Development, implementation and Validation of 3-D Failure Model for Aluminium 2024 for High Speed Impact Applications

Paul Du Bois, Murat Buyuk, Jeanne He, Steve Kan

NCAC-GWU

9th LS-DYNA Forum

October 12-13, 2010

Bamberg, Germany

Introduction

- Part of a research program conducted by FAA William J Hughes Technical Center (NJ)

- material testing performed by OSU
- ballistic testing performed by NASA/GRC
- numerical simulations performed by GWU-NCAC

- involved the implementation in LS-DYNA of a tabulated generalisation of the Johnson-Cook material law with regularisation to accommodate simulation of ductile materials

- previously published results in :

▪ A Generalized, Three Dimensional Definition, Description and Derived Limits of the Triaxial Failure of Metals, Carney, DuBois, Buyuk, Kan, Earth&Sky, march 2008

FAA engine safety working group

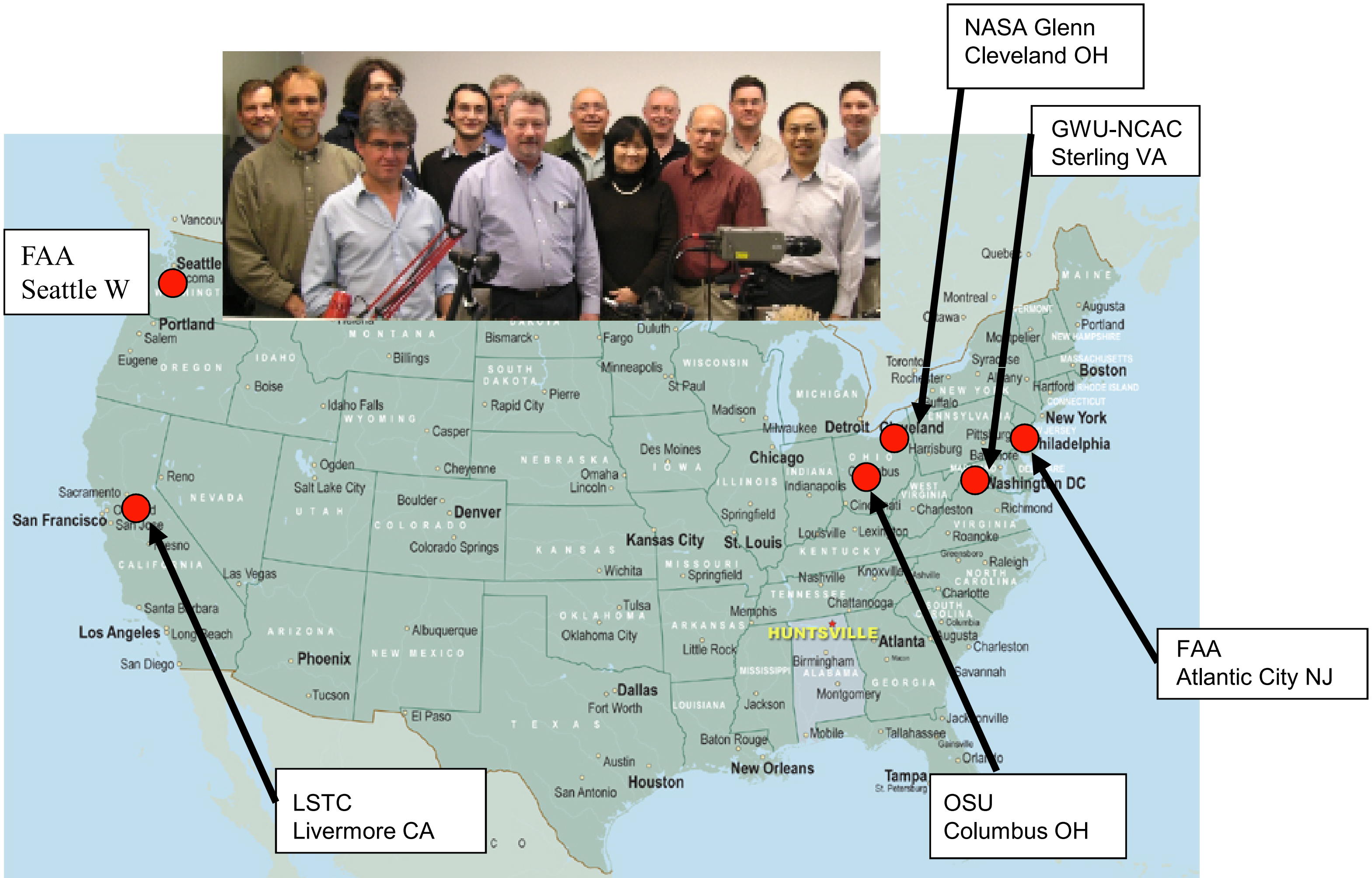

Background : blade-out events

- Aircraft Safety depends upon sound engine containment designs, and upon realistic evaluation of the damage from uncontained engine debris.
- The program addresses the modeling of impact between the blades and case, or between the fragments and non-engine aircraft structure
- The program has developed an extensive material test database and has modeled many different tests to evaluate the overall applicability of a single material model to the larger overall problem

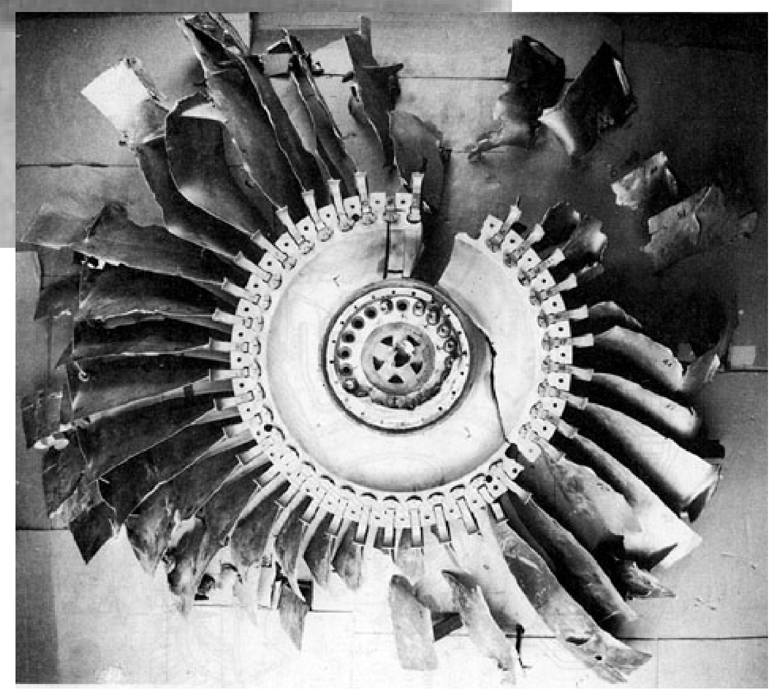

Sioux City, 1989

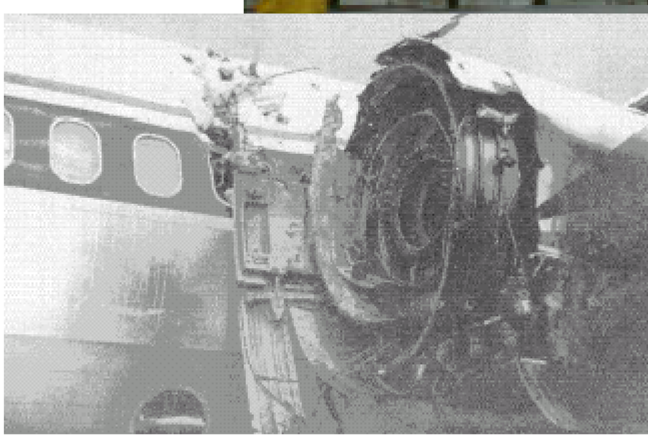

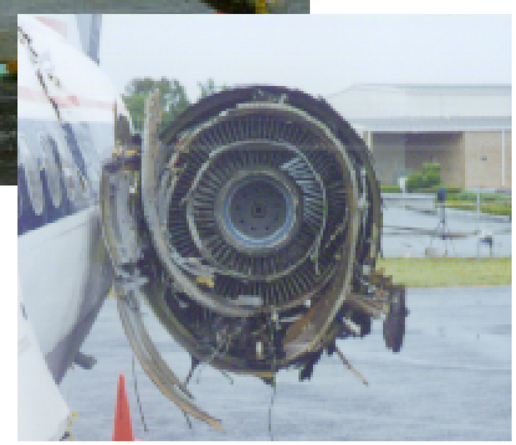

Pensacola RTO, 1996

Development, Implementation and Validation of 3-D Failure Model for Aluminium 2024

Mandatory full scale engine containment test

Fan blades of Trent

Development, Implementation and Validation of 3-D Failure Model for Aluminium 2024

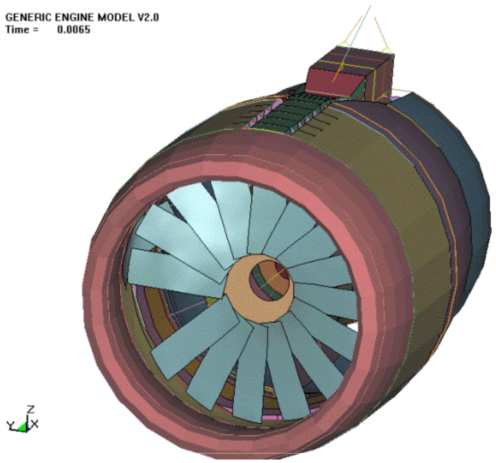

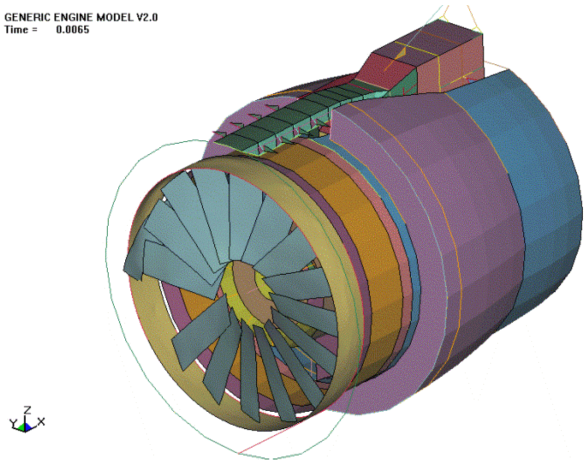

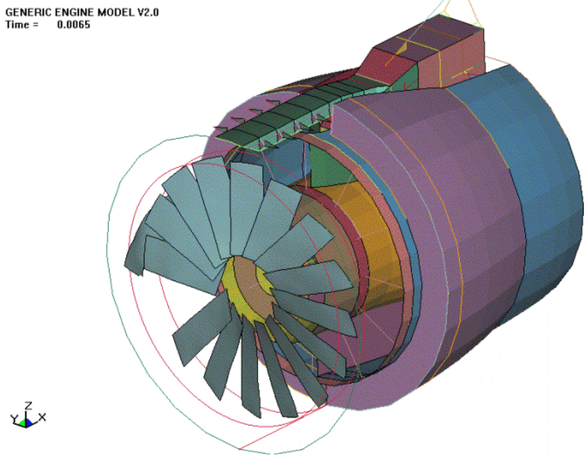

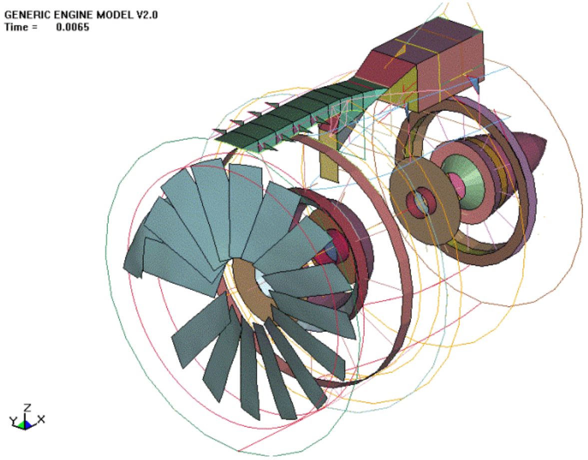

Development, Implementation and Validation of 3-D Failure Model for Aluminium 2024

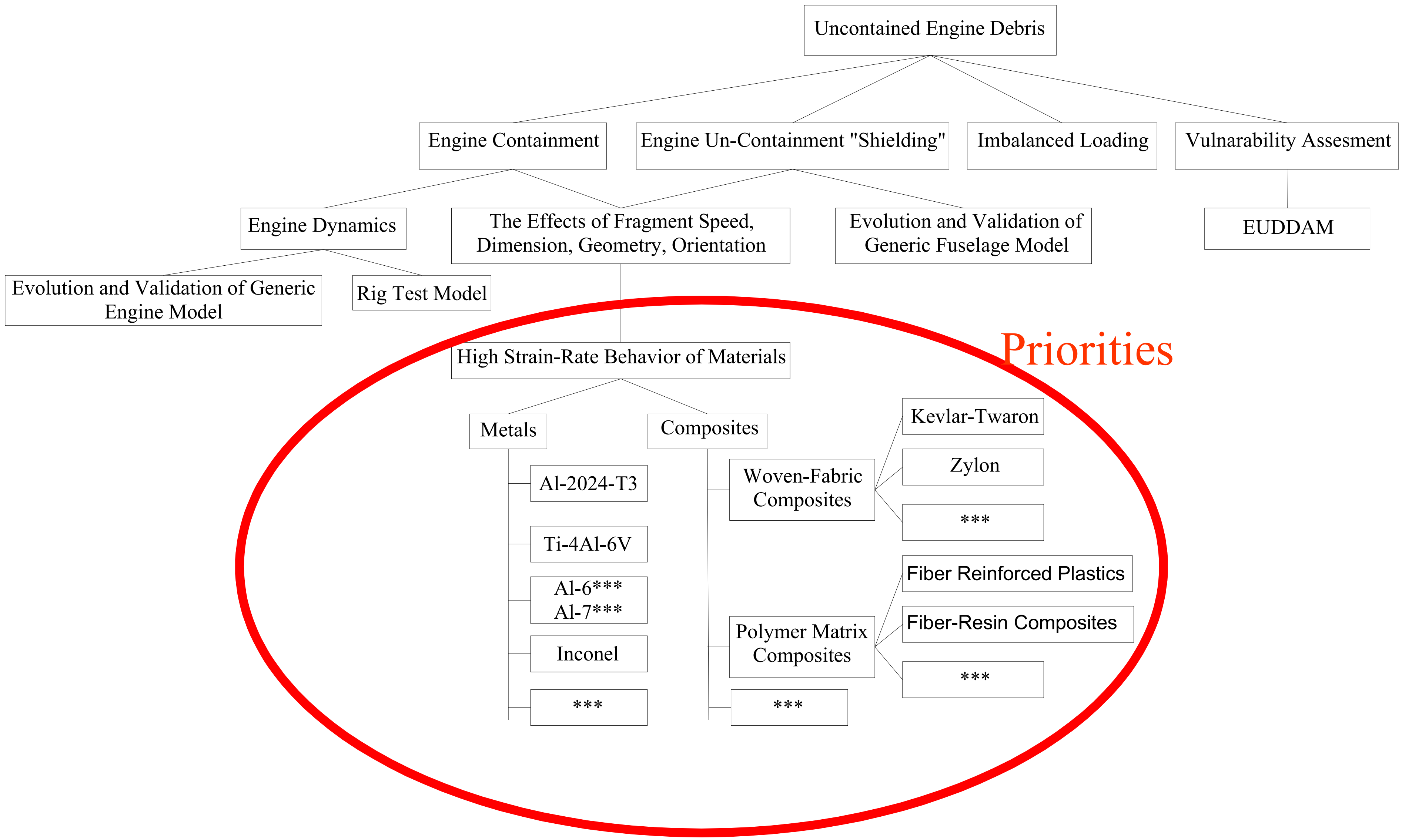

Failure Mode Transition with Material Thickness and Projectile Energy

1/16” plate - 1035 ft/s
Petaling &
Bending-Necking

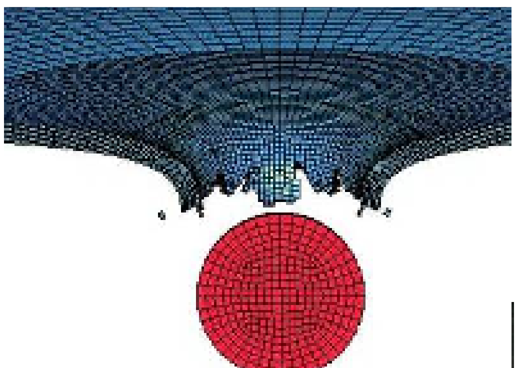


1/8” plate - 1140 ft/s
Mixed mode
Bending-Spalling

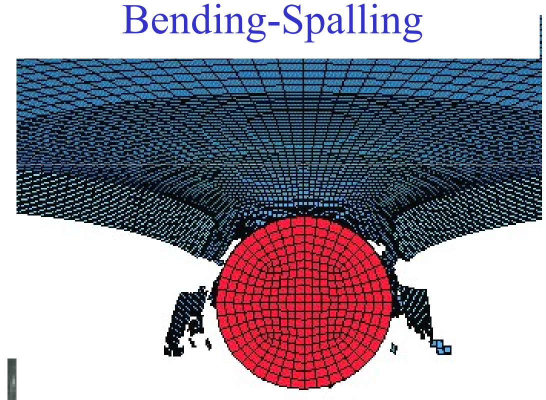


1/4” plate - 1875 ft/s
Plugging &
Shearing-Spalling


Pre MAT224 analysis requires adjusting the material failure model to the design condition

DOT/FAA/AR-07/26 Ballistic testing and simulation

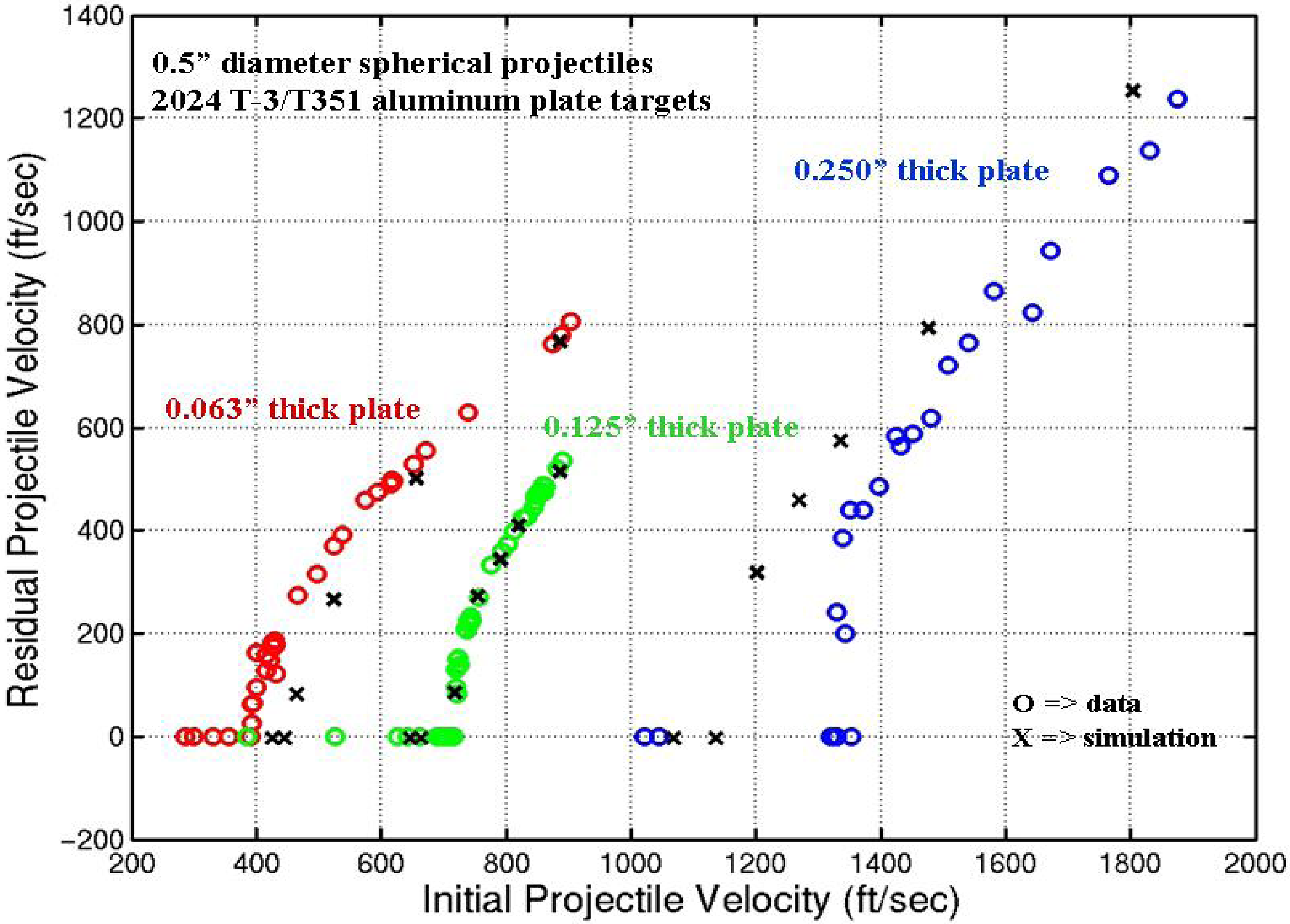

DOT/FAA/AR-08/36 Ballistic Limit Data

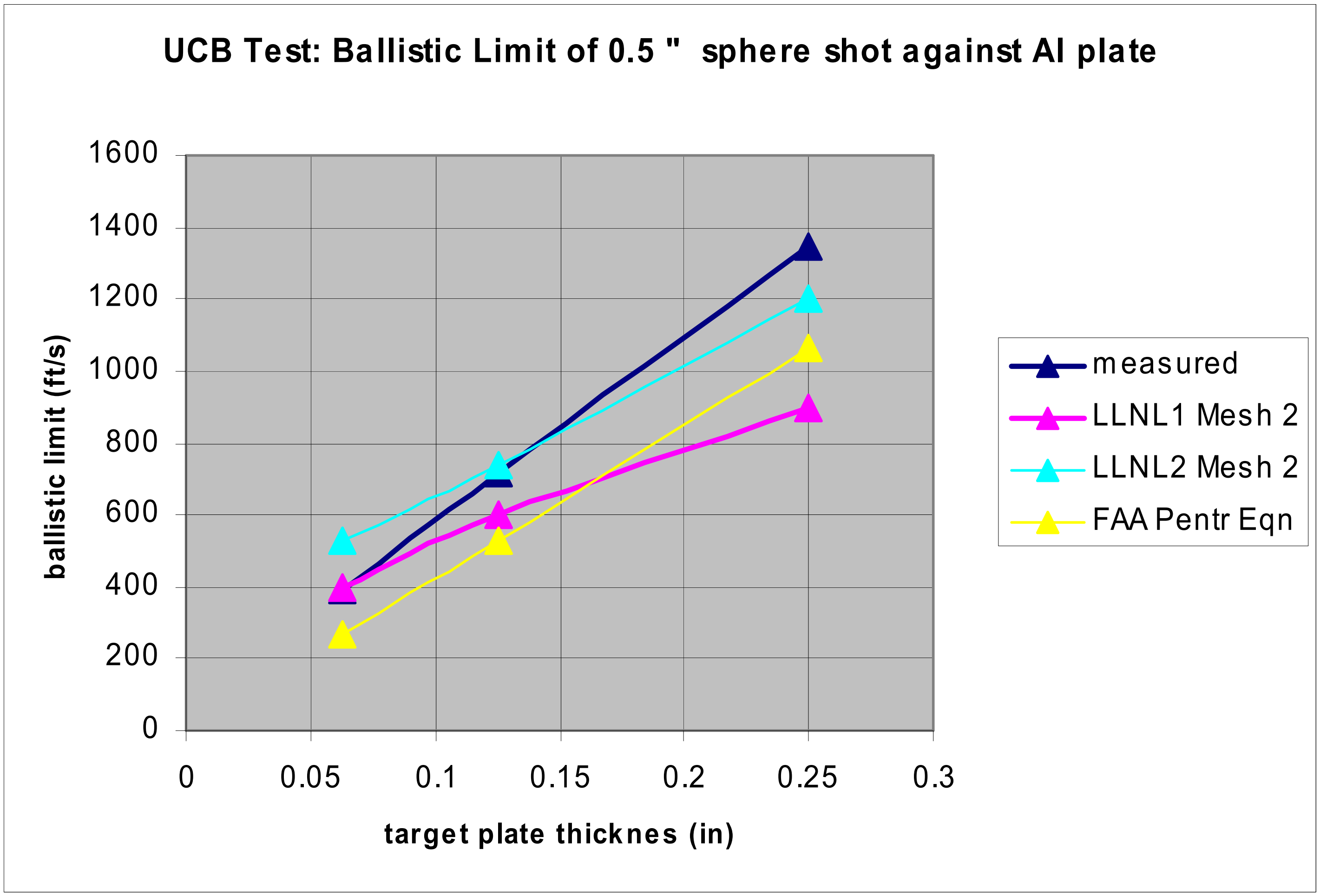

DOT/FAA/AR-08/36 Ballistic Limit Data

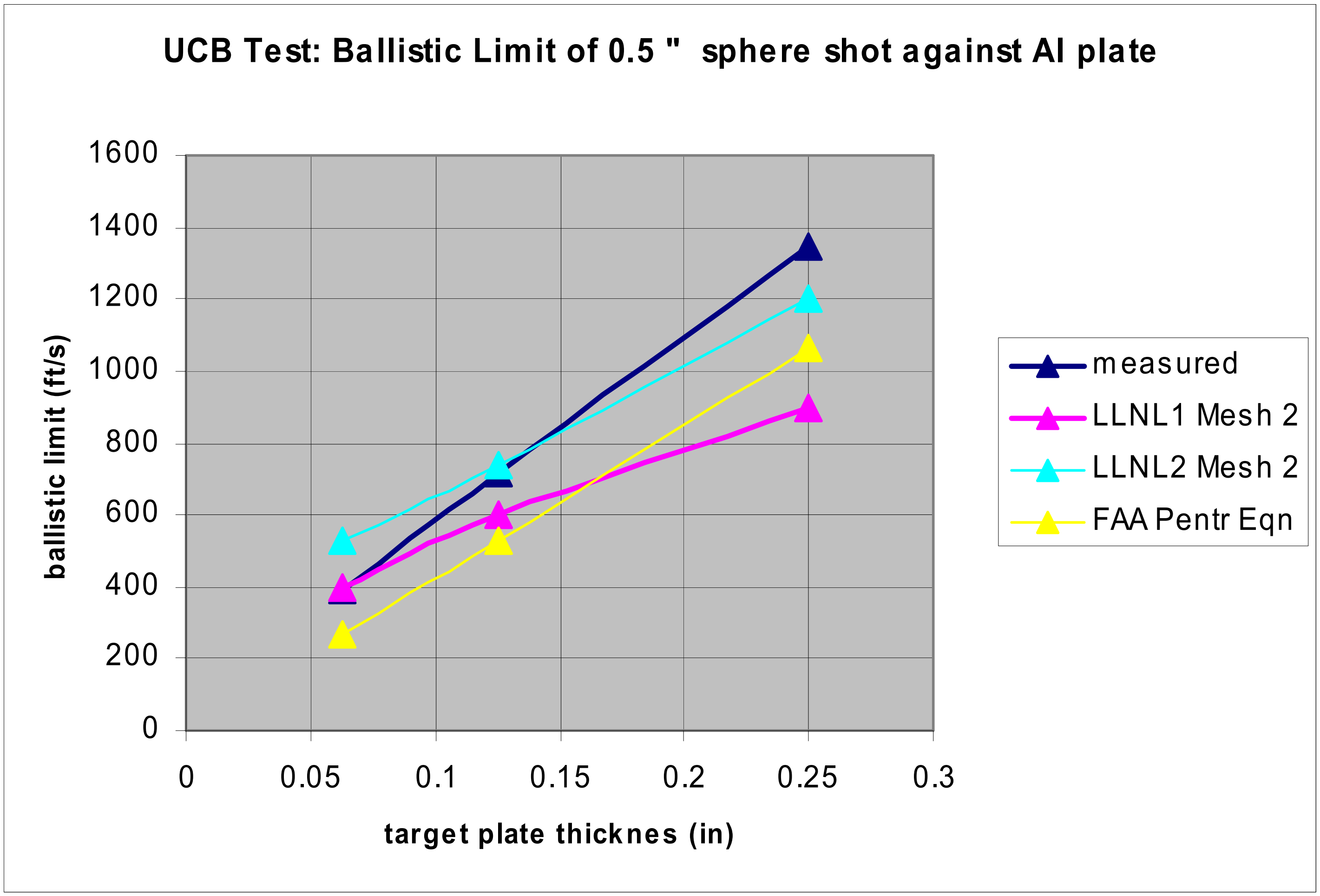

Part 1 :

OVERVIEW OF MAT_224

Development of MAT_224 in LS-DYNA

• The Johnson-Cook material law is based on a multiplicative decomposition of strain hardening, strain rate hardening and thermal softening :

$$\sigma_y = (a + b\varepsilon_p^n)\left(1 + c\ln\left(\frac{\dot{\varepsilon}}{\dot{\varepsilon}_0}\right)\right)\left(1 - \left(\frac{T - T_R}{T_m - T_R}\right)^m\right)$$

• A similar formulation is used for the plastic failure strain in function of state of stress (triaxiality), temperature and strain rate

$$\varepsilon_{pf} = \left(D_1 + D_2 e^{D_3 \frac{p}{\sigma_{vm}}}\right)\left(1 + D_4 \ln\left(\frac{\dot{\varepsilon}}{\dot{\varepsilon}_0}\right)\right)\left(1 + D_5\left(\frac{T - T_R}{T_m - T_R}\right)\right)$$

•A damage variable with scalar accumulation is used as failure criterion :

$$d = \int \frac{d\varepsilon_p}{\varepsilon_{pf}} \leq 1$$

• Exactly the same approach is followed in MAT_224
• analytical formulations are replaced by tabulated generalisation

Development of MAT_224 in LS-DYNA

- regularisation of the displacement at failure is added to account for the inevitable mesh-dependency of the simulations after necking in ductile materials
- started development in november 2006
- production version available in ls971-R4.2
- current presentation is based on implementation in ls971-R5.0
- developed on the basis of MAT_024 with VP=1
- available for fully and underintegrated shell and solid elements
- full keyword code : *MAT_TABULATED_JOHNSON_COOK

MAT_224 : material law

*MAT_TABULATED_THERMO_VISCOPLASTICITY_WITH_FAILURE

TITLE

1	MID	RO	E	PR	CP	TR	BETA
	4	2.7e-009	0.7466e + 005	0.3	8.75e + 006	300.0	1.0
2	k1	kt	f	g	h	i	
	11	12	15	16	17	18	0.0

k1 : table of rate dependent
isothermal hardening curves
or load curve defining
quasistatic hardening curve

kt : table of temperature dependent
quasistatic hardening curves

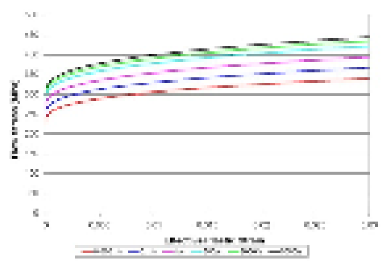

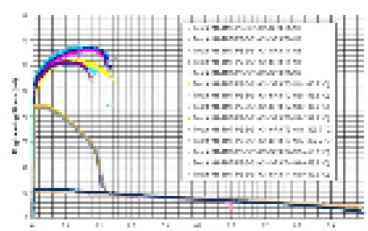

$$\sigma_y = k1(\varepsilon_p, \dot{\varepsilon}_p) \cdot kt(\varepsilon_p, T)$$

$$\varepsilon_p = \int \dot{\varepsilon}_p$$

$$T = T_R + \frac{\beta}{C_p \rho} \int \sigma_y \dot{\varepsilon}_p$$

MAT_224 : failure model

*MAT_TABULATED_THERMO_VISCOPLASTICITY_WITH_FAILURE

TITLE

1	MID	RO	E	PR	CP	TR	BETA
	4	2.7e-009	0.7466e + 005	0.3	8.75e + 006	300.0	1.0
2	k1	kt	f	g	h	i	
	11	12	15	16	17	18	0.0

f : table of load curves giving failure plastic strain in function of triaxiality at constant Lode angle
g : scaling function for rate effects
h : scaling function for temperature
i : regularisation curve

$$\varepsilon_{pf} = f\left(\frac{p}{\sigma_{vm}}\right) g\left(\dot{\varepsilon}_p\right) h\left(T\right) i\left(l_c\right)$$

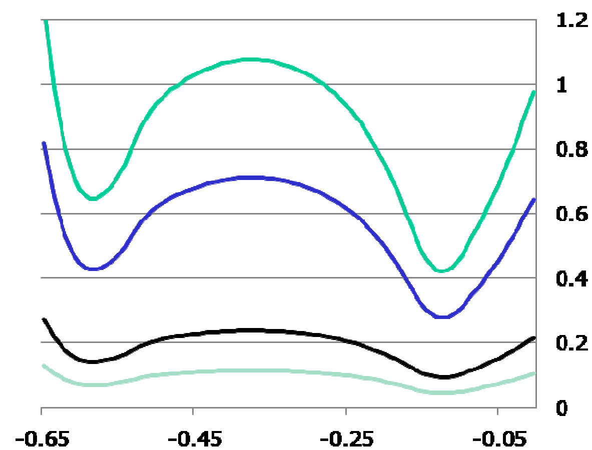

MAT_224 : material law : basic example

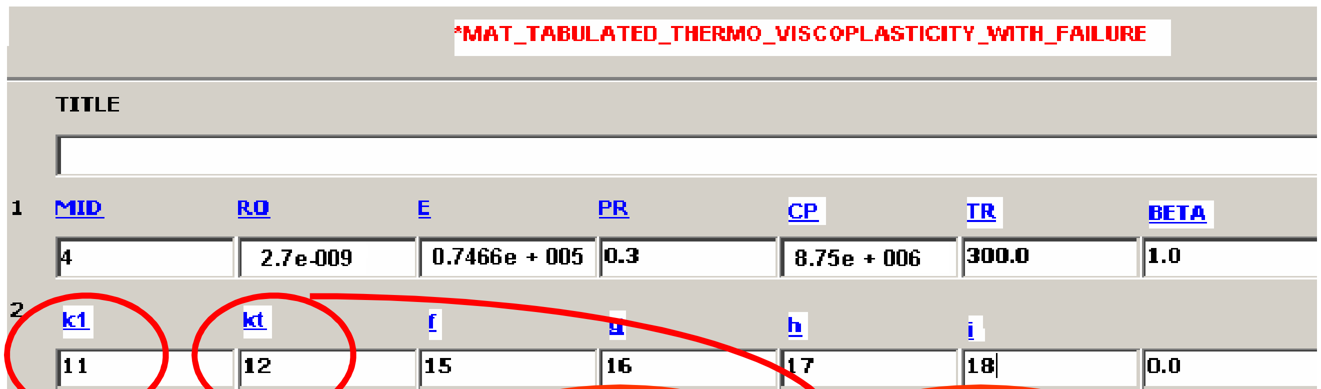

$$\sigma_y = k1(\varepsilon_p, \dot{\varepsilon}_p) \cdot kt(\varepsilon_p, T)$$

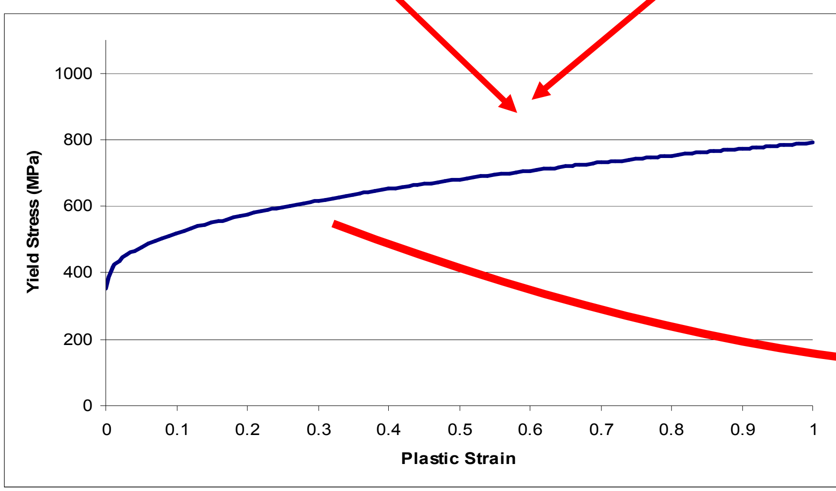

T	ε	σ
TR	$\sigma_y = k1(\varepsilon_p, \dot{\varepsilon}_p)$	
TM	0	

TR = 300 K
TM = 775 K

MAT_224 : failure law : basic example

*MAT_TABULATED_THERMO_VISCOPLASTICITY_WITH_FAILURE

TITLE

1	MID	RO	E	PR	CP	TR	BETA
	4	2.7e-009	0.7466e + 005	0.3	8.75e + 006	300.0	1.0
2	k1	kt	f	g	h	i	
	11	12	15	16	17	18	0.0

$\dot{\varepsilon}$	ε_f
0	1
1000000	1

TR	1
TM	1

TR = 300 K
TM = 775 K

0	1
l_{max}	1

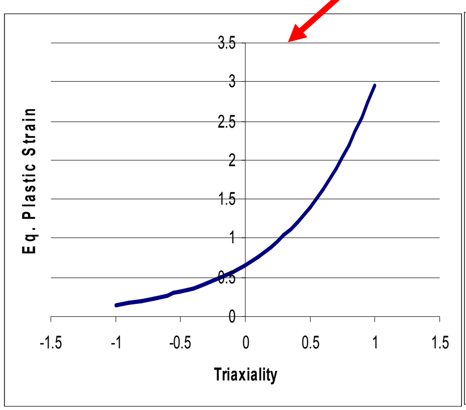

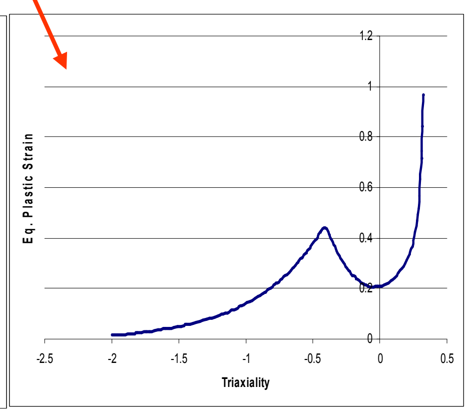

$$\varepsilon_{pf} = f\left(\frac{p}{\sigma_{vm}}\right) g\left(\dot{\varepsilon}_p\right) h\left(T\right) i\left(l_c\right)$$

$$d = \int \frac{d\varepsilon_p}{\varepsilon_{pf}} \leq 1$$

MAT_224 : failure law : regularisation

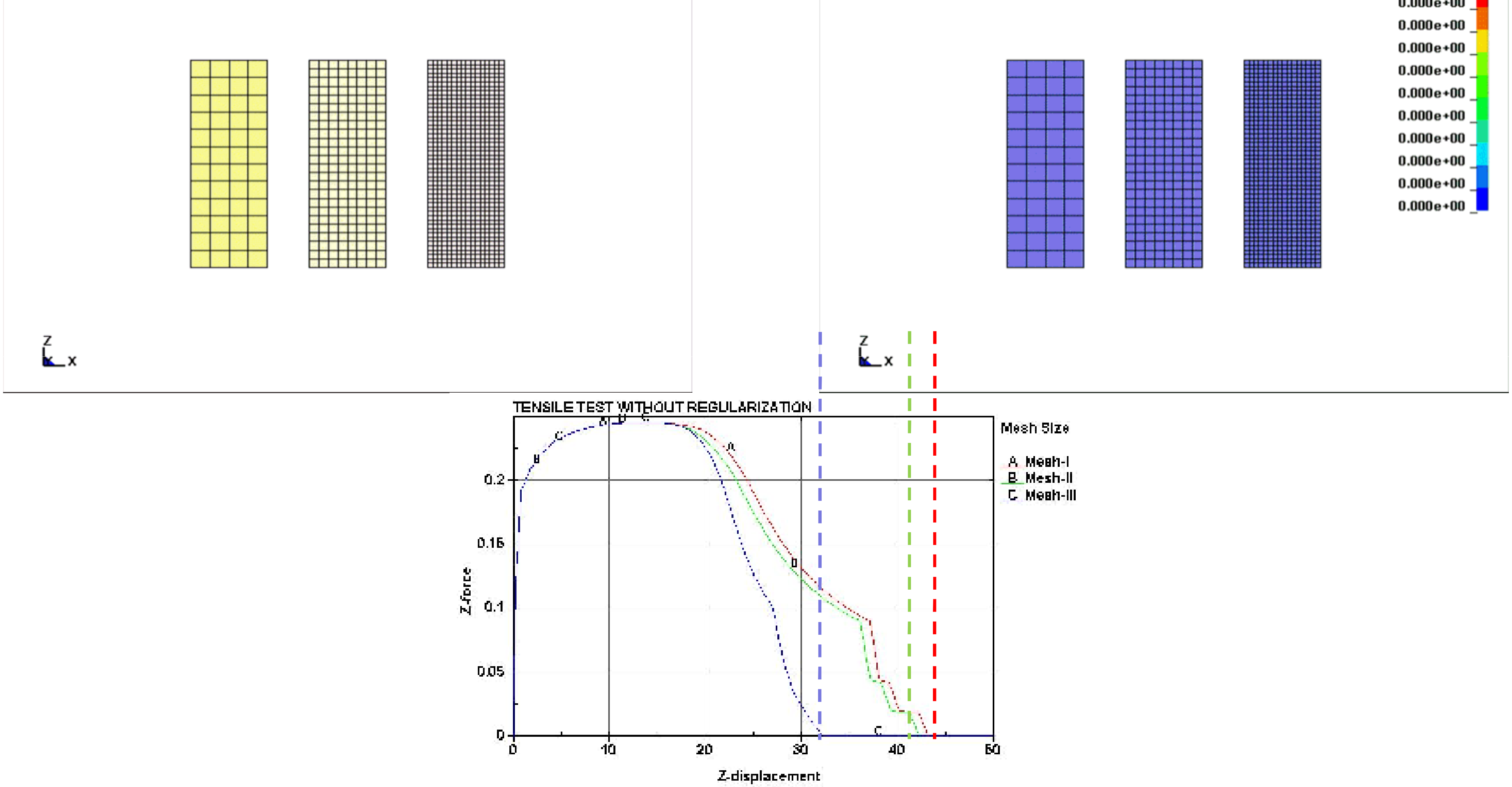

Differences in the Elongation Due to Mesh Dependency; Even if Characterized Failure Strain is Used

MAT_224 : failure law : regularisation

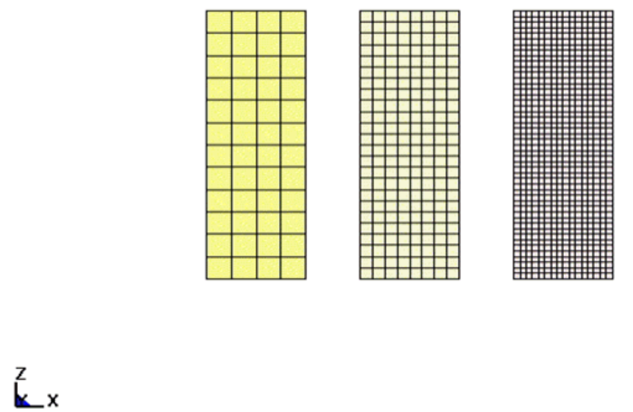

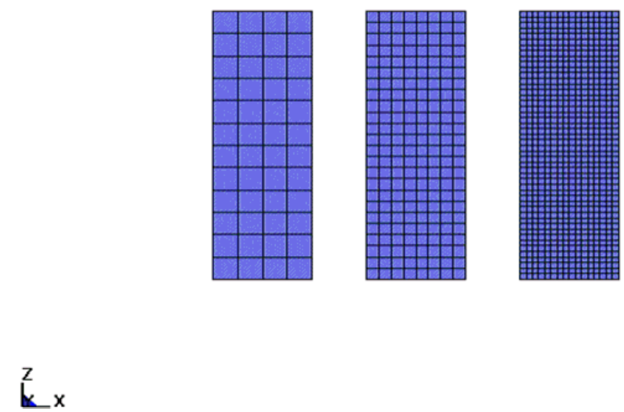

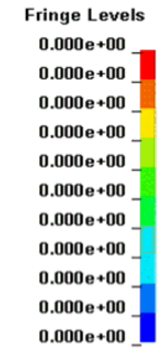

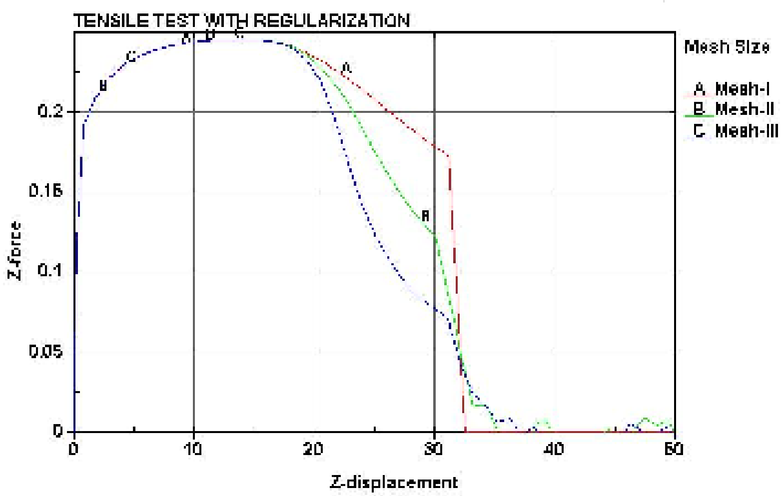

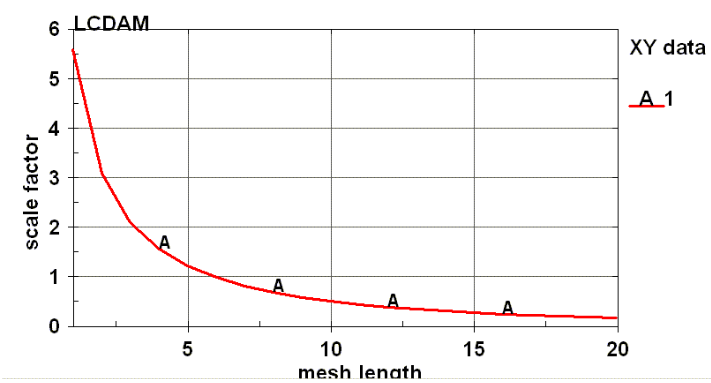

Regularized Failure Strain According to the Mesh Size

MAT_224 : Verification Process

- extensive verification needs to be performed
- some elementary single solid element tests are shown next
- resuls must be compared to reliably implemented material laws in LS-DYNA : natural choices are MAT_024 and MAT_015
- in particular verify the influence of thermal softening and stress triaxiality

Development, Implementation and Validation of 3-D Failure Model for Aluminium 2024

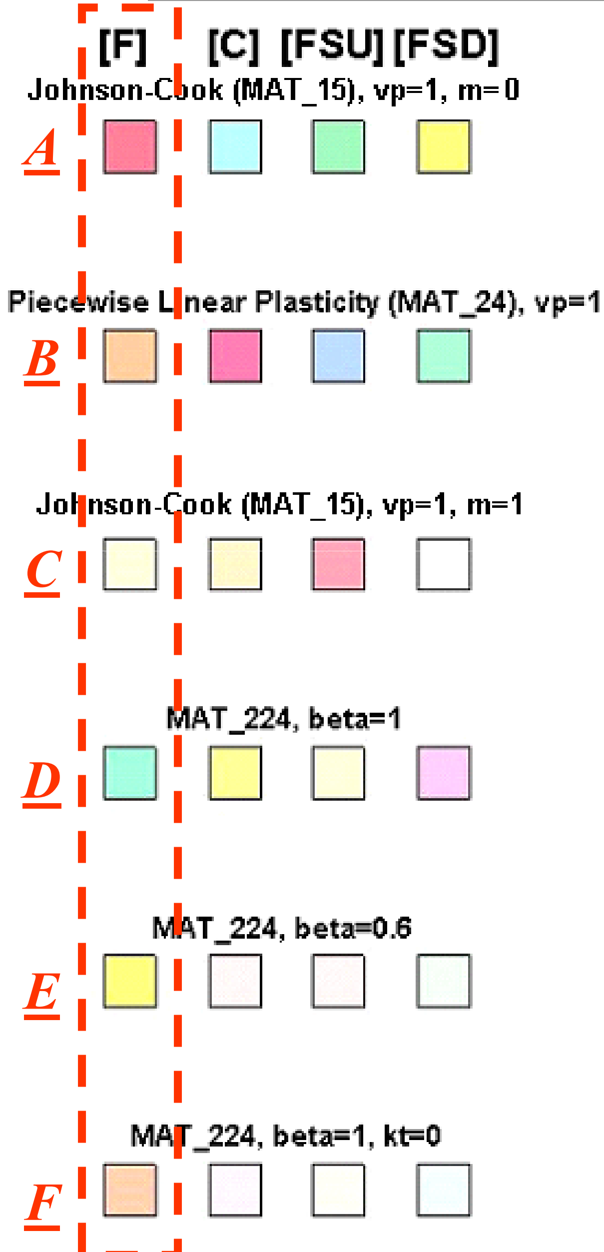

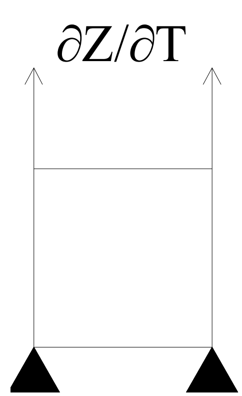

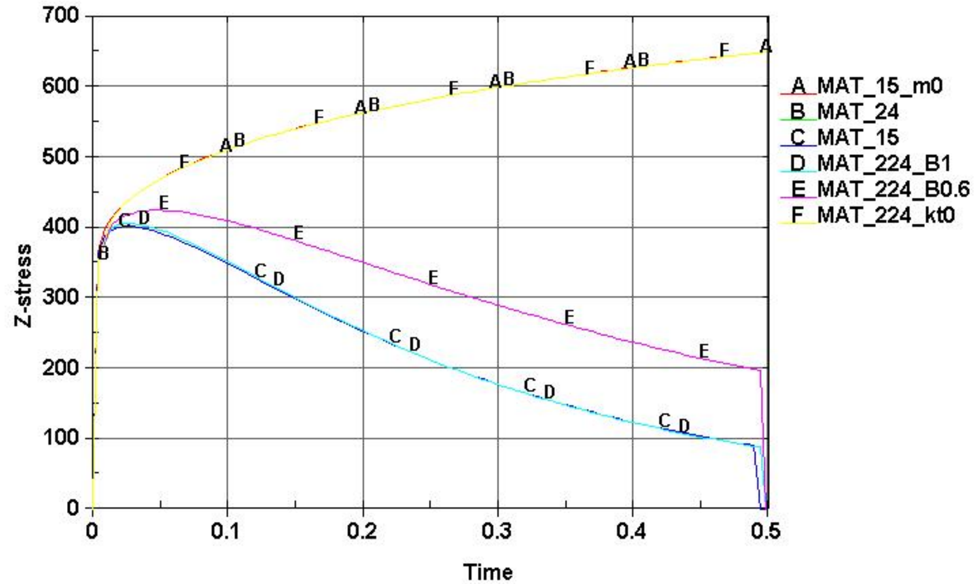

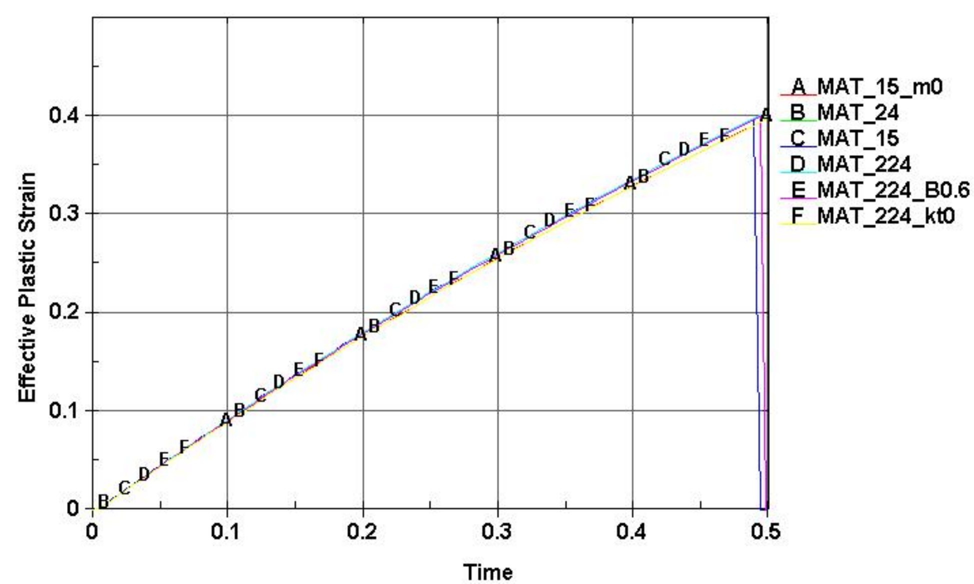

Development, Implementation and Validation of 3-D Failure Model for Aluminium 2024

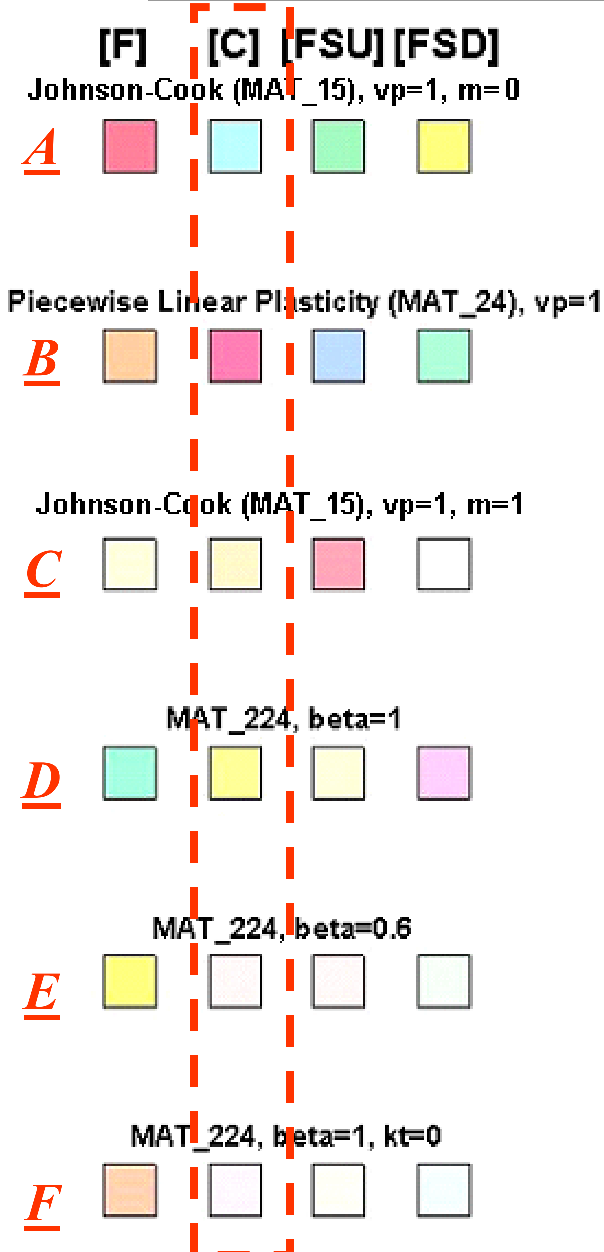

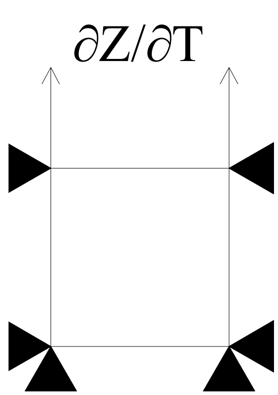

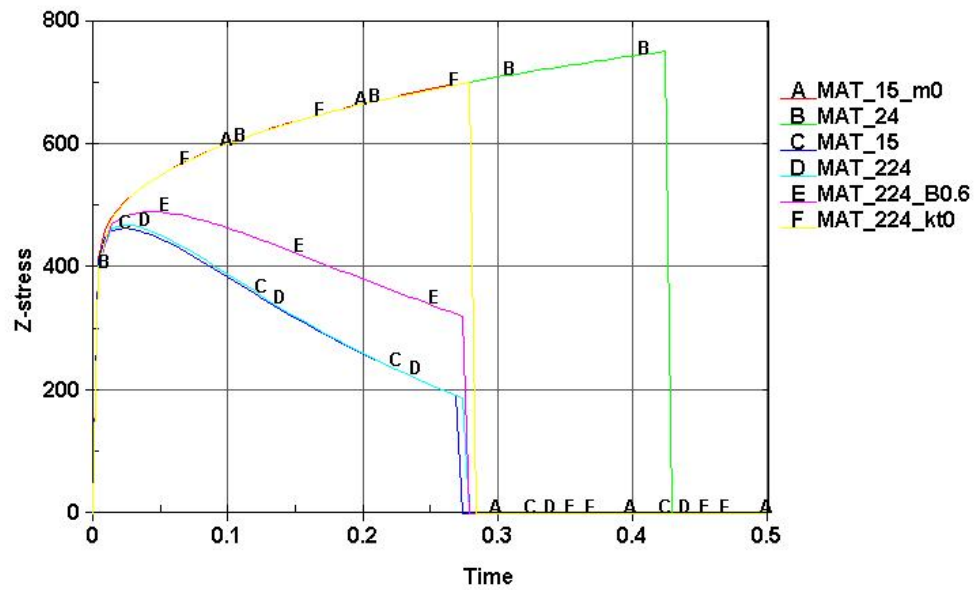

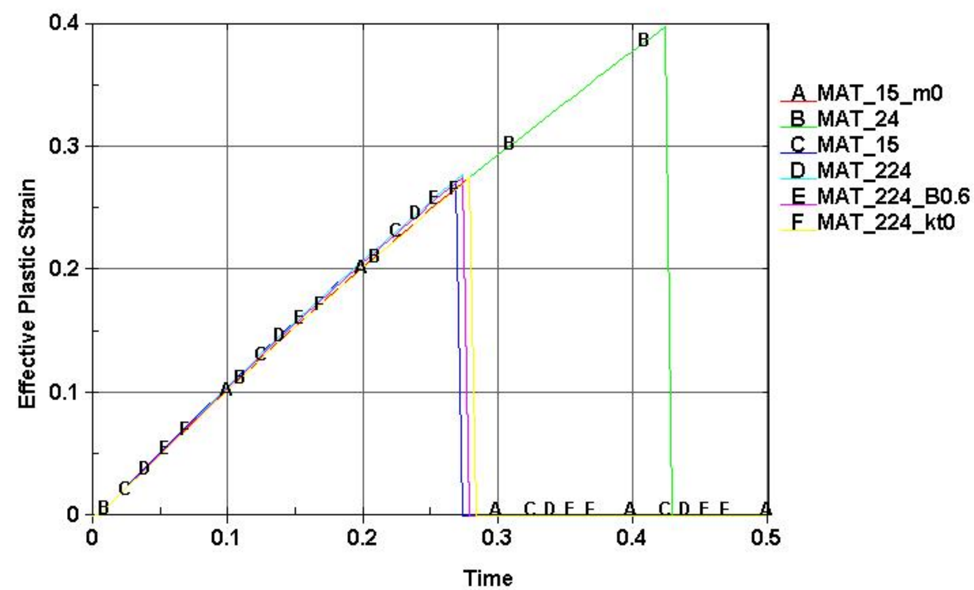

Development, Implementation and Validation of 3-D Failure Model for Aluminium 2024

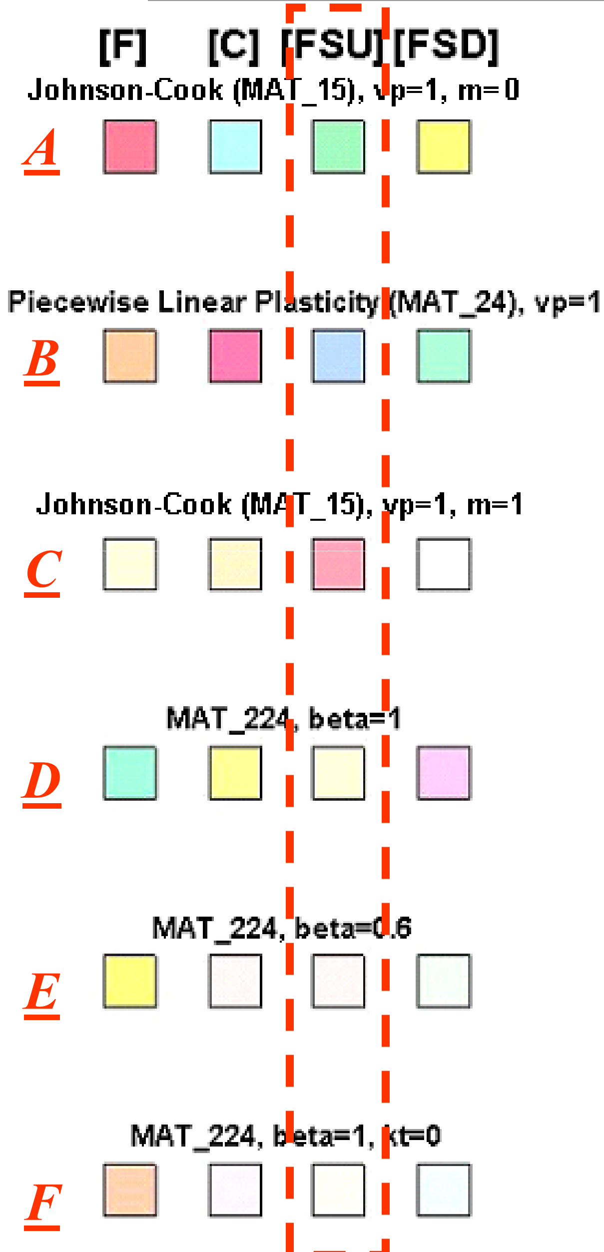

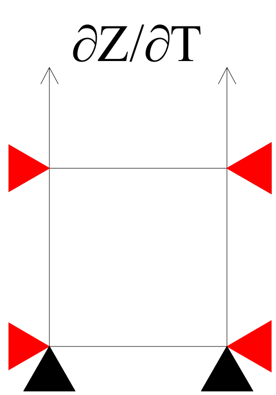

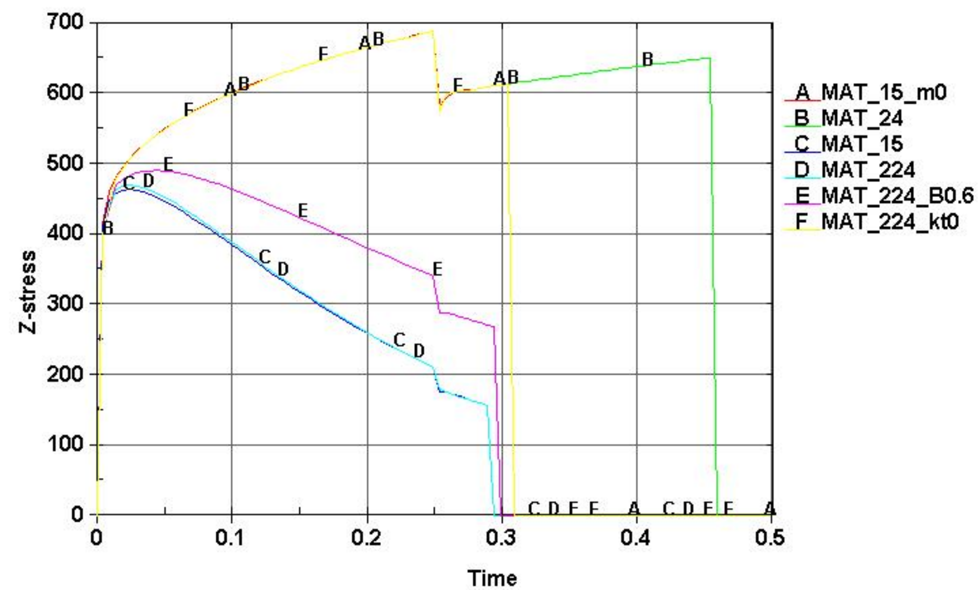

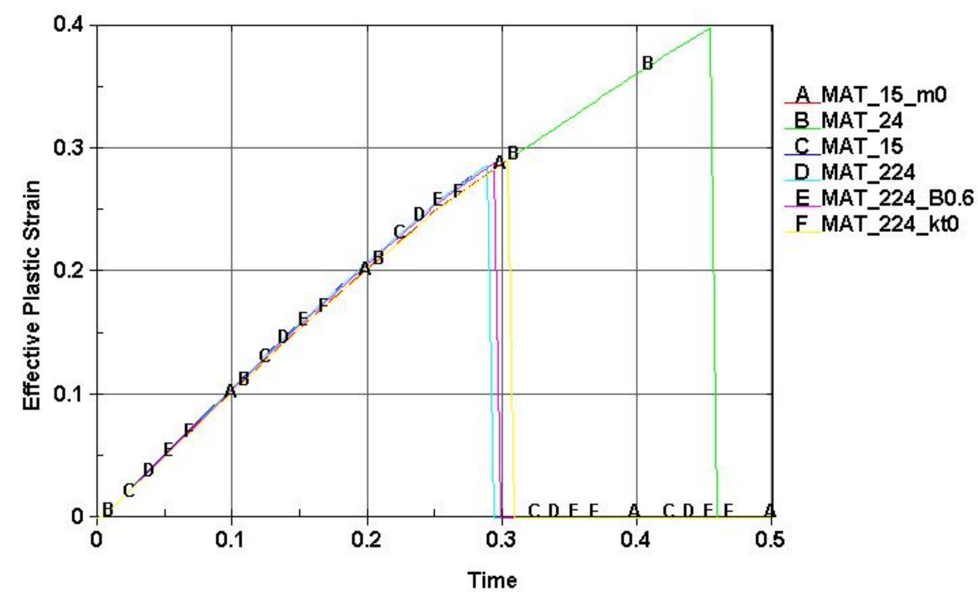

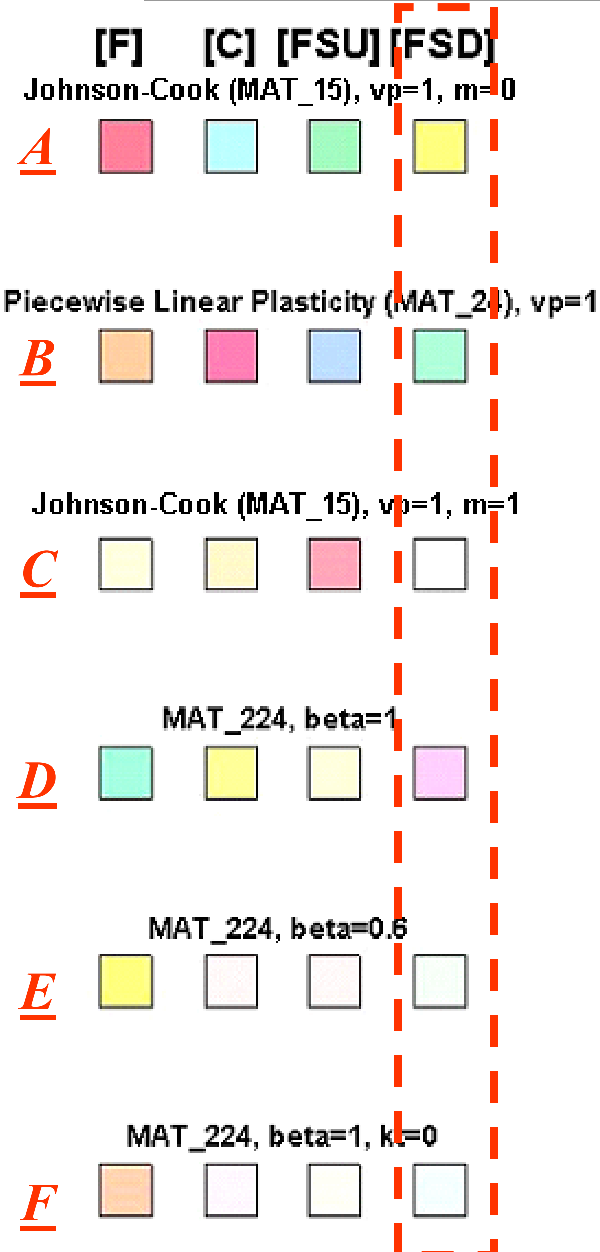
[F] [C] [FSU] [FSD]
Johnson-Cook (MAT_15), vp=1, m=0
A
Piecewise Linear Plasticity (MAT_24), vp=1
B
Johnson-Cook (MAT_15), vp=1, m=1
C
MAT_224, beta=1
D
MAT_224, beta=0.6
E
MAT_224, beta=1, kt=0
F

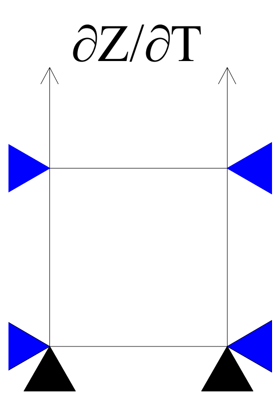
∂Z/∂T

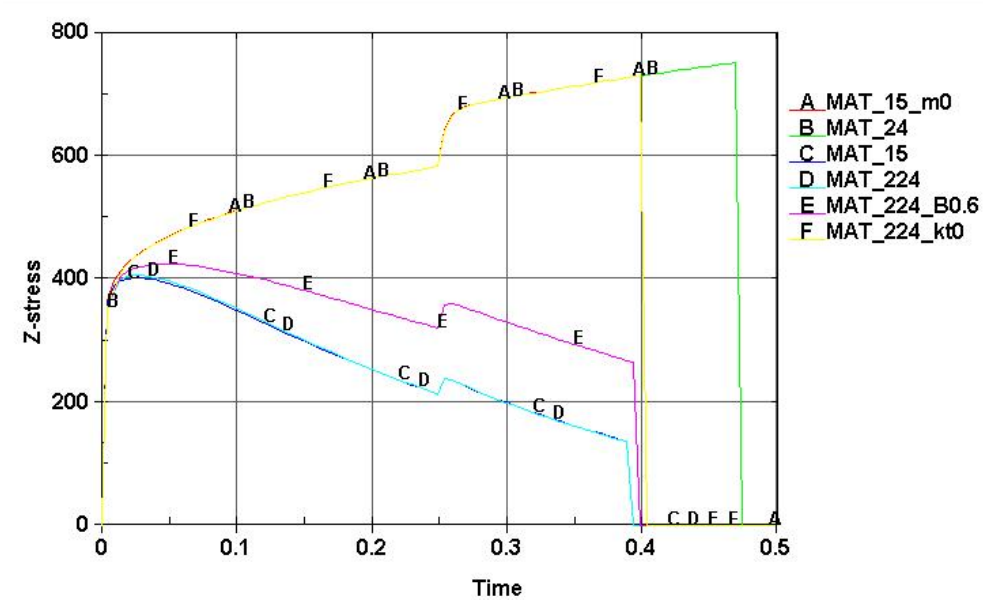
Z-stress
Time
A MAT_15_m0
B MAT_24
C MAT_15
D MAT_224
E MAT_224_B0.6
F MAT_224_kt0

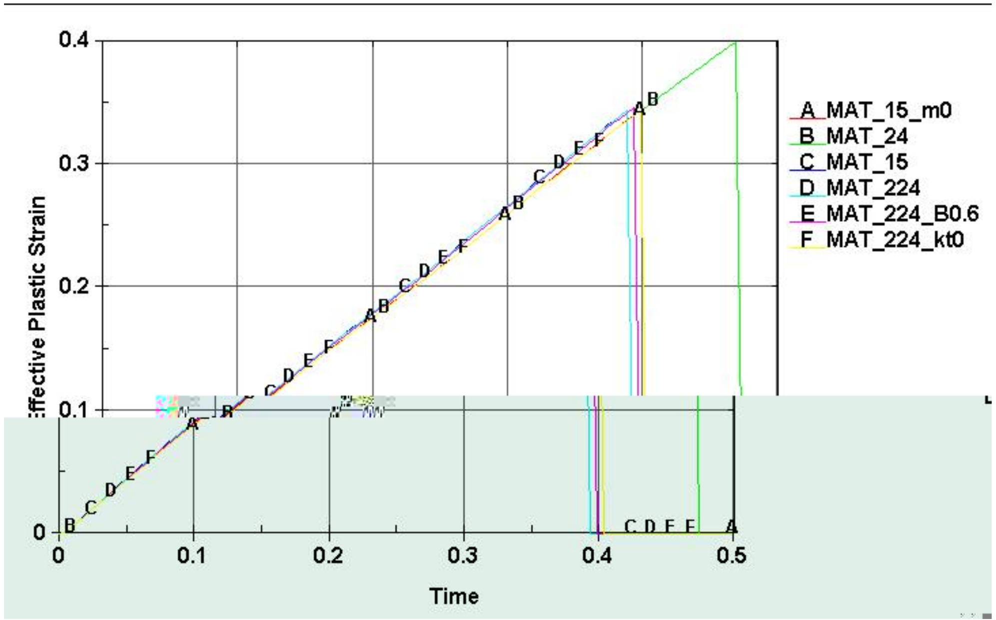
Effective Plastic Strain
Time
A MAT_15_m0
B MAT_24
C MAT_15
D MAT_224
E MAT_224_B0.6
F MAT_224_kt0

Once and for all : the history variables :

HV	Shell	Solid
1	Plastic strain rate	
5		Plastic strain rate
7	Plastic work	
8	Plastic strain/failure strain	Plastic failure strain
9	Element size	triaxiality
10	temperature	Lode angle
11	Plastic failure strain	Plastic work
12	Triaxiality	Plastic strain/failure strain
13		Element size
14		temperature

Part 2 :

FAILURE MODEL DESCRIPTION DEPENDENCY UPON THE STATE-OF-STRESS

$$\textbf{Triaxiality} = \frac{p}{\sigma_{vm}}$$

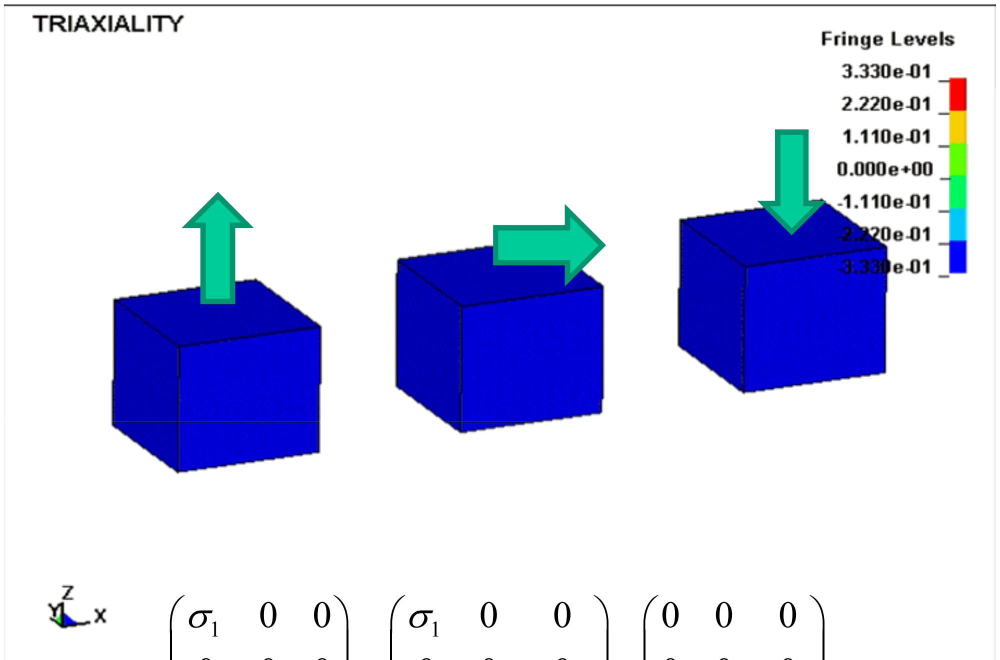

$$\begin{pmatrix} \sigma_1 & 0 & 0 \\ 0 & 0 & 0 \\ 0 & 0 & 0 \end{pmatrix} \quad \begin{pmatrix} \sigma_1 & 0 & 0 \\ 0 & 0 & 0 \\ 0 & 0 & -\sigma_1 \end{pmatrix} \quad \begin{pmatrix} 0 & 0 & 0 \\ 0 & 0 & 0 \\ 0 & 0 & \sigma_3 \end{pmatrix}$$

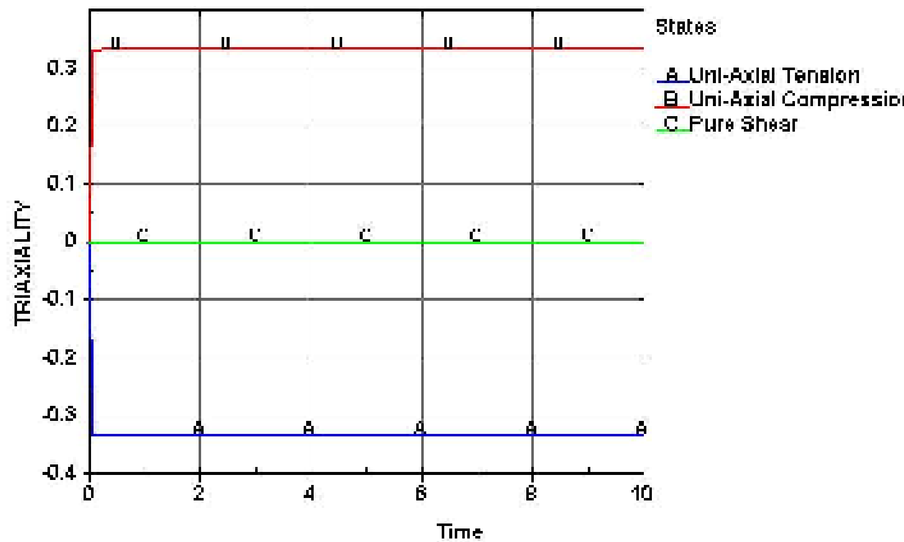

Single Finite Elements Under Different States-of-Stress

Lode angle $= \dfrac{27 J_3}{2\sigma_{vm}^3}$

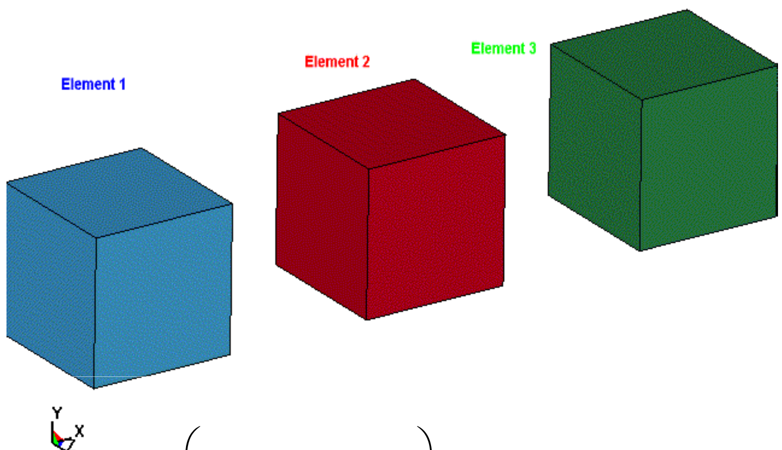

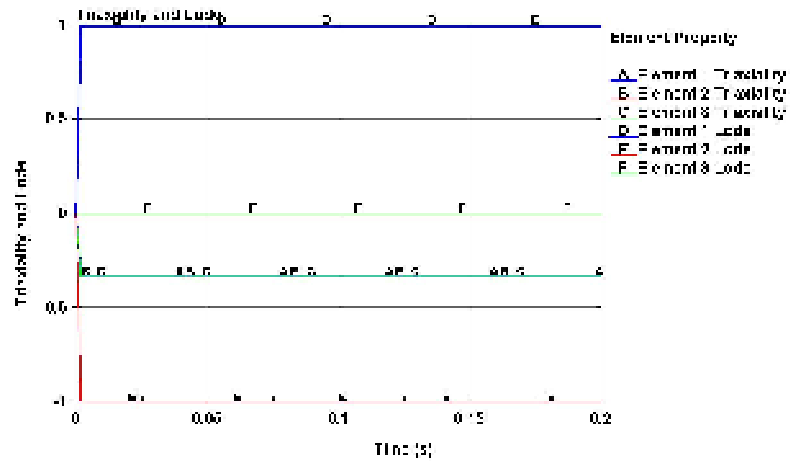

$$\begin{pmatrix} \sigma_1 & 0 & 0 \\ 0 & 0 & 0 \\ 0 & 0 & 0 \end{pmatrix} \quad \begin{pmatrix} \sigma_1 & 0 & 0 \\ 0 & \sigma_1 & 0 \\ 0 & 0 & -\dfrac{\sigma_1}{2} \end{pmatrix} \quad \begin{pmatrix} \sigma_1 & 0 & 0 \\ 0 & a\sigma_1 & 0 \\ 0 & 0 & (2a-1)\sigma_1 \end{pmatrix}$$

$$a = \frac{\sqrt{3}-1}{2}$$

3 very different load paths all have a triaxiality = -1/3
A second parameter is needed to distinguish between them
The Lode angle is a good practical choice since it is always comprised between -1 and 1

Representation of the state of stress :

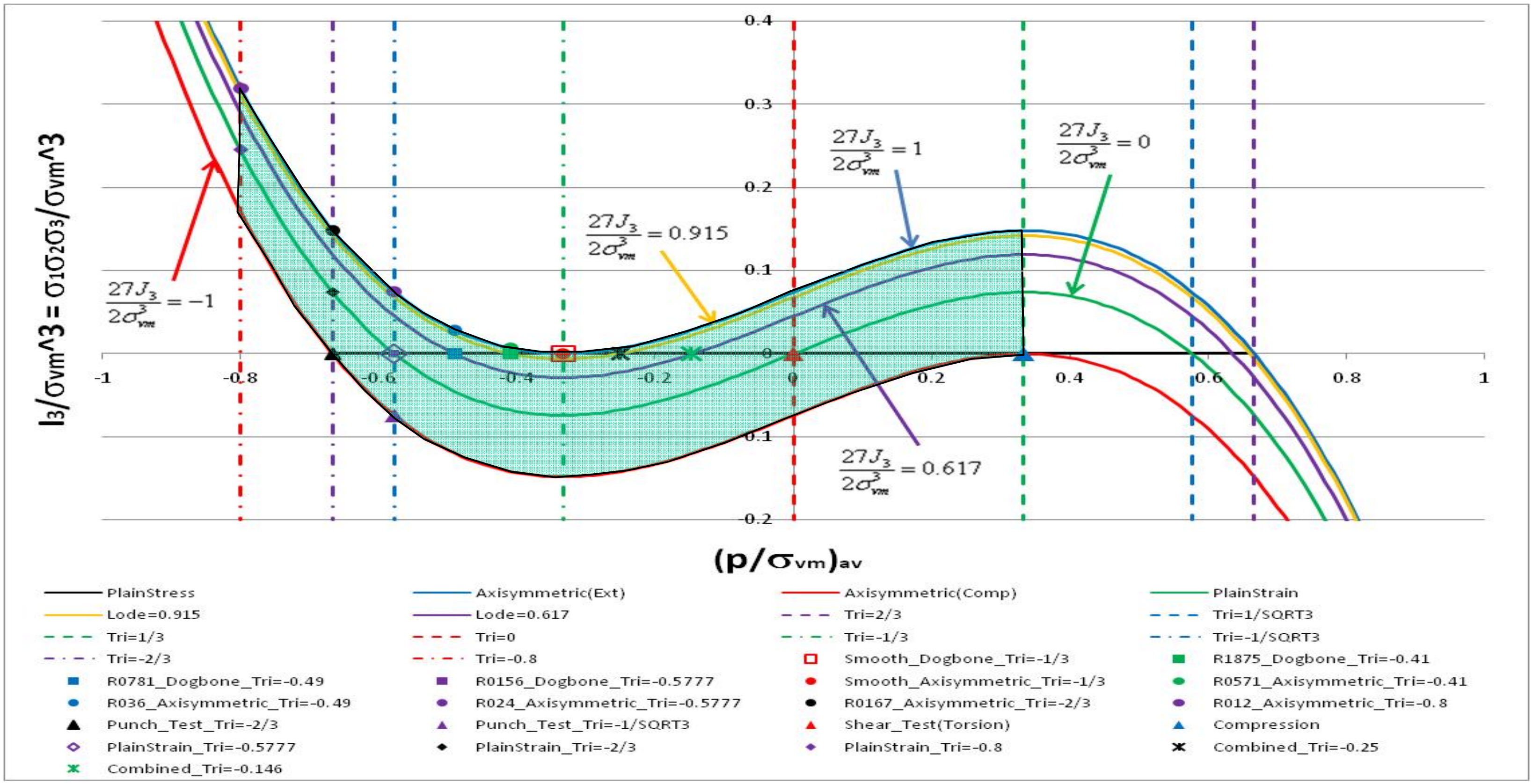

In this diagram the horizontal line comprises all possible states of plane stress

NASA Ballistic Tests

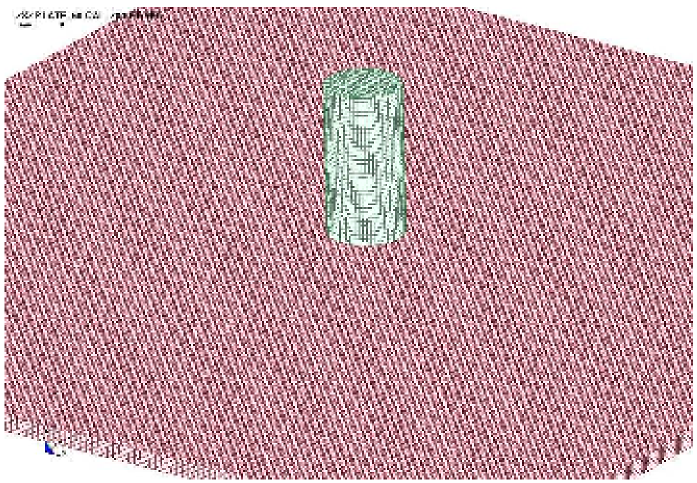

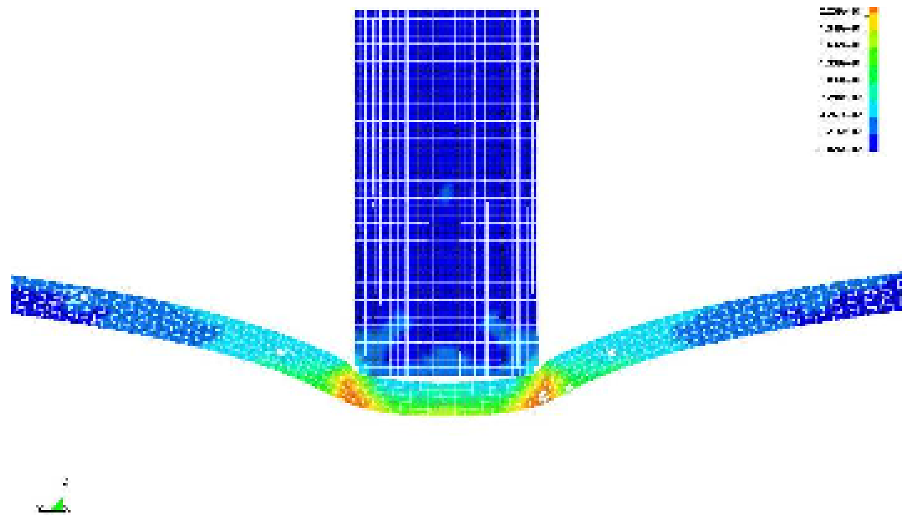

NASA Ballistic Tests

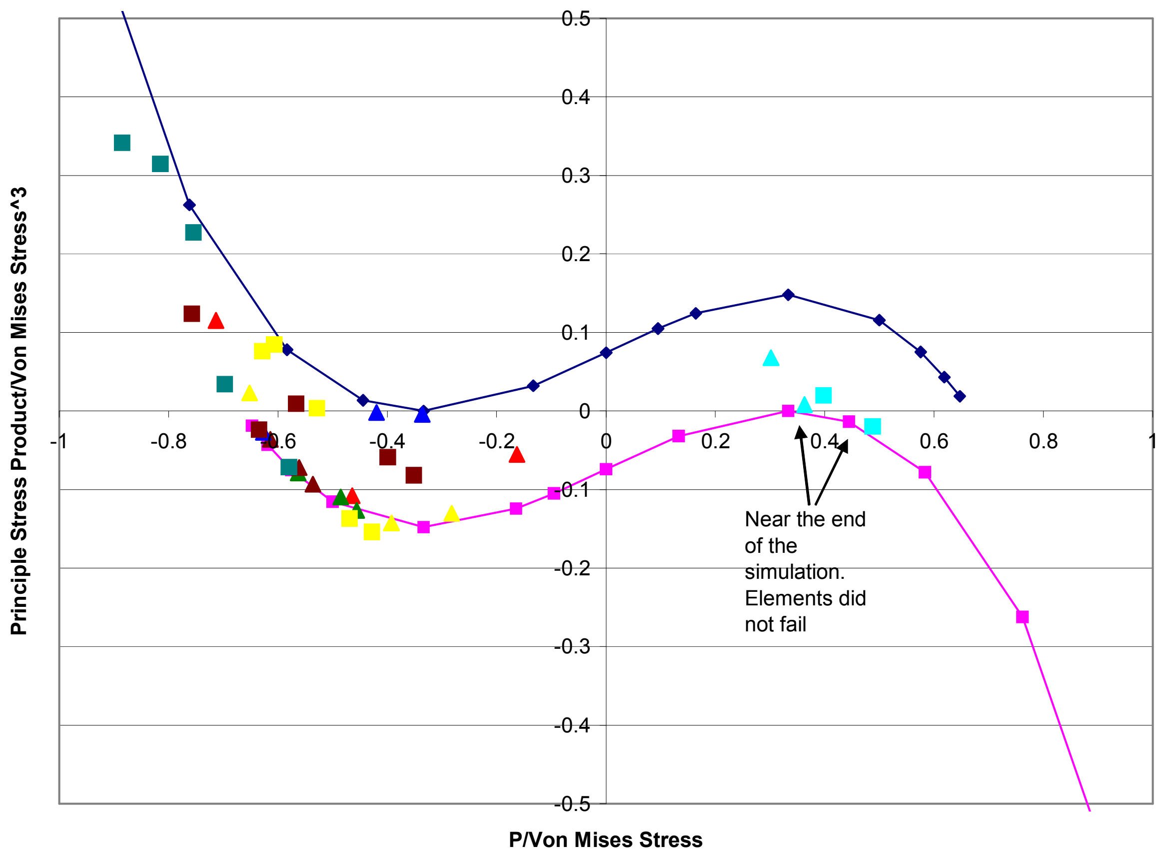

Carney K.S., DuBois P.A., ***Buyuk M.****, Kan S.*, "A generalized, three dimensional definition, description and derived limits of the triaxial failure of metals", *Journal*

MAT_224 : failure criterion

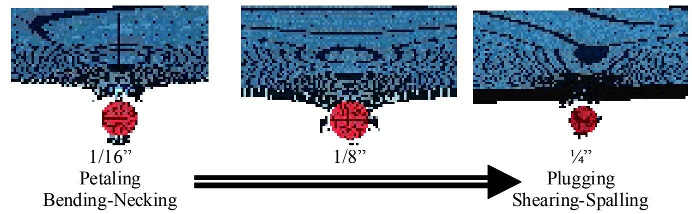

Failure Locus will be Covered by the Experimental Program

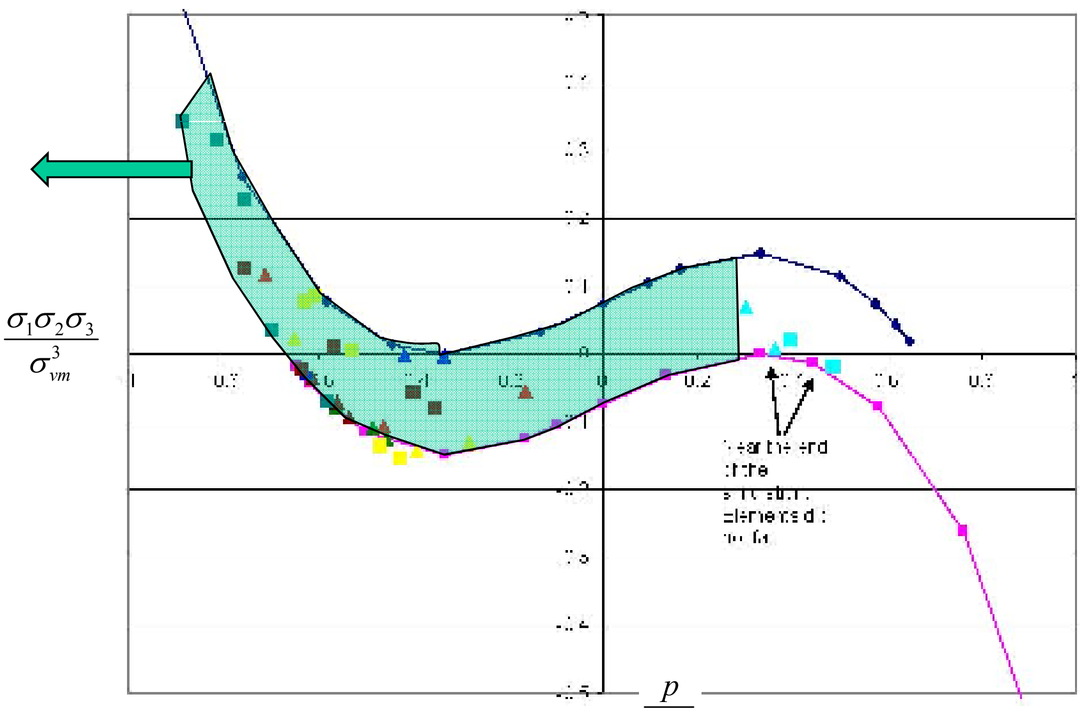

Domain Constituted and Populated by All Possible States-of-Stress upon Impact

material tests for failure criterion

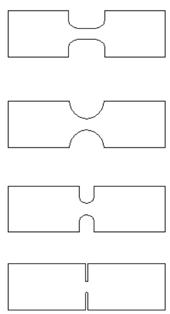

	Dog-Bone Specimens	Triaxiality	Lode-Angle
1		-0.333	1
2		-0.41	0.915
3		-0.49	0.617
4		-0.577	0

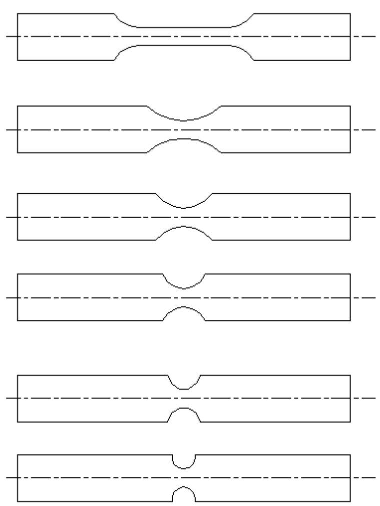

	Axi-Symmetric Specimens	Triaxiality	Lode-Angle
1		-0.333	1
2		-0.41	1
3		-0.49	1
4		-0.577	1
5		-0.666	1
6		-0.8	1

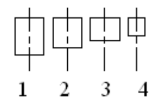

Compression Cylinders	Triaxiality	Lode-Angle
D20xL25 D20xL20 D20xL15 D12xL12	0.333	-1

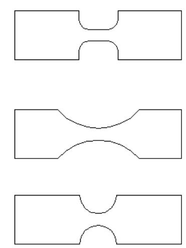

	Grooved Plates	Triaxiality	Lode-Angle
1		-0.577	0
2		-0.666	0
3		-0.8	0

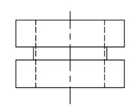

	Shear	Triaxiality	Lode-Angle
1		0	0

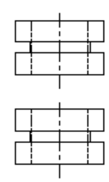

	Combined Loading	Triaxiality	Lode-Angle
1		-0.2505	0.915
2		-0.1466	0.617

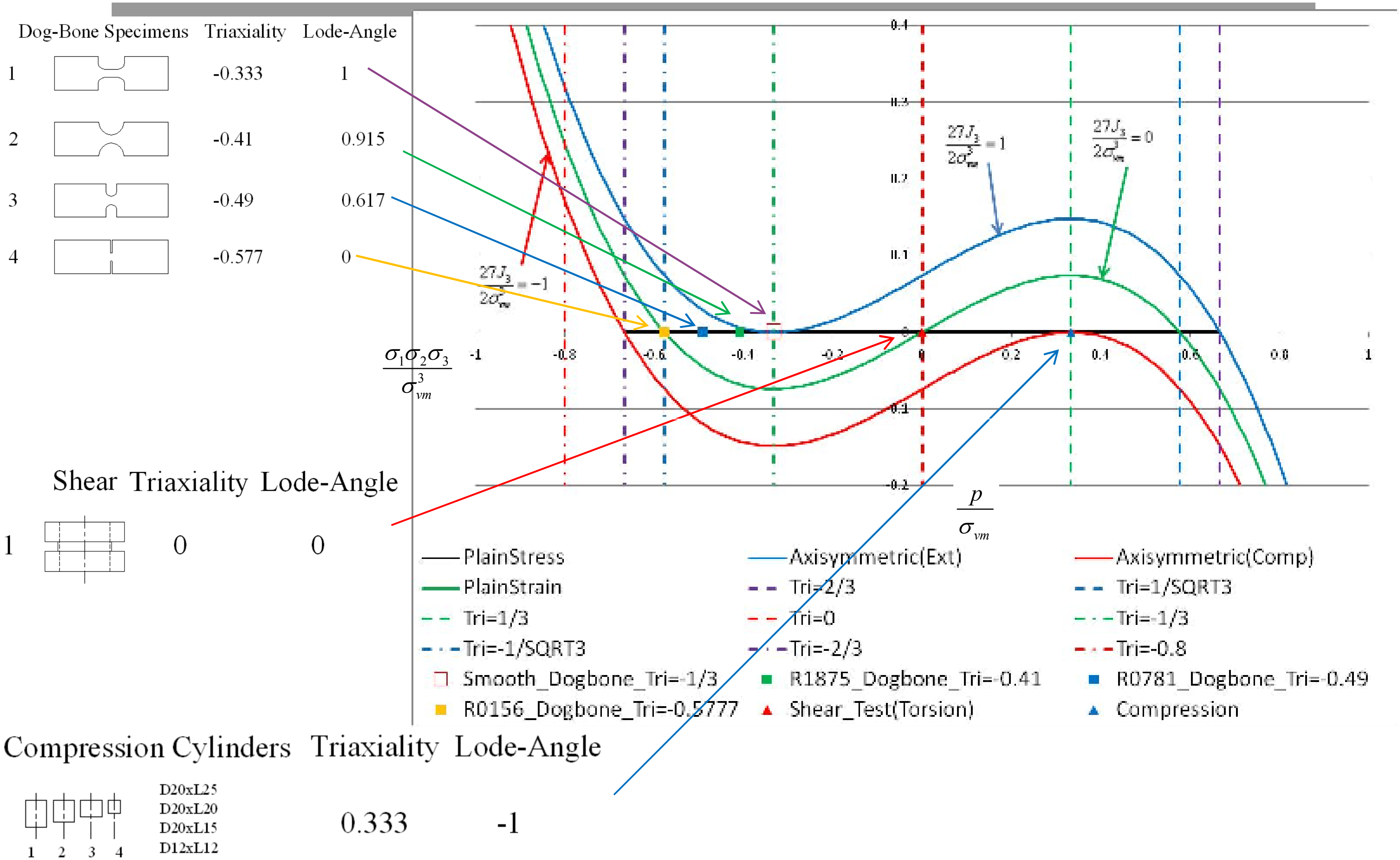
Dog-Bone Specimens Triaxiality Lode-Angle
1 -0.333 1
2 -0.41 0.915
3 -0.49 0.617
4 -0.577 0
Shear Triaxiality Lode-Angle
1 0 0
Compression Cylinders Triaxiality Lode-Angle
D20xL25
D20xL20
D20xL15
D12xL12
1 2 3 4
0.333 -1
$\frac{\sigma_1\sigma_2\sigma_3}{\sigma_{vm}^3}$
$\frac{p}{\sigma_{vm}}$
$\frac{27J_3}{2\sigma_{vm}^3}=-1$
$\frac{27J_3}{2\sigma_{vm}^3}=1$
$\frac{27J_3}{2\sigma_{vm}^3}=0$
PlainStress
Axisymmetric(Ext)
Axisymmetric(Comp)
PlainStrain
Tri=2/3
Tri=1/SQRT3
Tri=1/3
Tri=0
Tri=-1/3
Tri=-1/SQRT3
Tri=-2/3
Tri=-0.8
Smooth_Dogbone_Tri=-1/3
R1875_Dogbone_Tri=-0.41
R0781_Dogbone_Tri=-0.49
R0156_Dogbone_Tri=-0.5777
Shear_Test(Torsion)
Compression

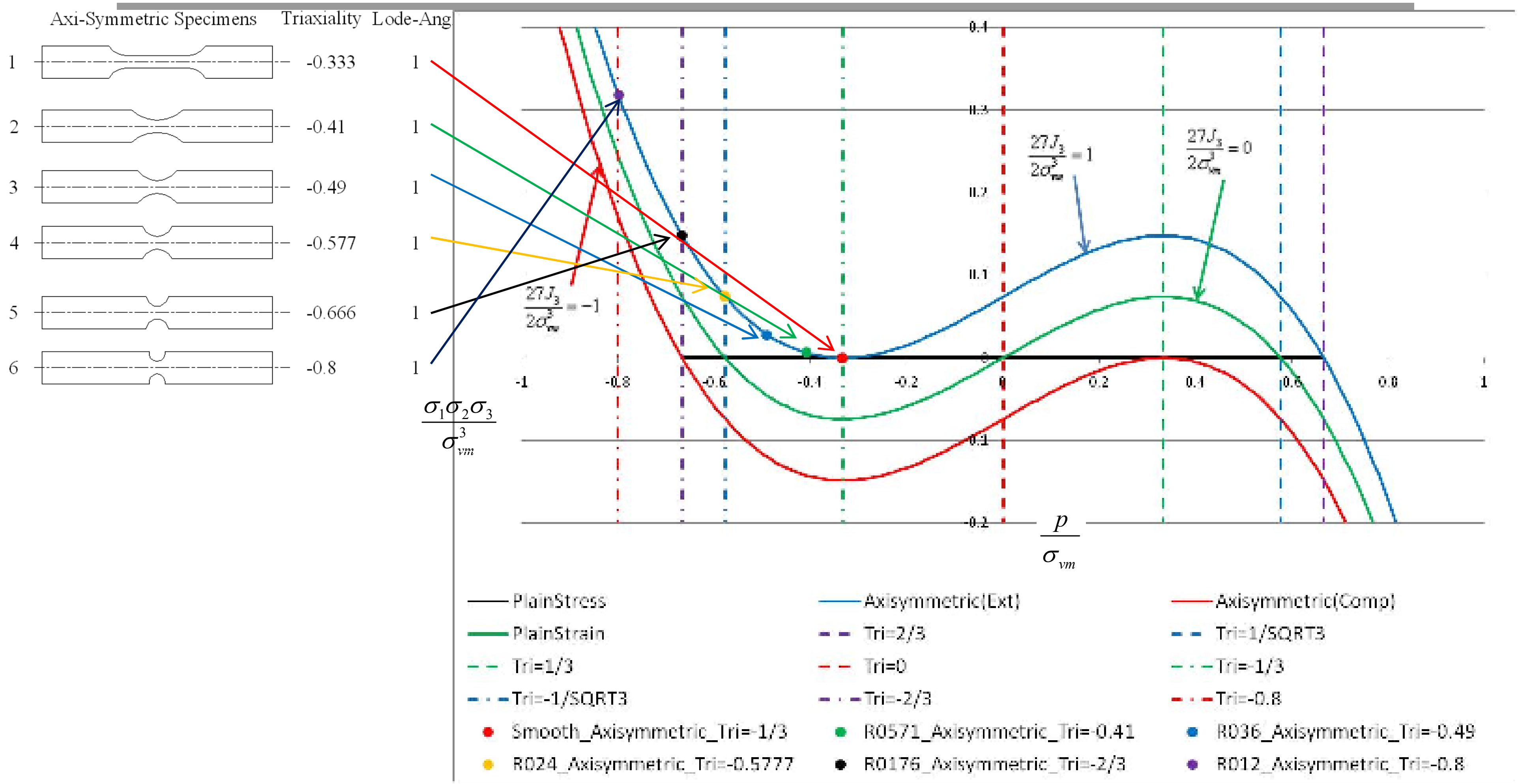

Axi-Symmetric Specimens
Triaxiality
Lode-Ang
1 -0.333 1
2 -0.41 1
3 -0.49 1
4 -0.577 1
5 -0.666 1
6 -0.8 1
$\frac{\sigma_1\sigma_2\sigma_3}{\sigma_{vm}^3}$
$\frac{p}{\sigma_{vm}}$
$\frac{27J_3}{2\sigma_{vm}^3}=1$
$\frac{27J_3}{2\sigma_{vm}^3}=0$
$\frac{27J_3}{2\sigma_{vm}^3}=-1$
PlainStress
Axisymmetric(Ext)
Axisymmetric(Comp)
PlainStrain
Tri=2/3
Tri=1/SQRT3
Tri=1/3
Tri=0
Tri=-1/3
Tri=-1/SQRT3
Tri=-2/3
Tri=-0.8
Smooth_Axisymmetric_Tri=-1/3
R0571_Axisymmetric_Tri=-0.41
R036_Axisymmetric_Tri=-0.49
R024_Axisymmetric_Tri=-0.5777
R0176_Axisymmetric_Tri=-2/3
R012_Axisymmetric_Tri=-0.8

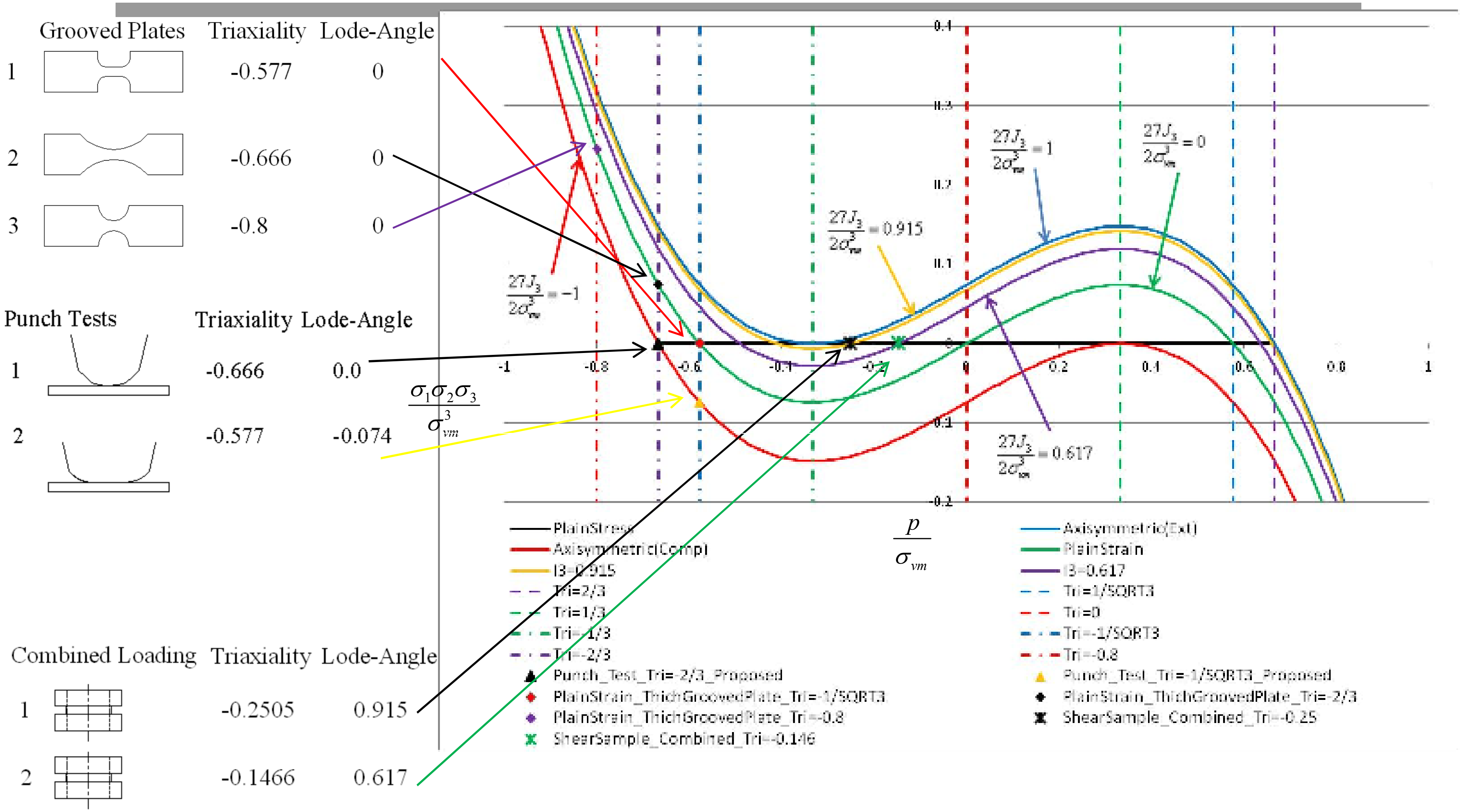

Grooved Plates
Triaxiality
Lode-Angle
1 -0.577 0
2 -0.666 0
3 -0.8 0
Punch Tests
Triaxiality
Lode-Angle
1 -0.666 0.0
2 -0.577 -0.074
Combined Loading
Triaxiality
Lode-Angle
1 -0.2505 0.915
2 -0.1466 0.617
$\frac{\sigma_1\sigma_2\sigma_3}{\sigma_{vm}^3}$
$\frac{p}{\sigma_{vm}}$
$\frac{27J_3}{2\sigma_{vm}^3} = -1$
$\frac{27J_3}{2\sigma_{vm}^3} = 0.915$
$\frac{27J_3}{2\sigma_{vm}^3} = 1$
$\frac{27J_3}{2\sigma_{vm}^3} = 0$
$\frac{27J_3}{2\sigma_{vm}^3} = 0.617$
PlainStress
Axisymmetric(Comp)
I3=0.915
Tri=2/3
Tri=1/3
Tri=-1/3
Tri=-2/3
Punch_Test_Tri=-2/3_Proposed
PlainStrain_ThichGroovedPlate_Tri=-1/SQRT3
PlainStrain_ThichGroovedPlate_Tri=-0.8
ShearSample_Combined_Tri=-0.146
Axisymmetric(Ext)
PlainStrain
I3=0.617
Tri=1/SQRT3
Tri=0
Tri=-1/SQRT3
Tri=-0.8
Punch_Test_Tri=-1/SQRT3_Proposed
PlainStrain_ThichGroovedPlate_Tri=-2/3
ShearSample_Combined_Tri=-0.25

~Lode	1	0.915	0.617	0	-1
~Triaxiality					
-0.8	Cylinder G6			Grooved Plate G3	
-0.666	Cylinder G5			Grooved Plate G2	Punch 1
-0.577	Cylinder G4			Dogbone G4 Grooved Plate G1	Punch 4
0.49	Cylinder G3		Dogbone G3		
-0.41	Cylinder G2	Dogbone G2			
-0.333	Cylinder G1 Dogbone G1				
-0.2505		Tension/Torsion			
-0.1466			Tension/Torsion		
0				Torsion Punch 6	
0.333					Compression

Spline-4

Spline-1

Free Points

Spline-2

Spline-3

Plane stress Failure criterion for Aluminium 2024

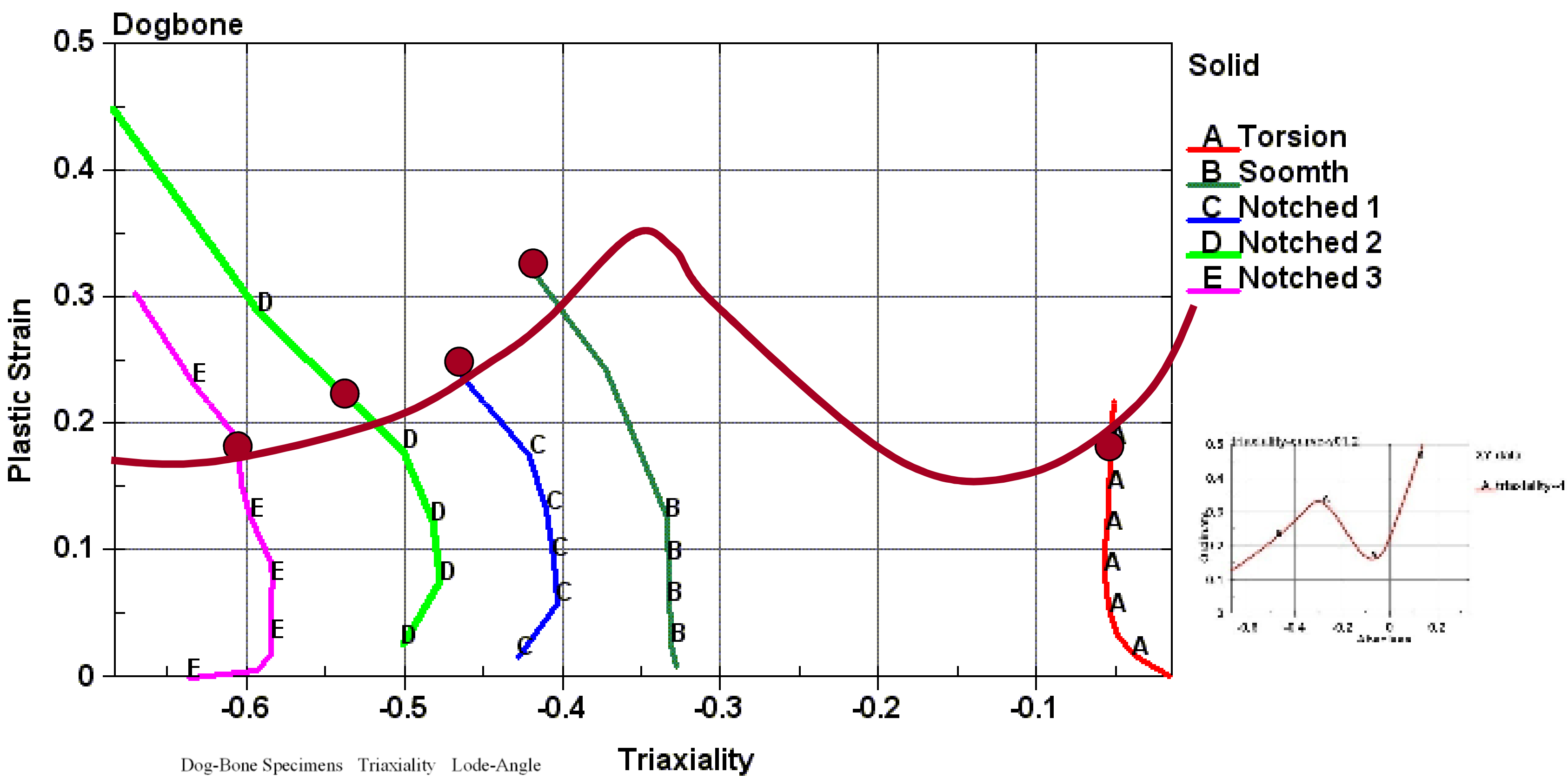

Dog-Bone Specimens	Triaxiality	Lode-Angle
1	-0.333	1
2	-0.41	0.915
3	-0.49	0.617
4	-0.577	0

Combined Loading	Triaxiality	Lode-Angle
1	-0.2505	0.915
2	-0.1466	0.617

Shear	Triaxiality	Lode-Angle
1	0	0

Plane stress Failure criterion for Aluminium 2024

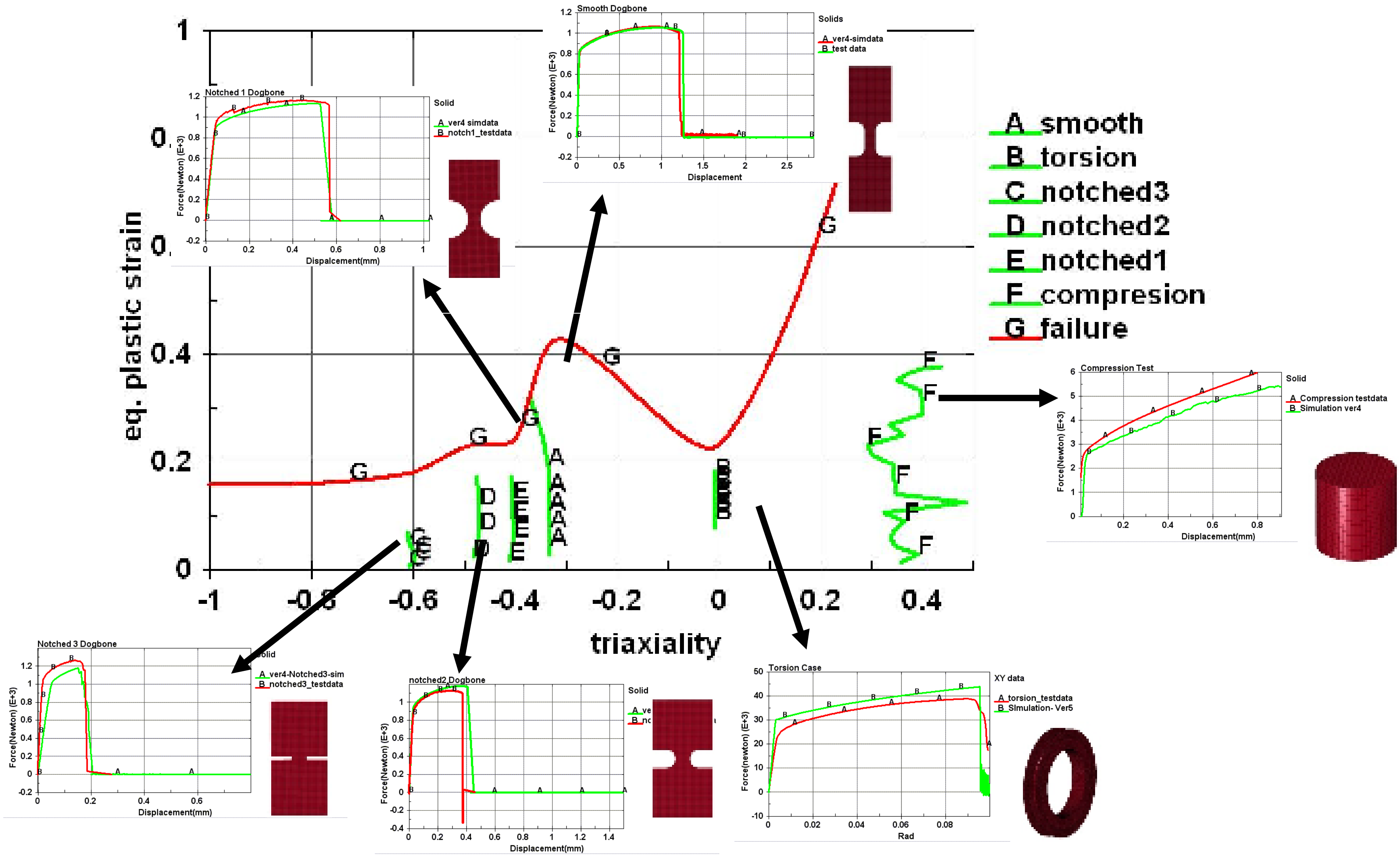

Comparison to JC failure criteria

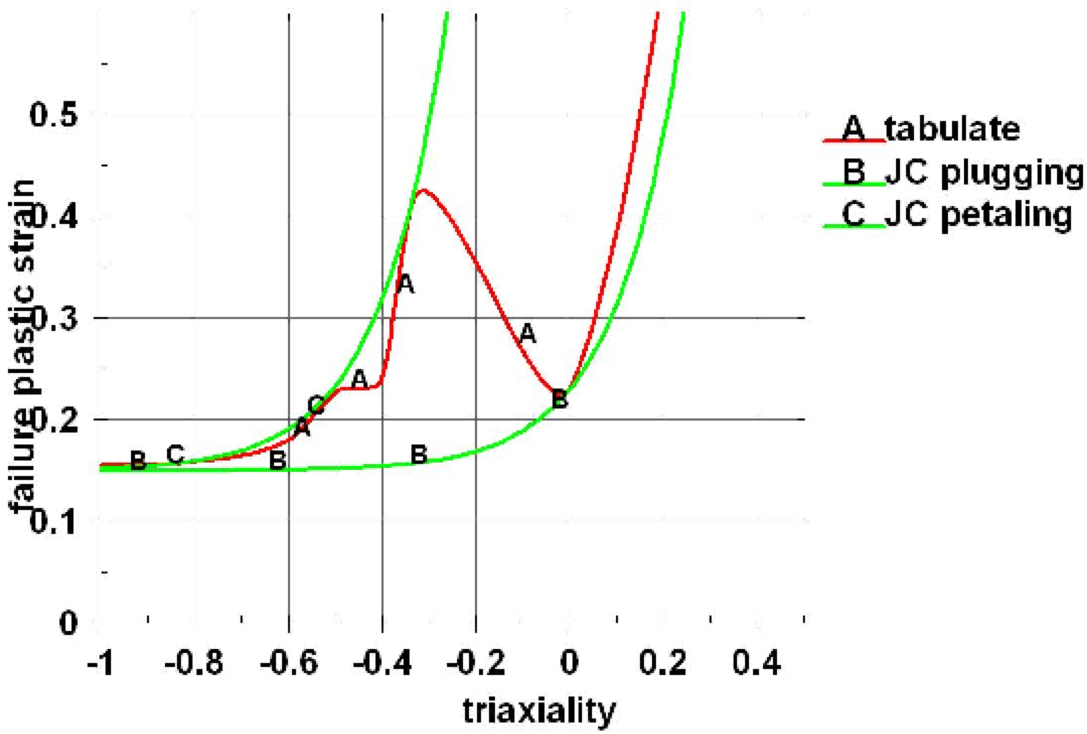

In fact the JC criterion usually cannot handle petaling (tensile) and plugging (shear) failure simultaneously

Example of AL2024, the physical failure criterion is more complex then JC

Basic splines for the 3D failure model

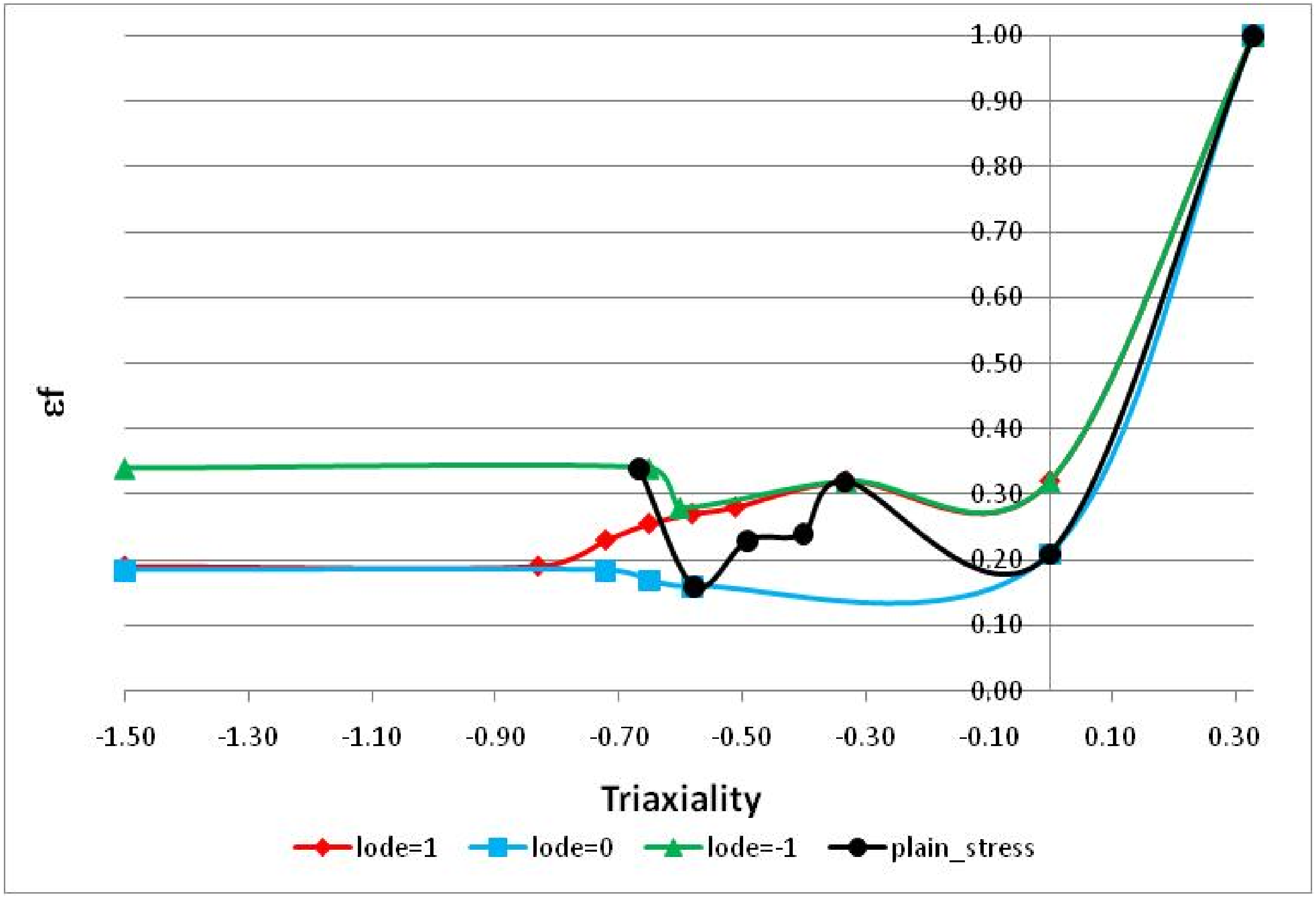

3-D Failure criterion for Aluminium 2024

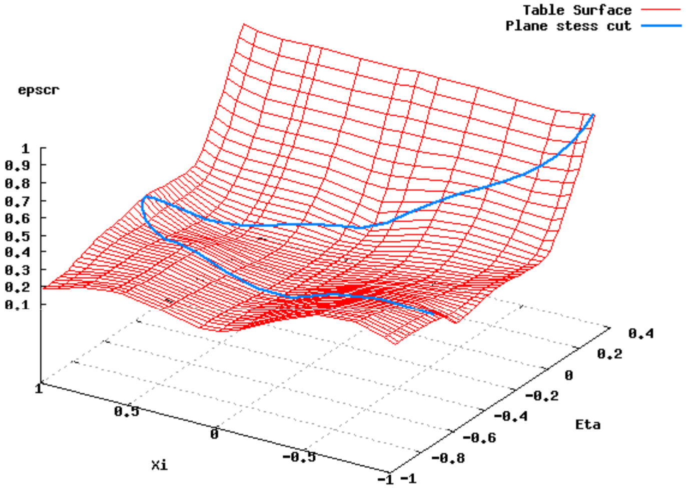

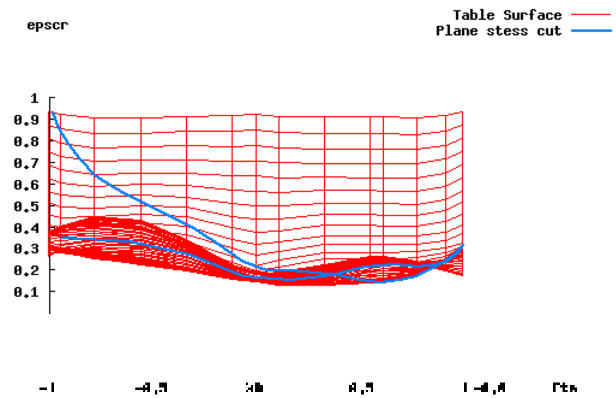

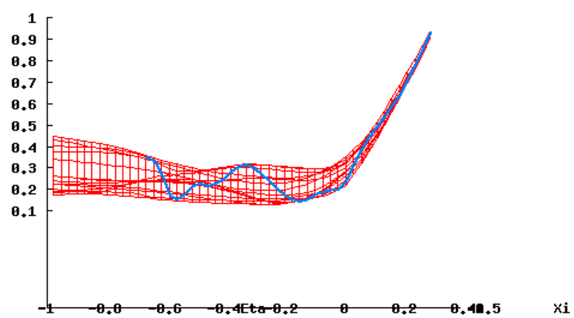

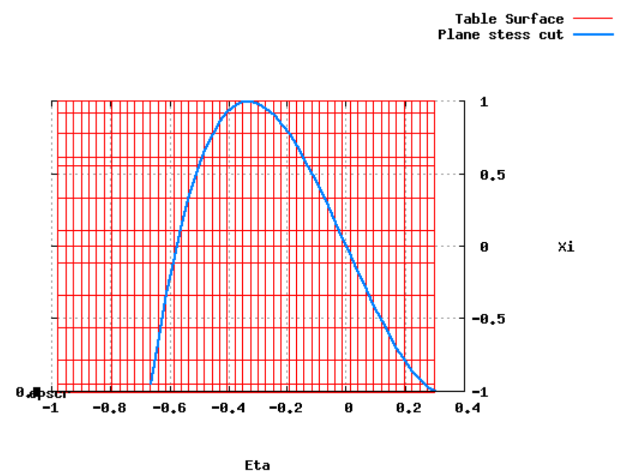

Development, Implementation and Validation of 3-D Failure Model for Aluminium 2024

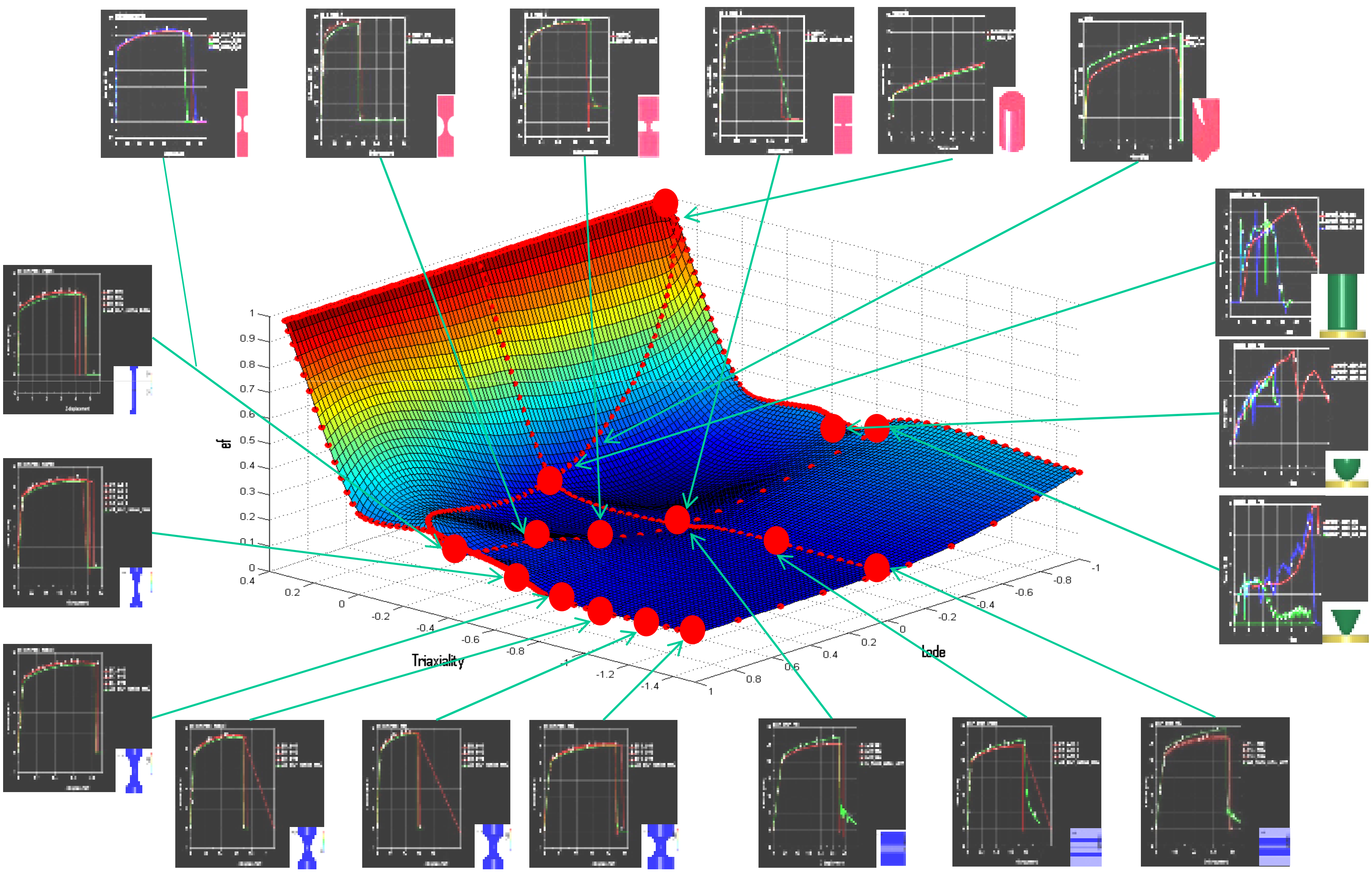

Part 3 :

DYNAMIC PUNCH TESTS
BALLISTIC TESTS

Dynamic punch testing on the SHB

- Controlled dynamic testing is performed on a SHB to examine failure of Aluminium 2024 before assessing the ballistic testing by NASA
- SHB at OSU is used for dynamic punch testing at 20 m/s using different punch shapes and a circular sample with D=14.56 mm and t=1.456 mm (10%)
- 3 different punch shapes were selected
- these tests allow validation of the failure criteria determined from quasistatic testing on samples with different shapes
- also failure criterion can be extended to states of stress lying on the compressive meridian
- crack patterns corresponding to different failure modes (petaling, plugging and combined) can be examined
- stop collars were used to arrest the impactor bar at predetermined values of the displacement allowing to study the crack growth in the samples

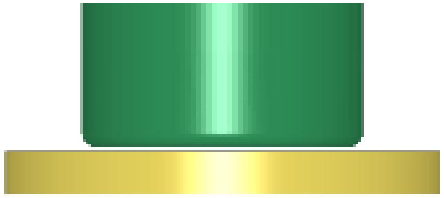

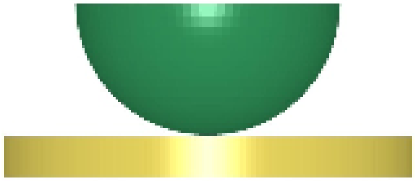

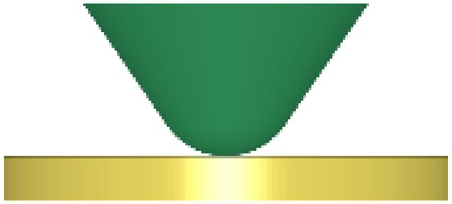

dynamic punch testing on the SHB

Punch 1 Punch 4 Punch 6

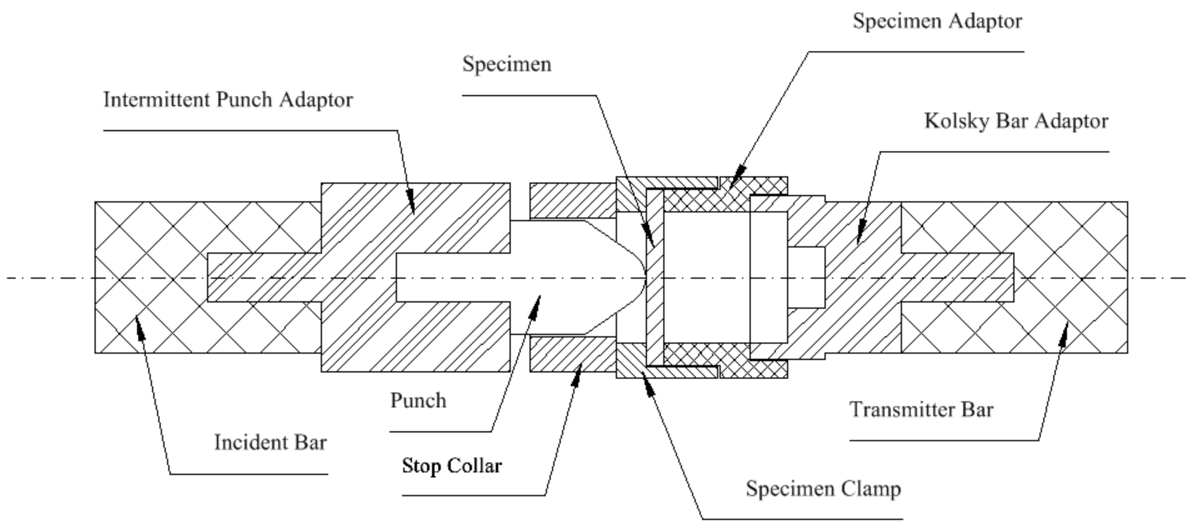

what happens during a punch test ?

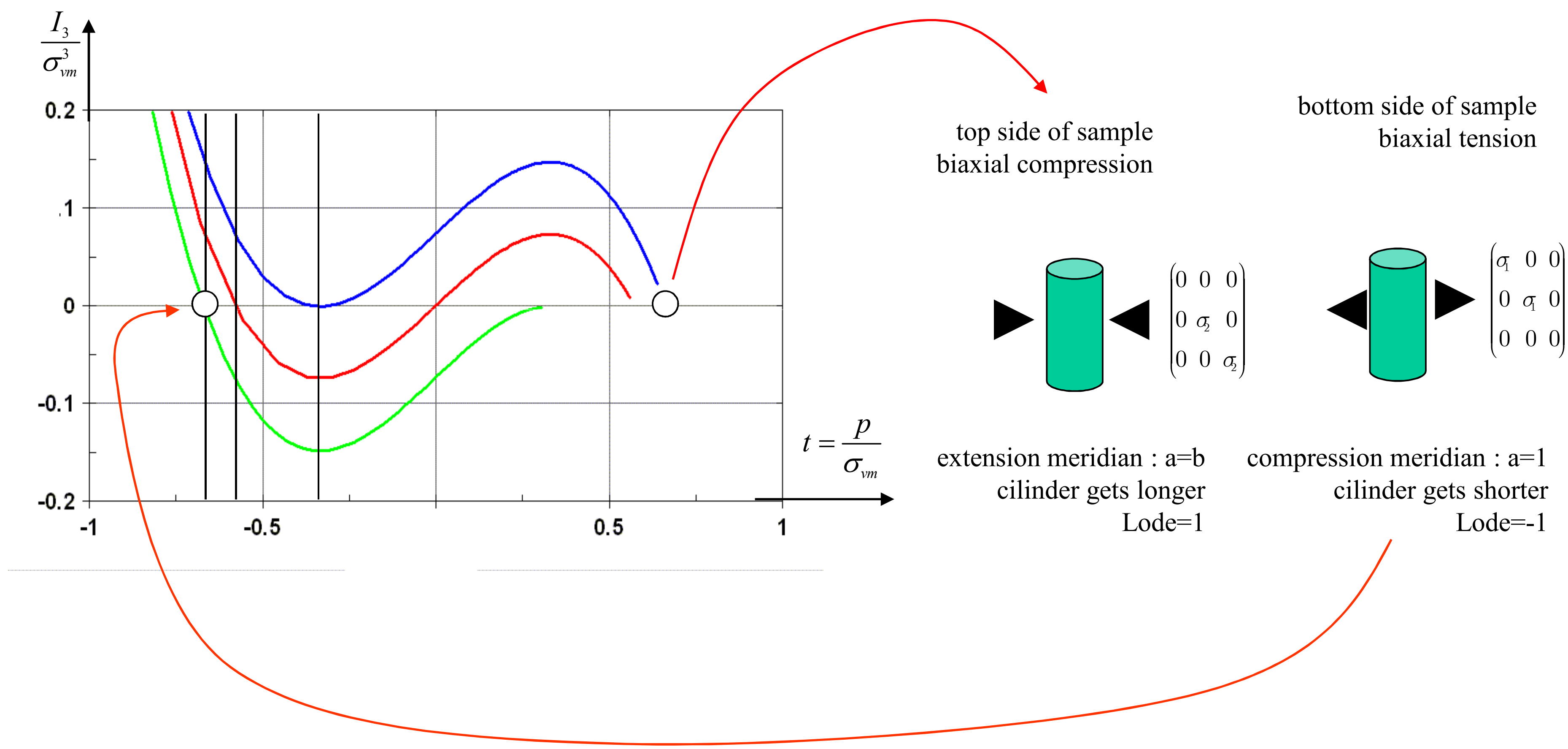

preliminary simulation results : punch 1

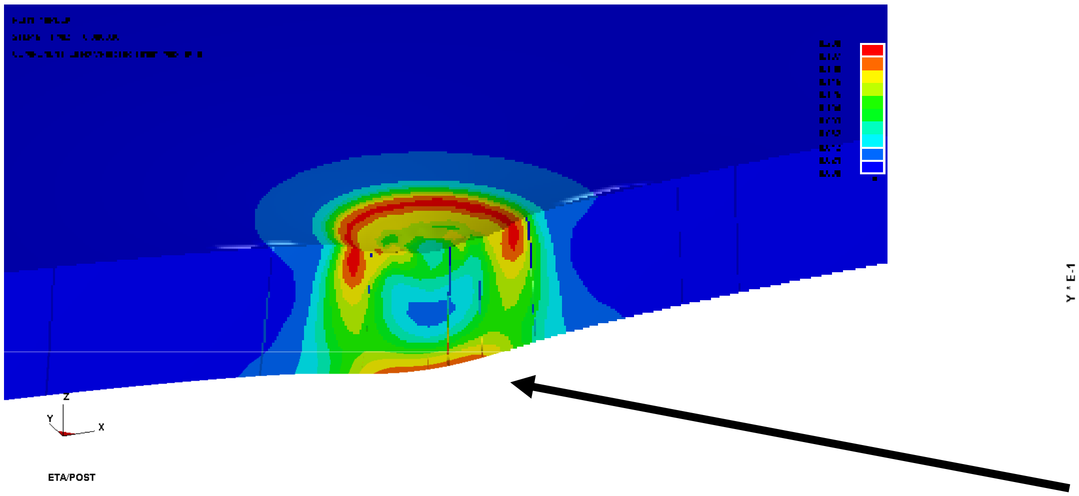

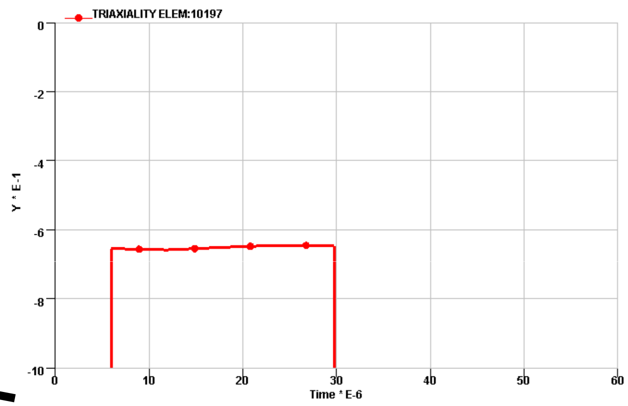

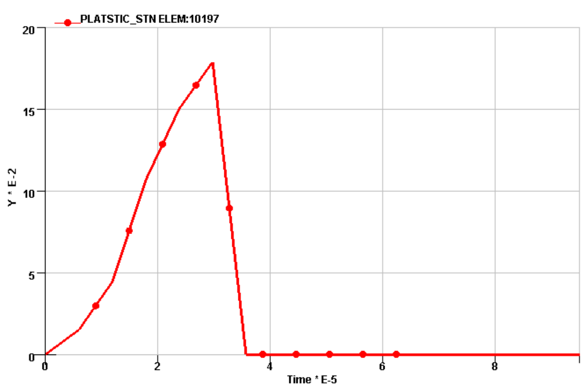

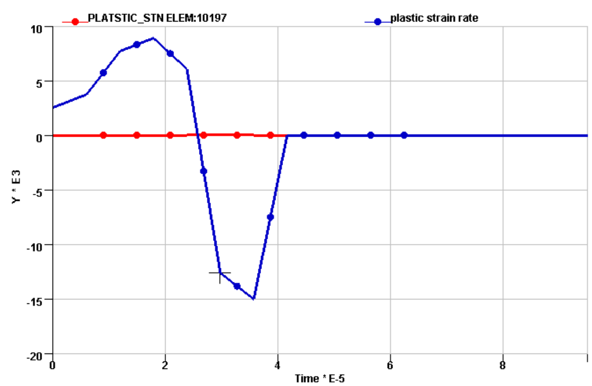

preliminary simulation results : punch 1

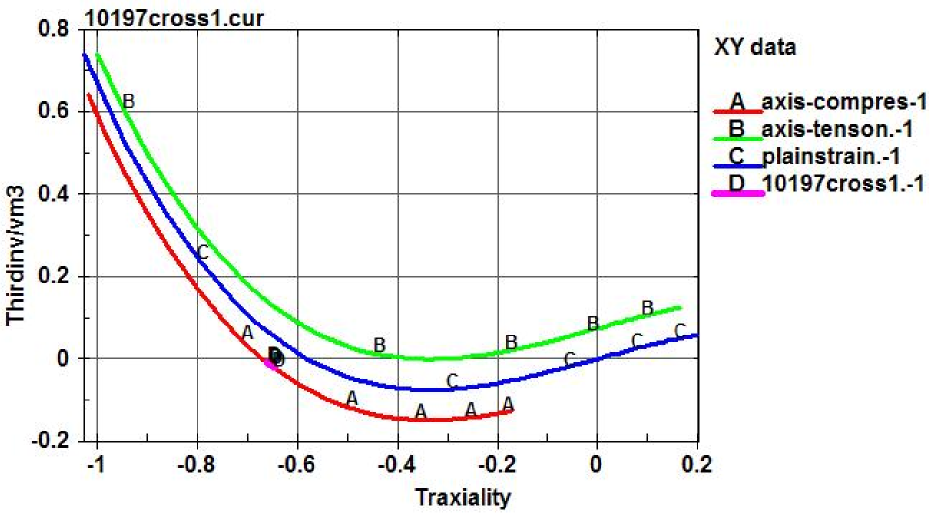

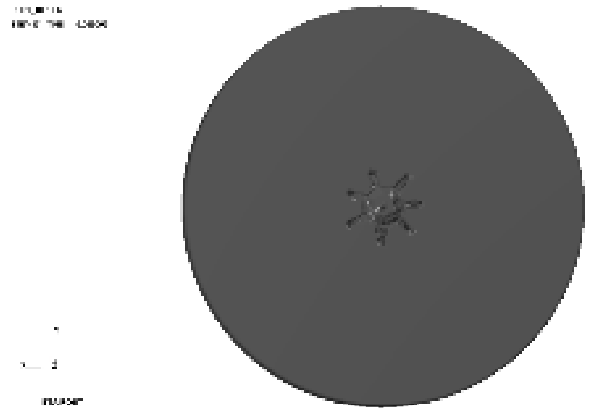

bottom view

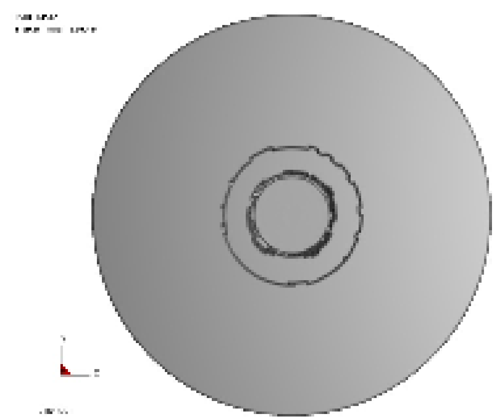

top view

preliminary simulation results : punch 4

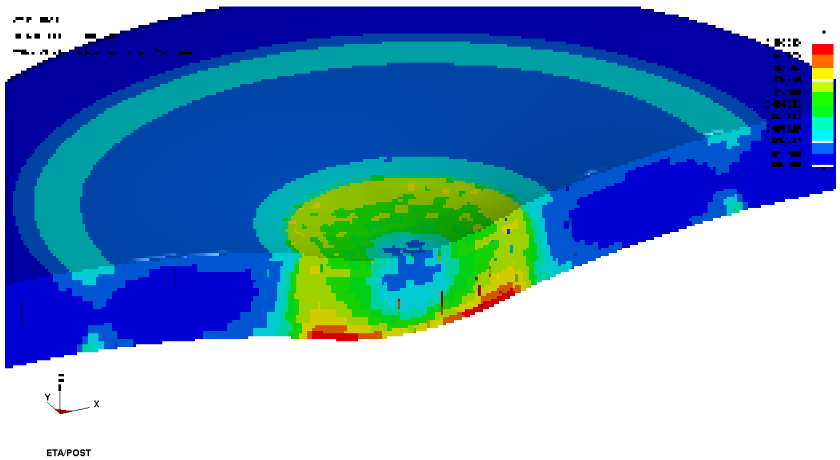

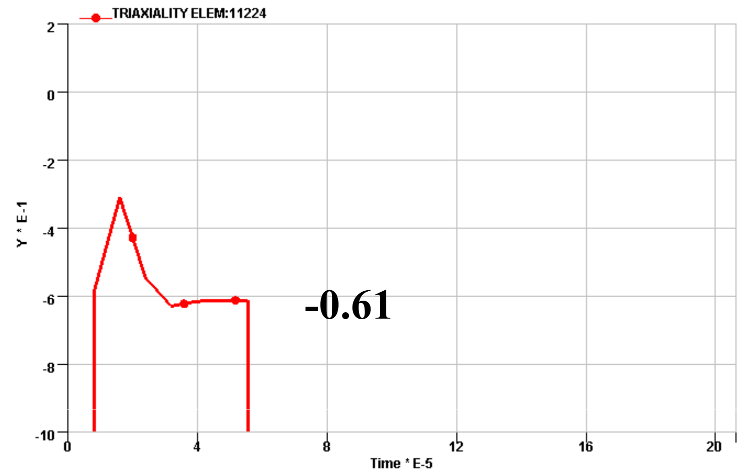

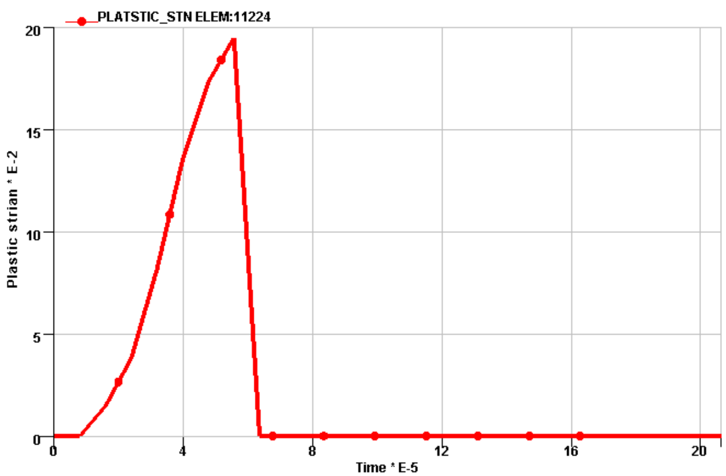

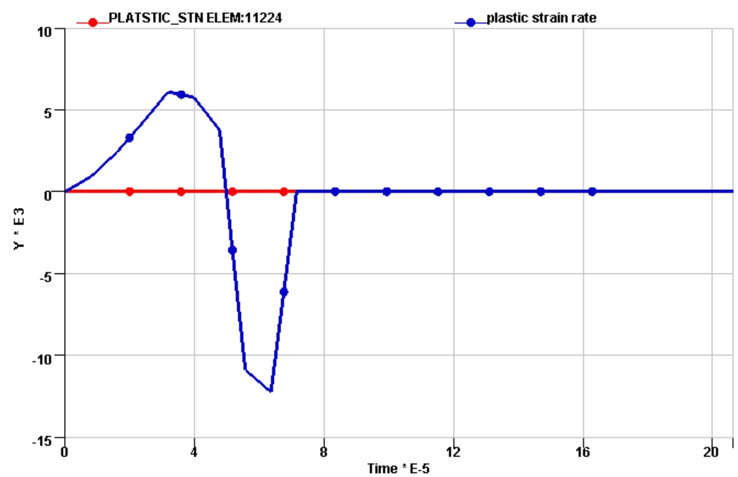

preliminary simulation results : punch 4

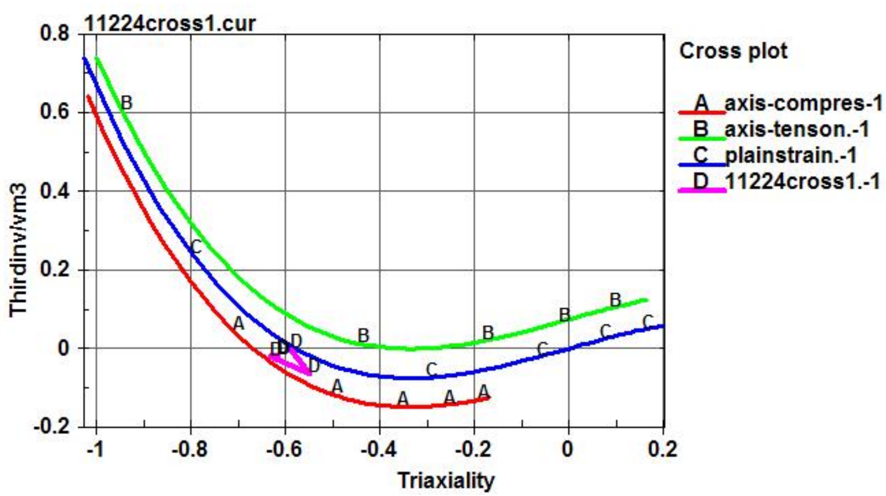

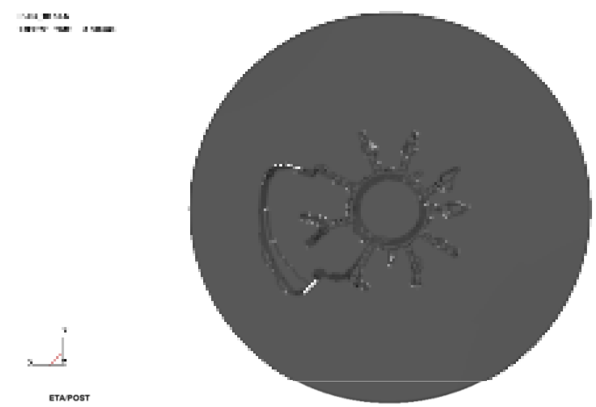

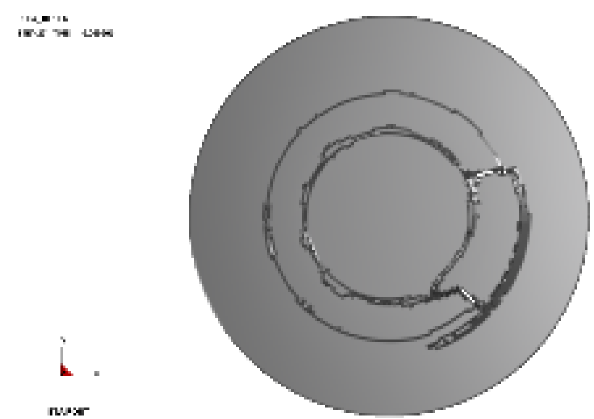

preliminary simulation results : punch 6

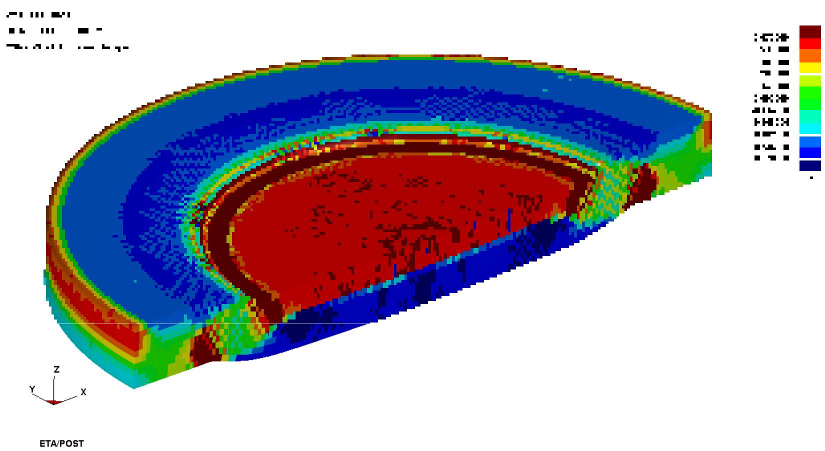

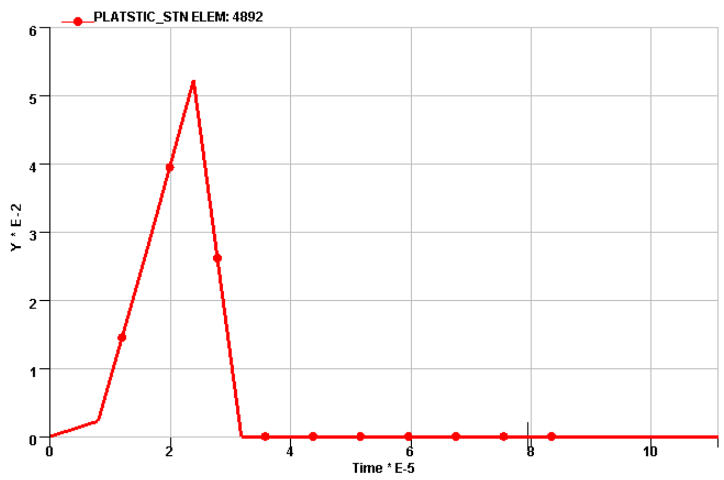

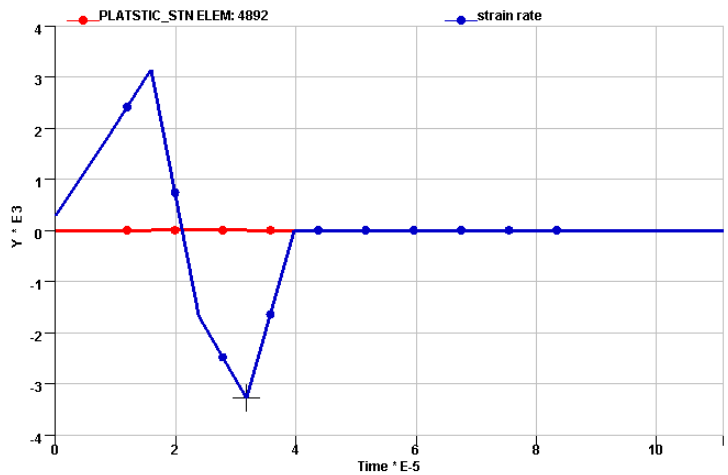

preliminary simulation results : punch 6

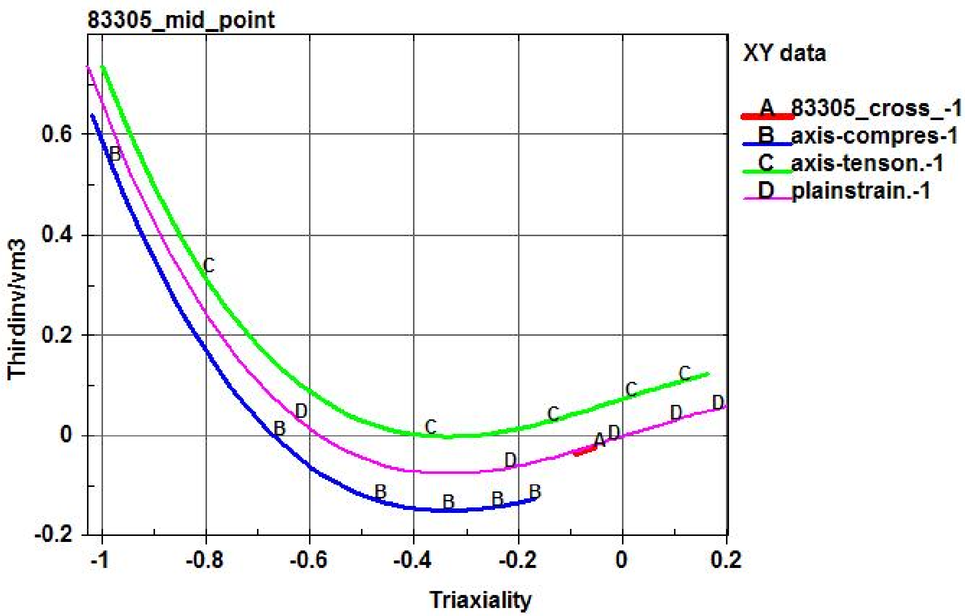

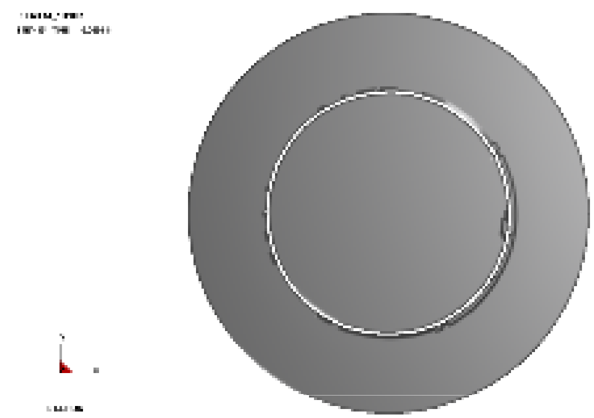

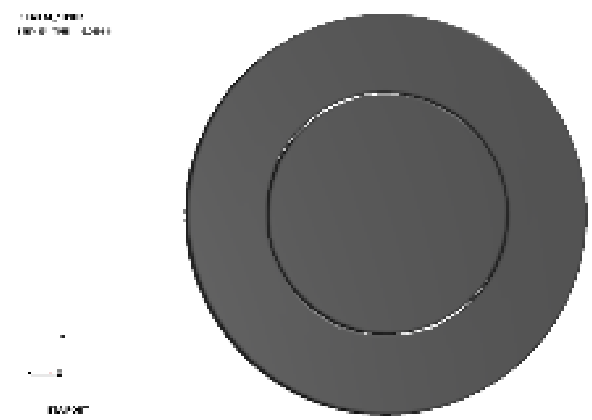

Comparison to SHB test results : 1mm displacement

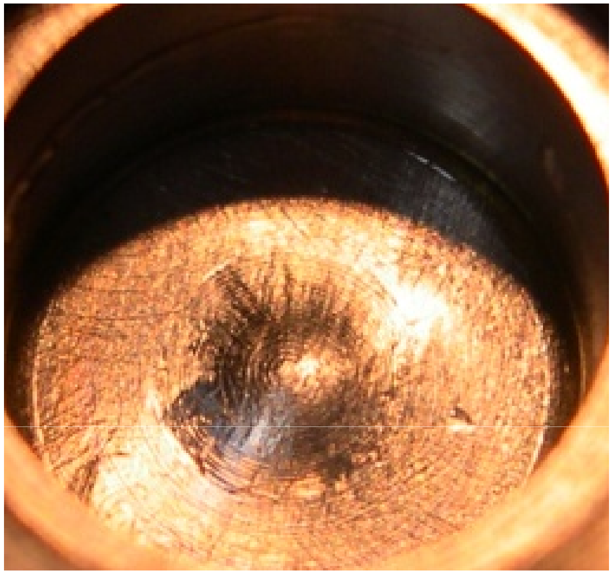

bottom no cracks yet top

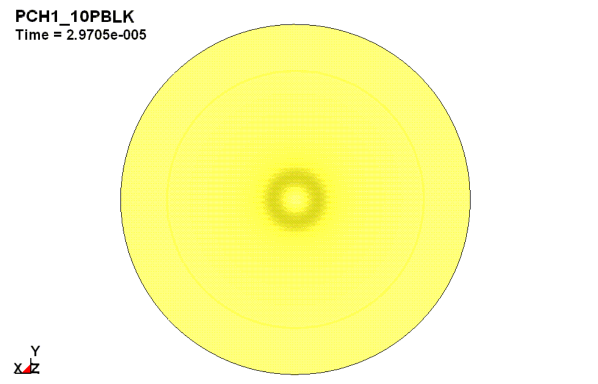

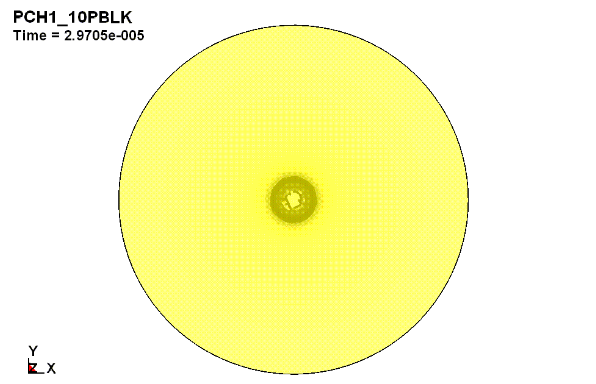

Comparison to SHB test results : 1.7mm displacement

circumferential crack at bottom side

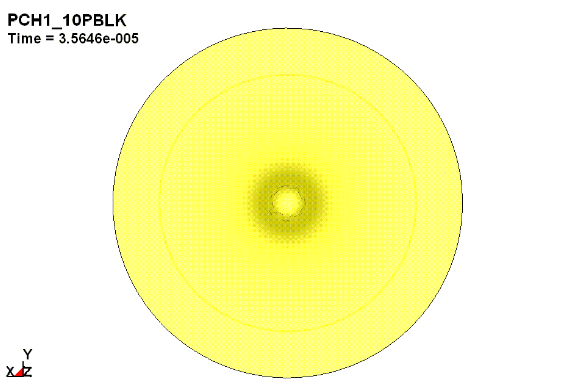

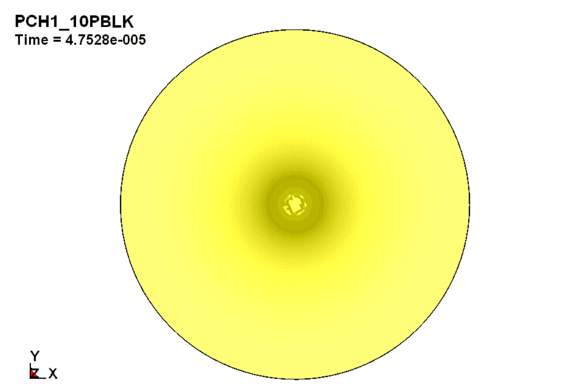

Comparison to SHB test results : 2.4mm displacement

radial cracks also appear at the bottom side

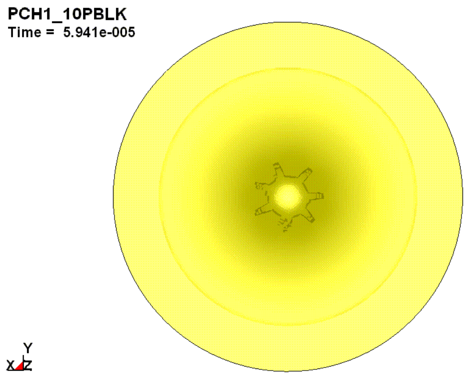

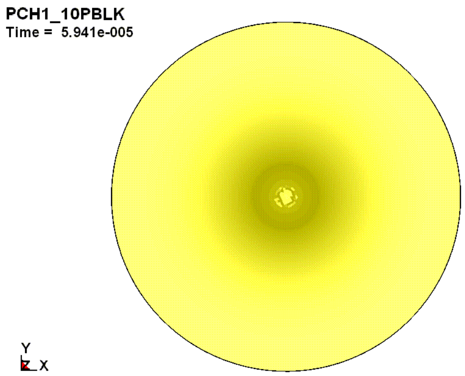

animated simulation results

Comparison to SHB test results : 2.4mm displacement

radial cracks also appear at the bottom side

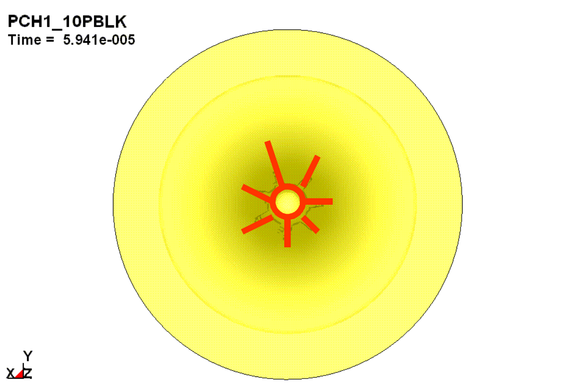

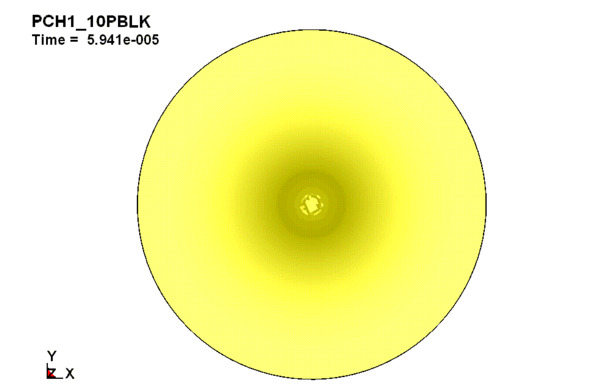

Punch #1 - Dynamic

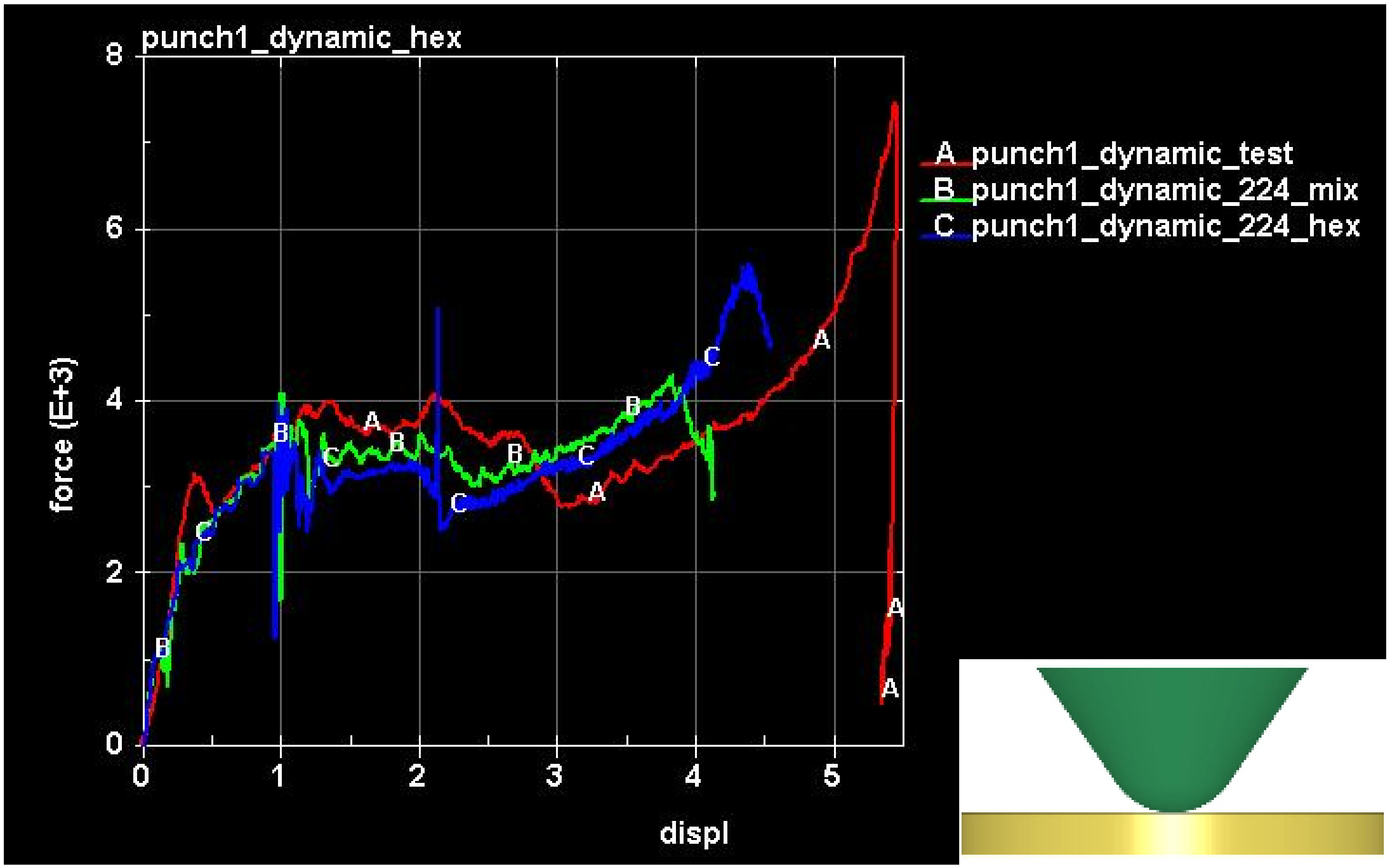

Punch #1

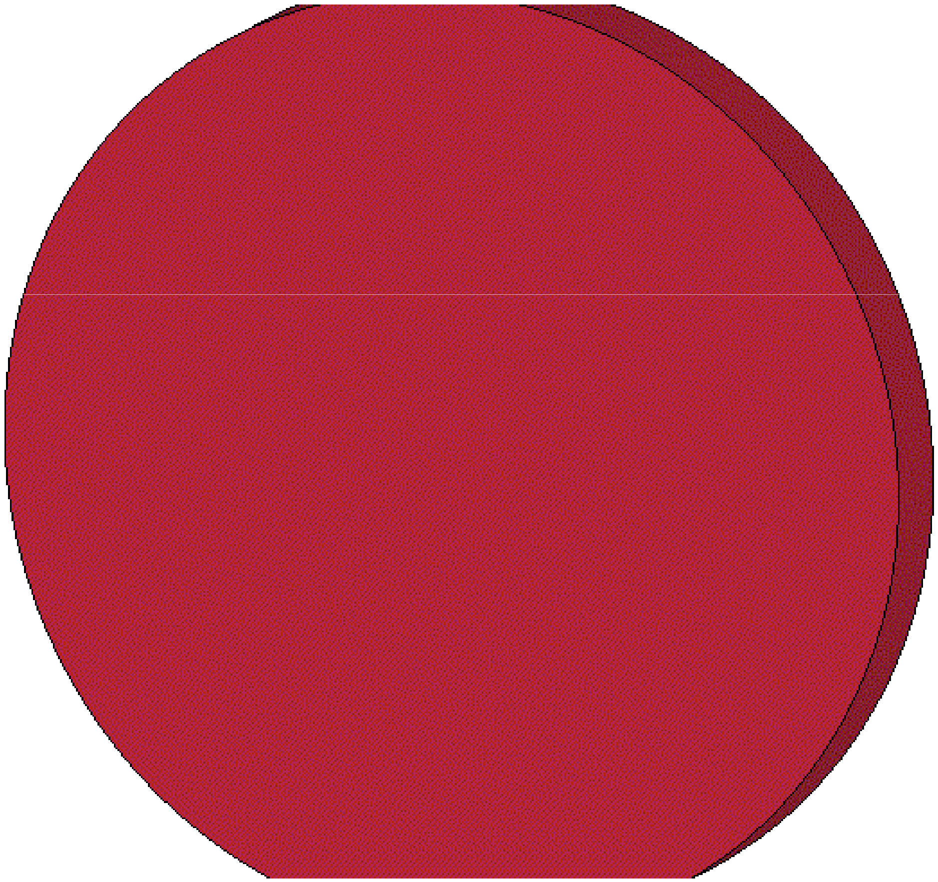

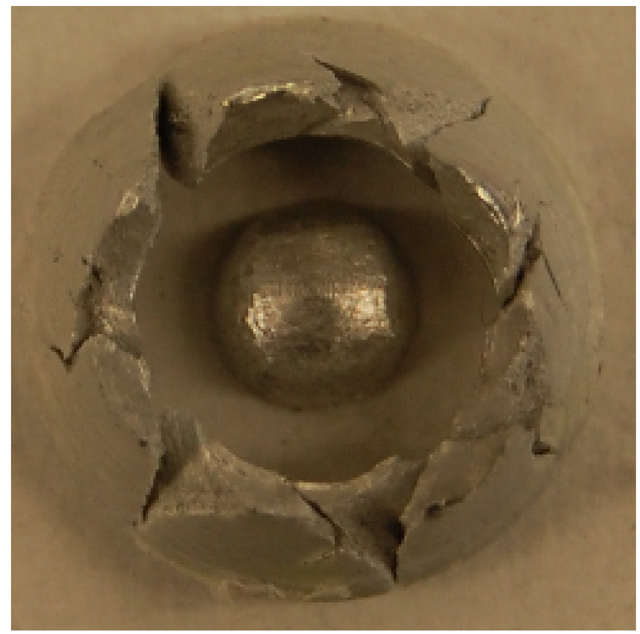

Punch #1 - Static

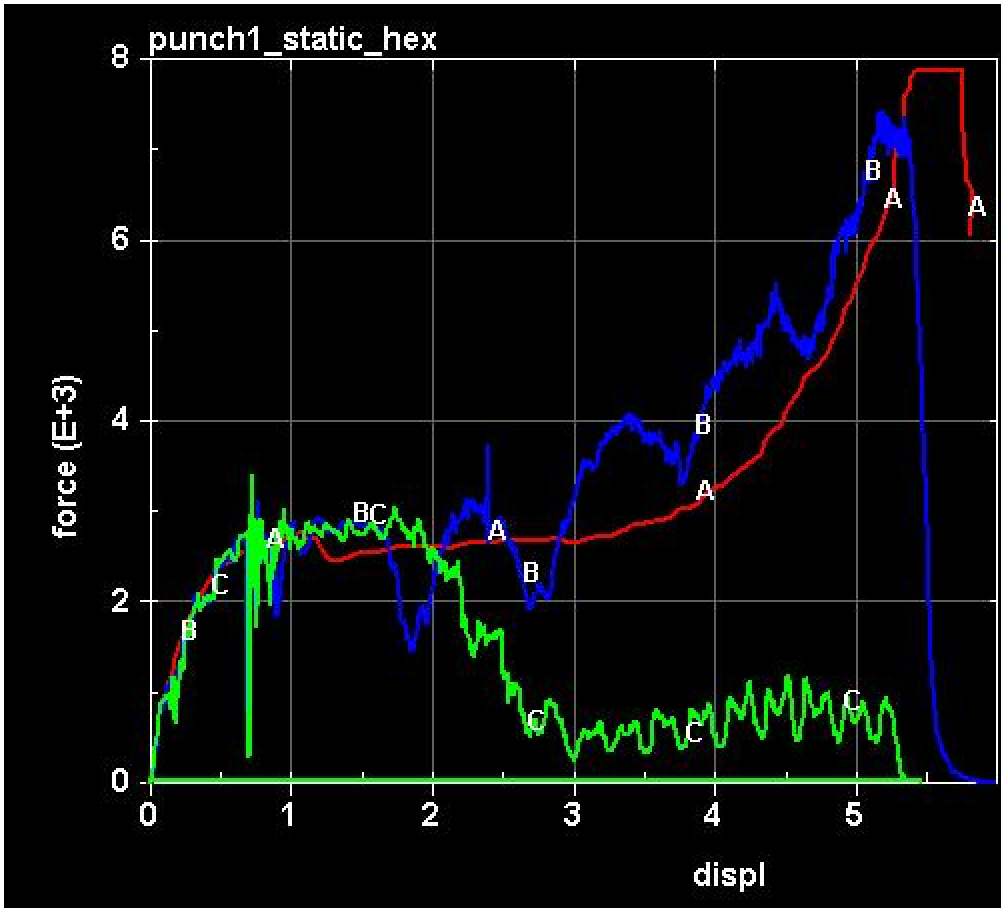

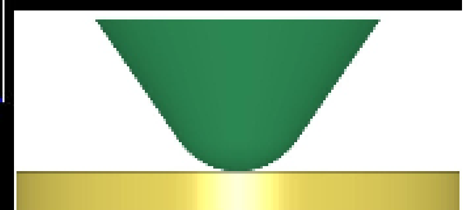

Punch #4 - Dynamic

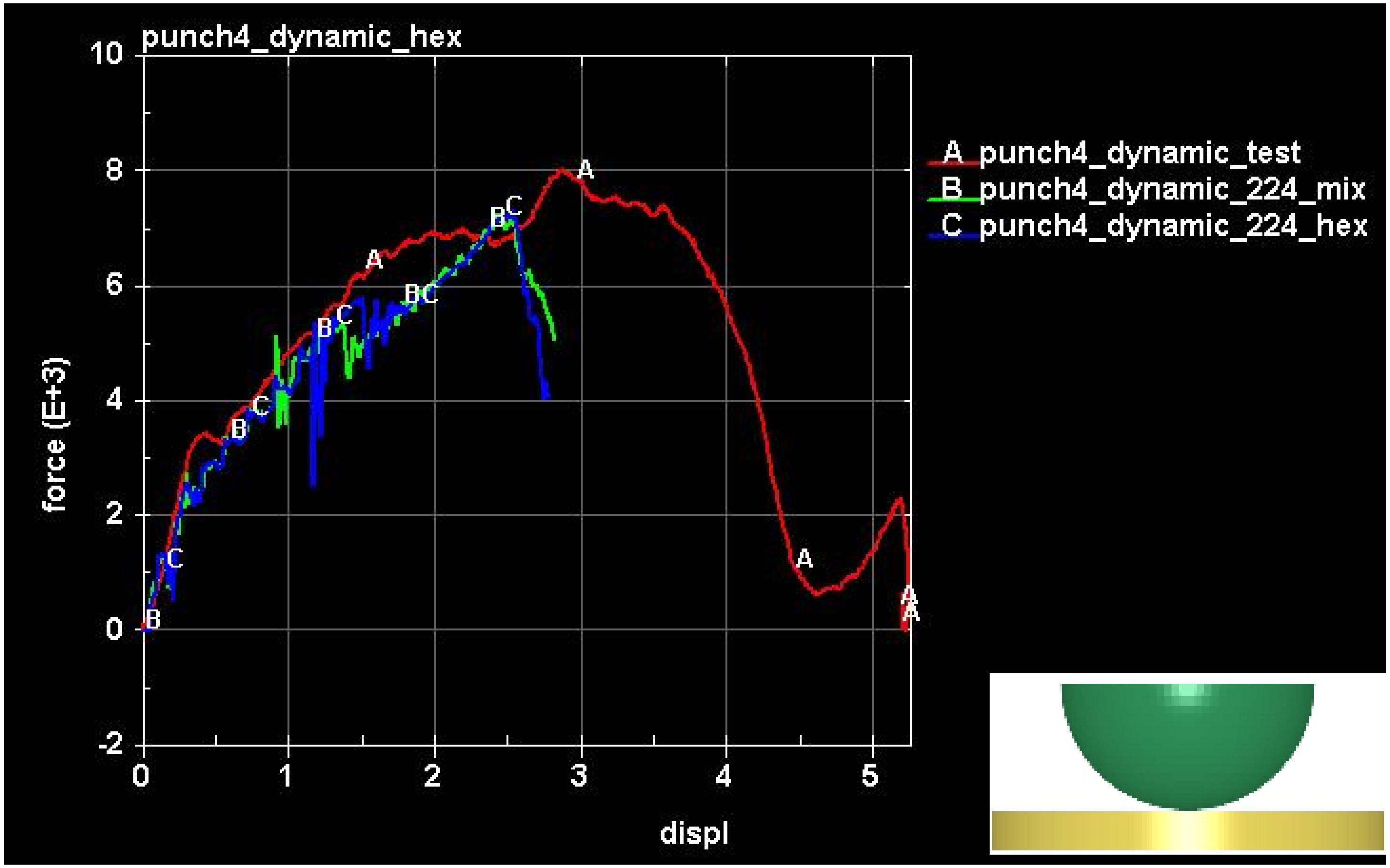

Punch #4

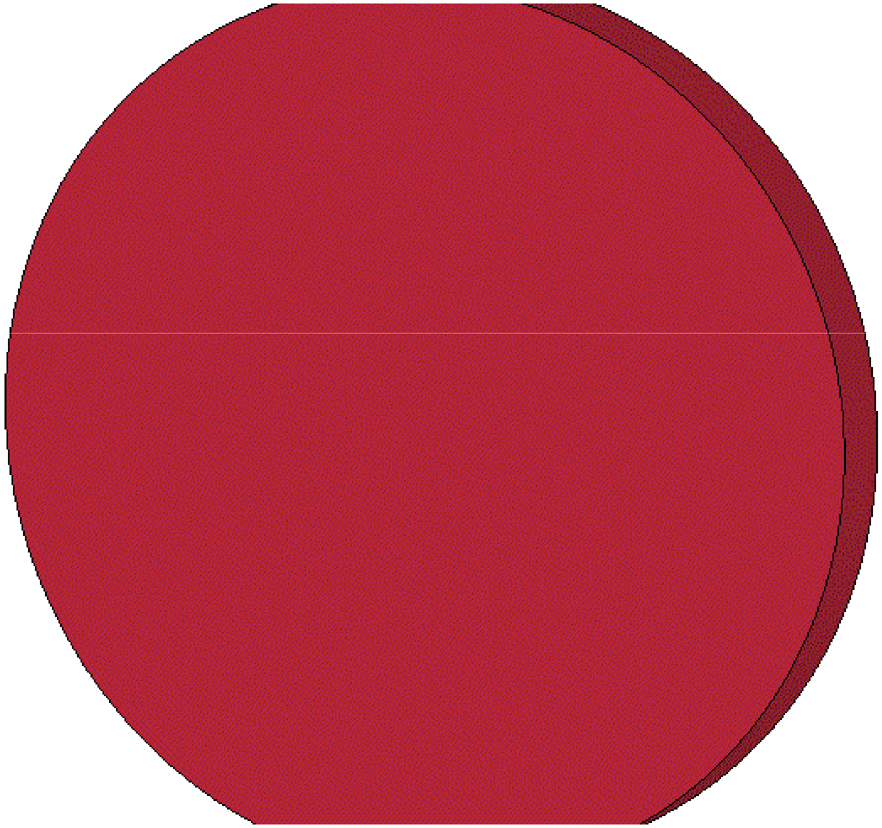

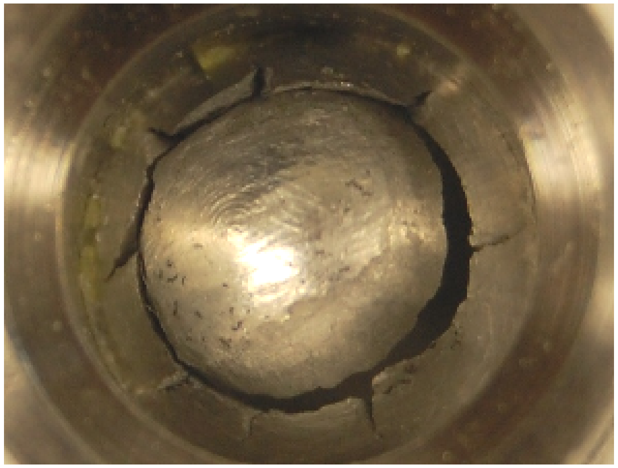

Punch #4 - Static

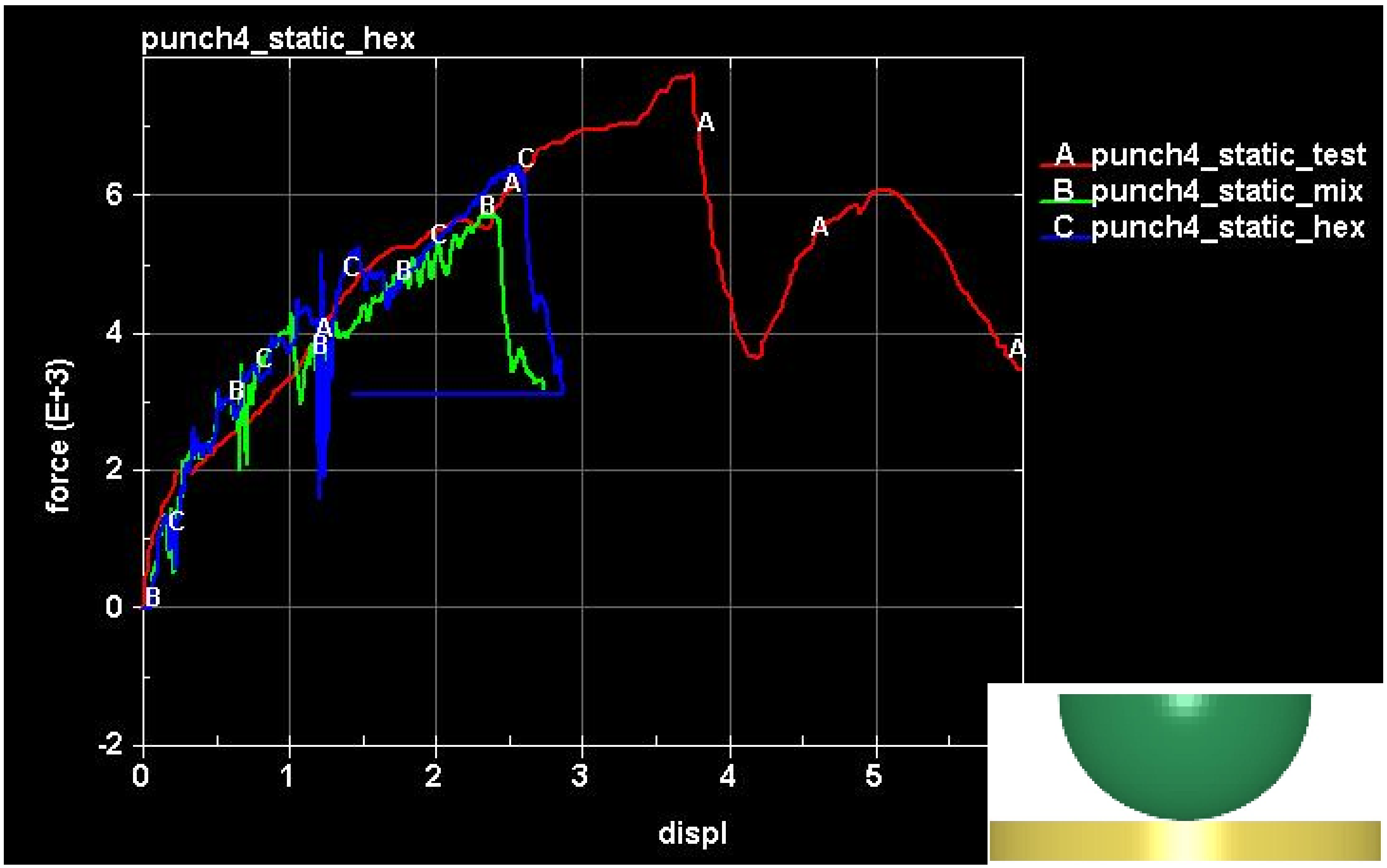

Punch #6 - Dynamic

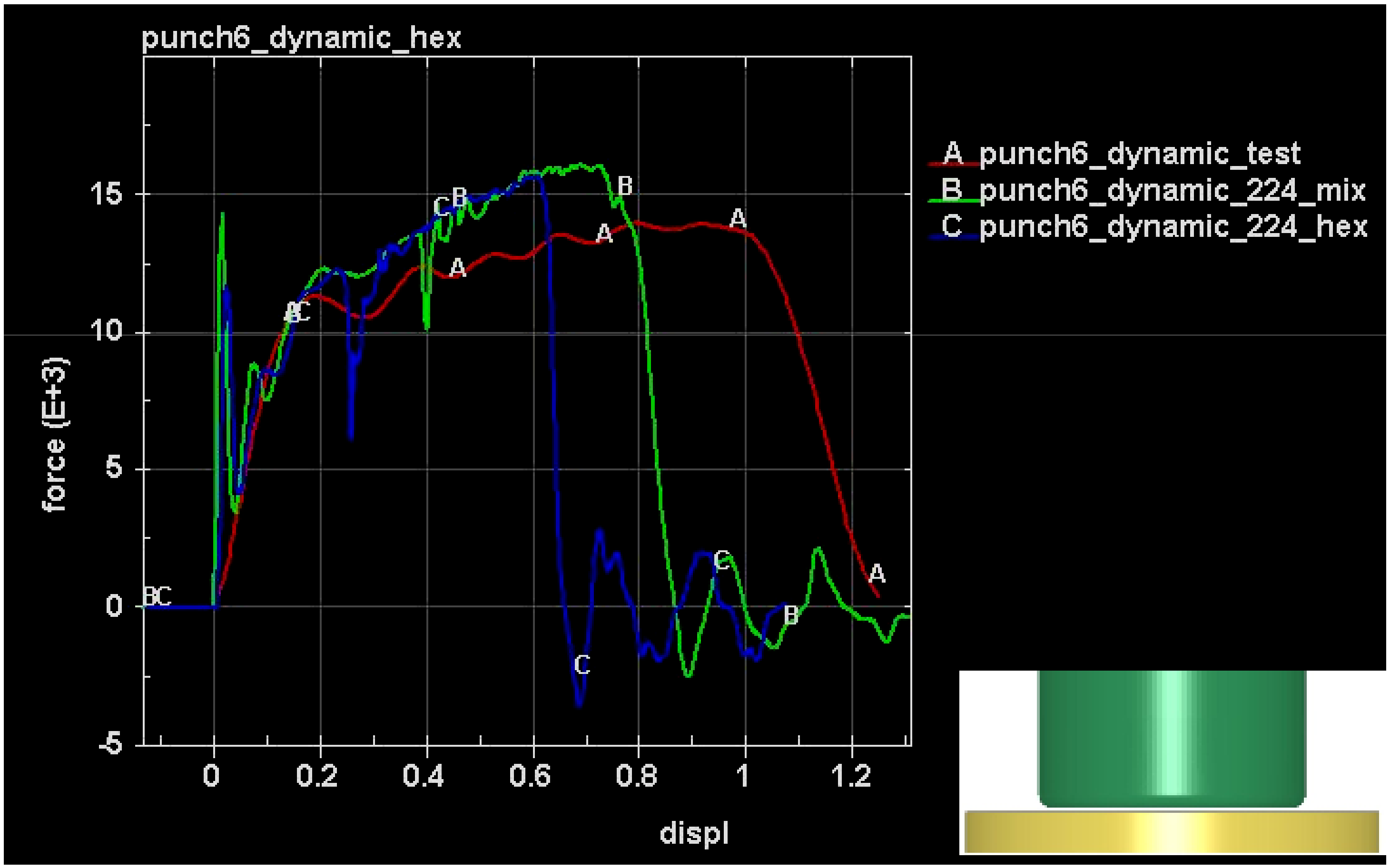

Punch #6

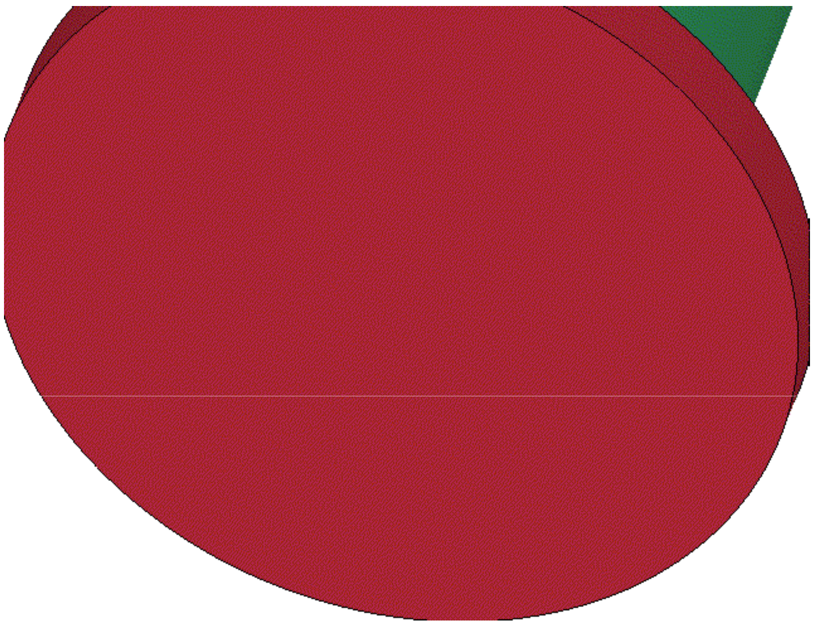

Punch Side

Punch #6 - Static

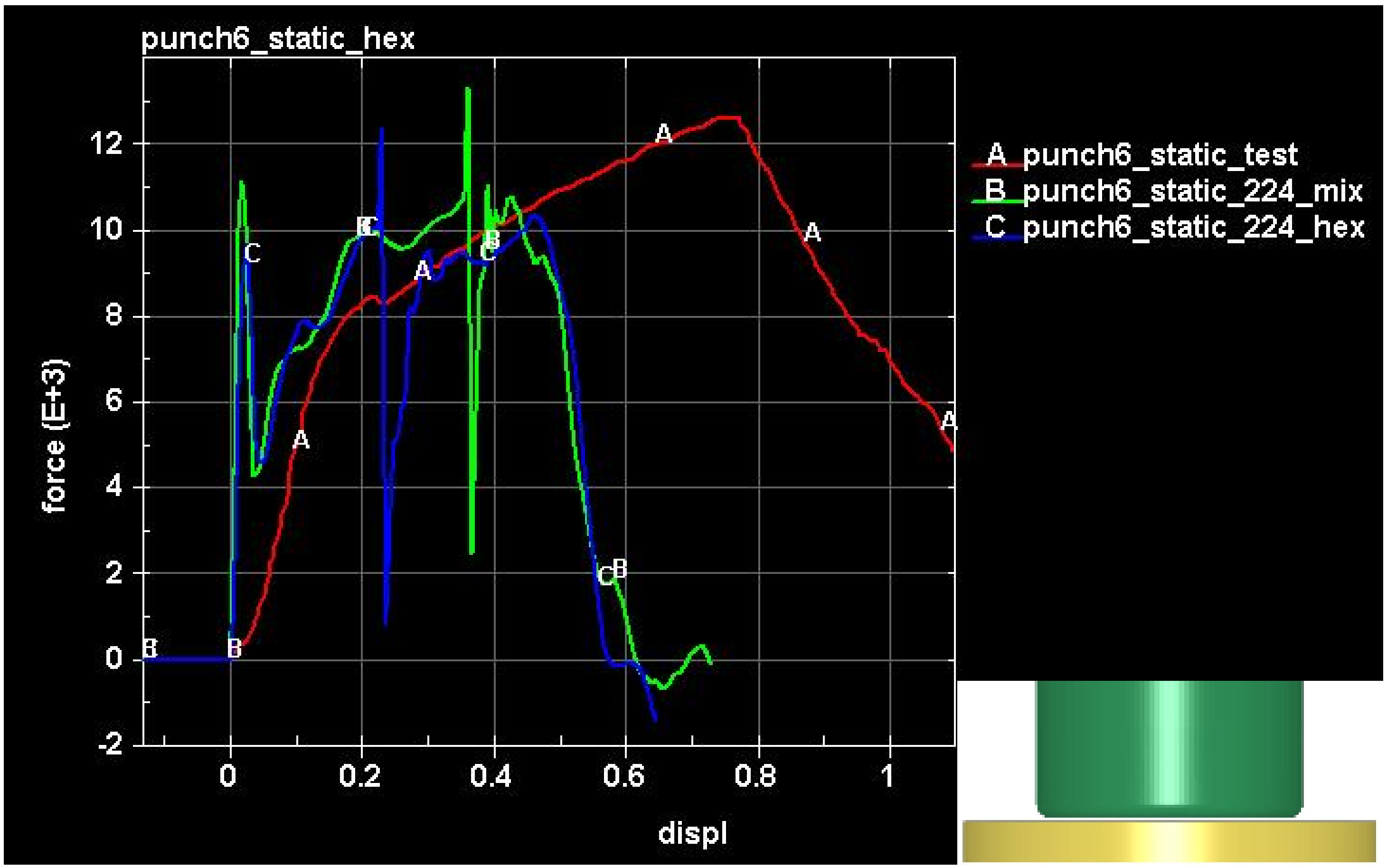

NASA Ballistic Tests

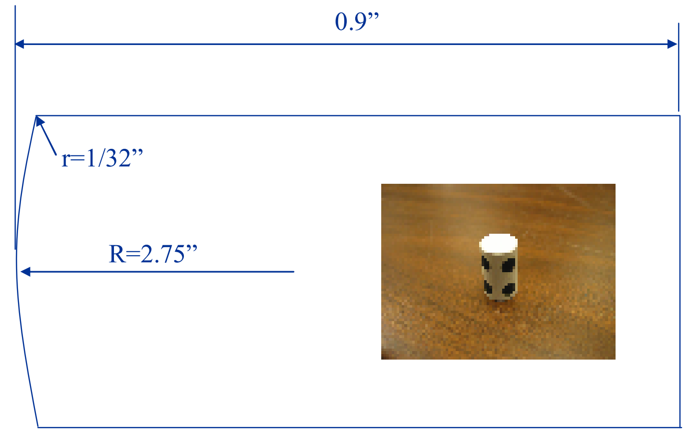

0.125” panels

- **0.5” dia, Ti-6-4, 0.7” long, ~ 9.9 g**

0.25” panels

- **0.5” dia, Ti-6-4, 0.9” long, ~12.8 g**

0.5” panels

- **0.5” dia, A2 tool steel, 1.125” long, ~28 g**
- **0.5” dia, A2 tool steel, 1.5” long, ~37.5 g**

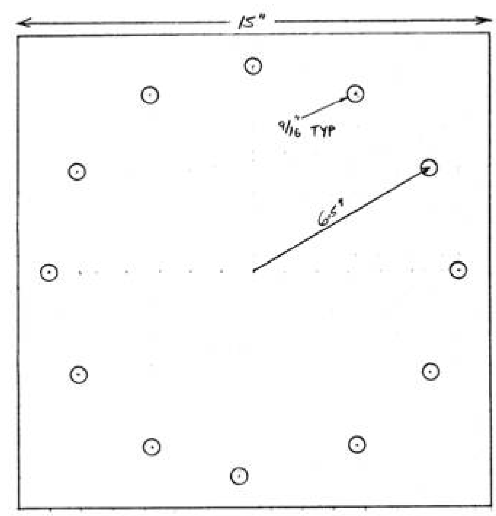

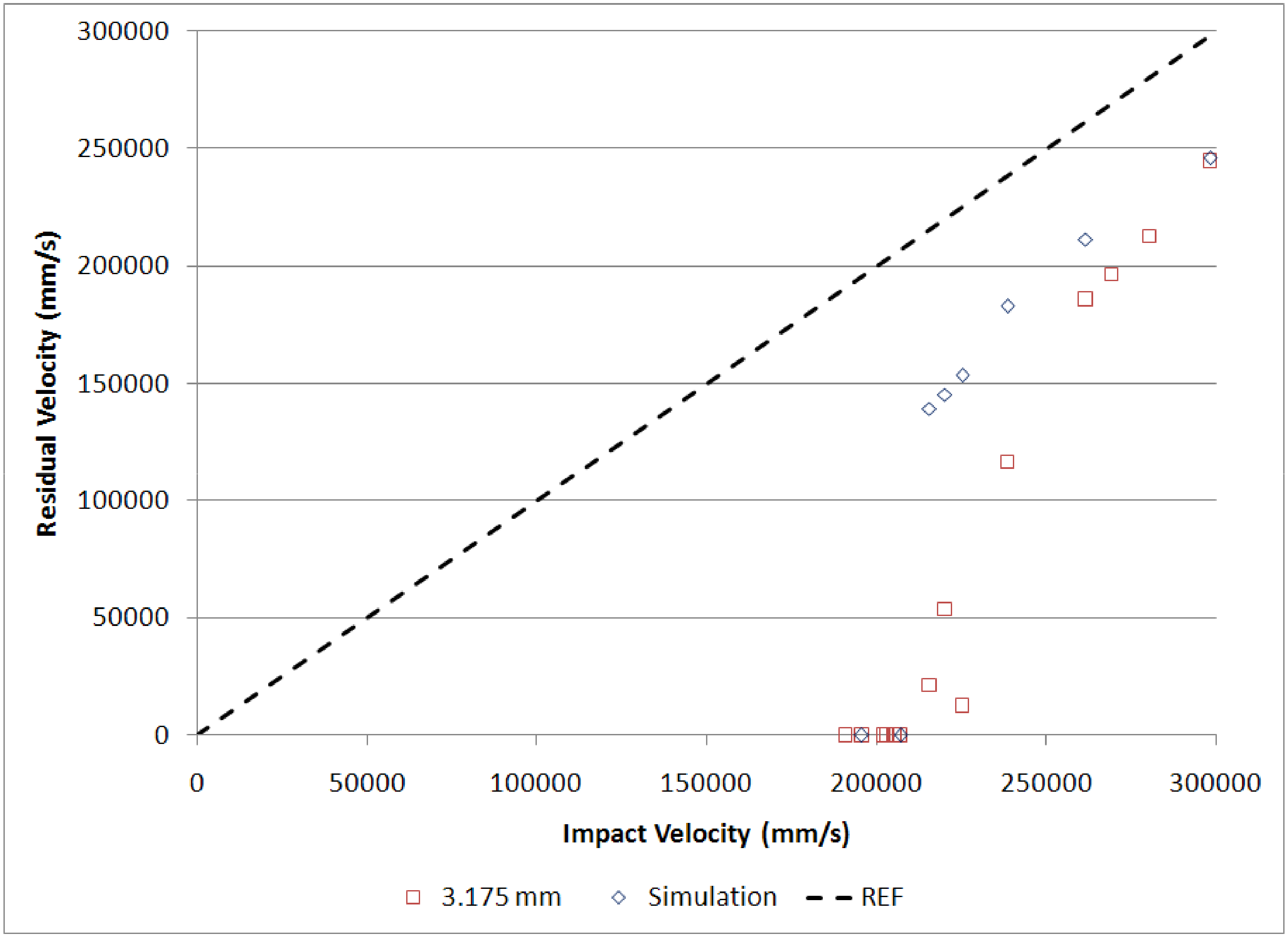

300000
250000
200000
150000
100000
50000
0
Residual Velocity (mm/s)
0
50000
100000
150000
200000
250000
300000
Impact Velocity (mm/s)
3.175 mm
Simulation
REF

Development, Implementation and Validation of 3-D Failure Model for Aluminium 2024

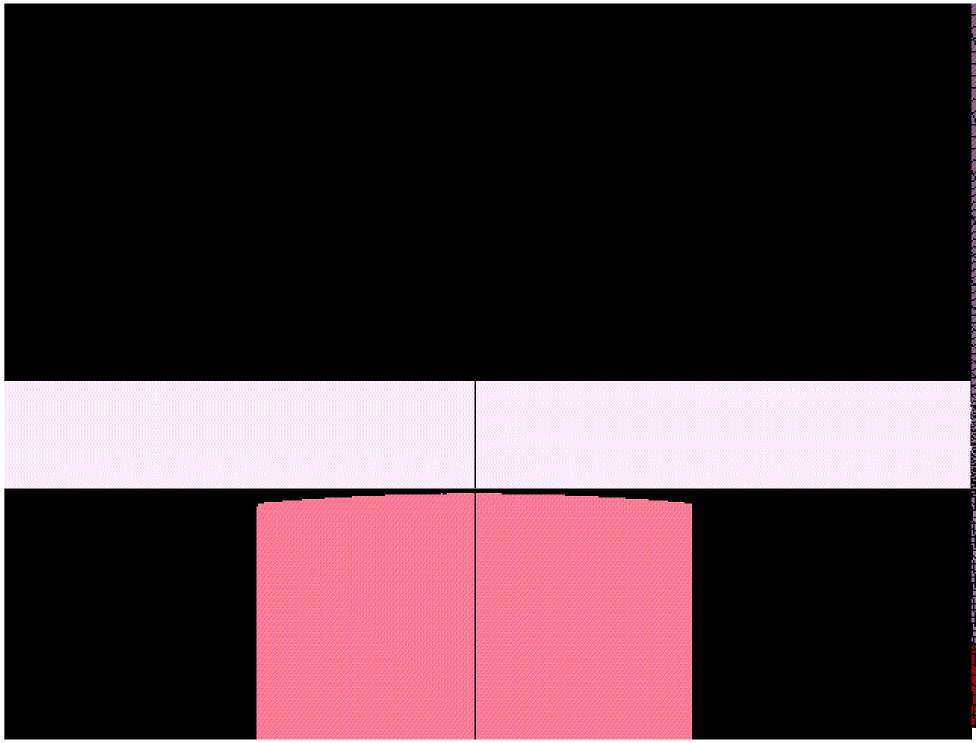

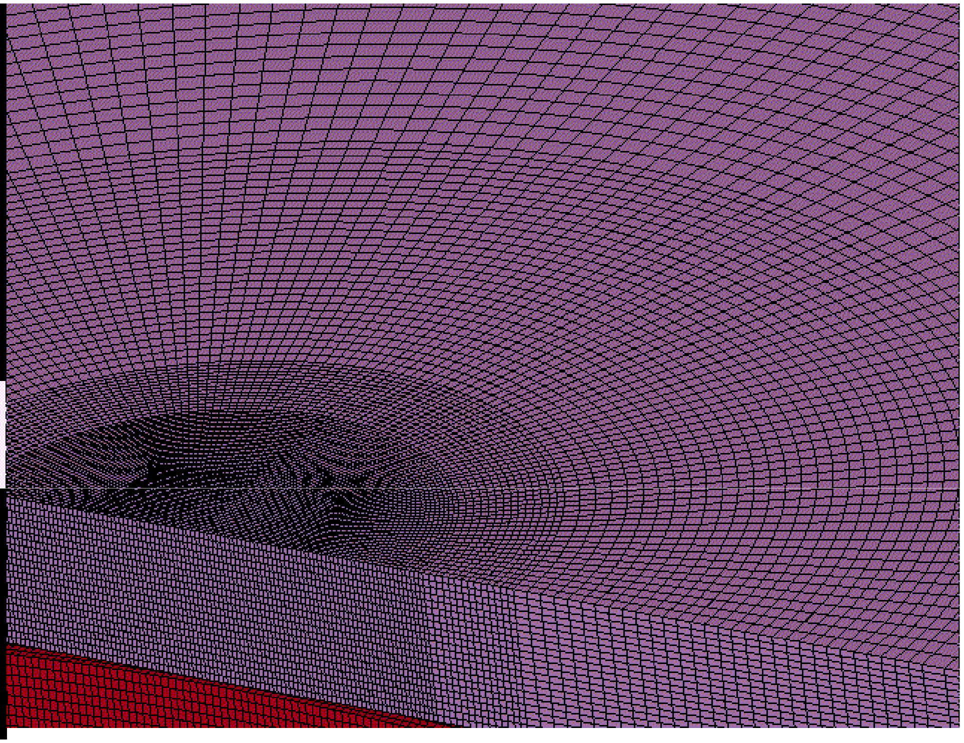

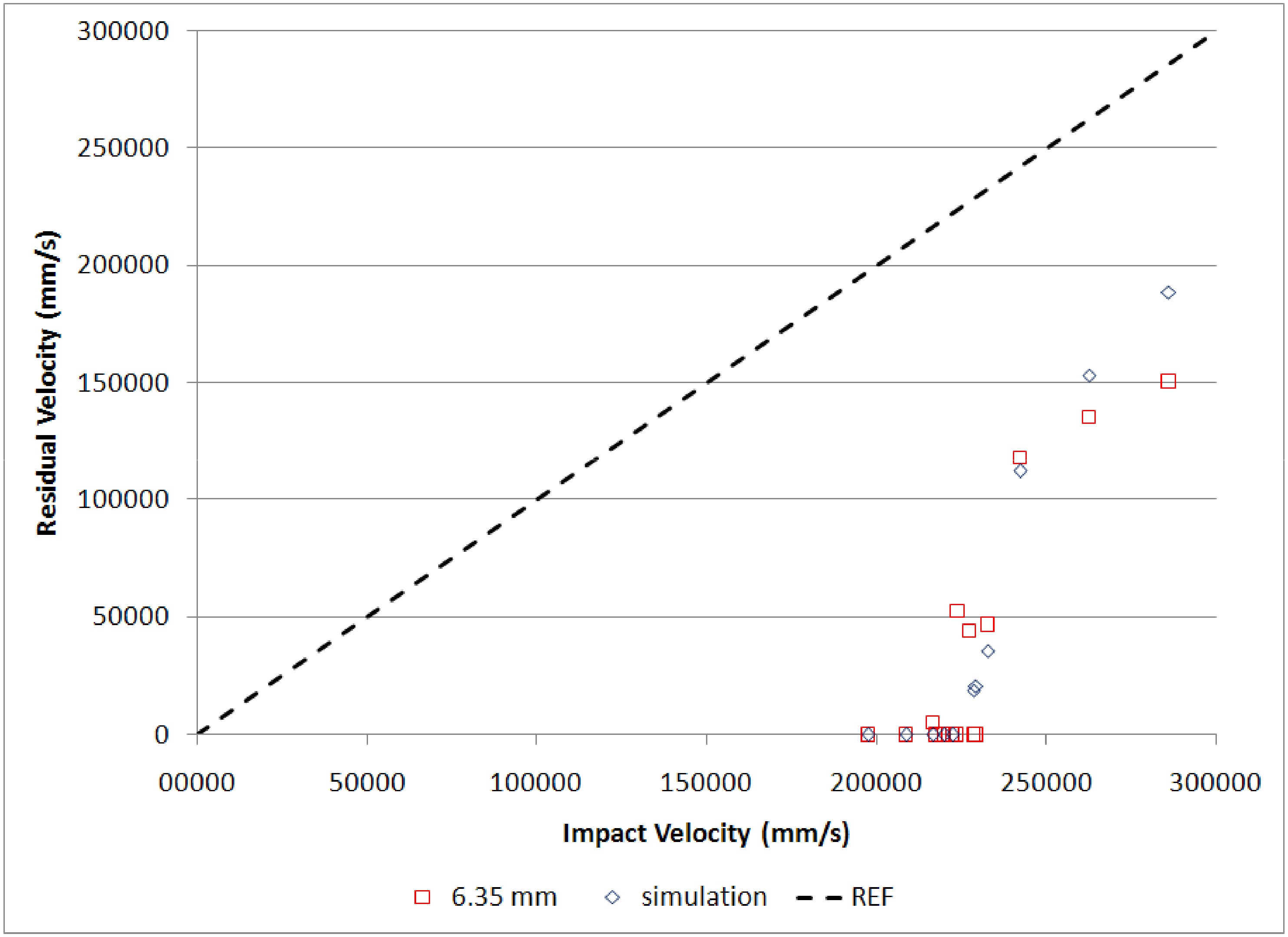
300000
250000
200000
150000
100000
50000
0
Residual Velocity (mm/s)
00000
50000
100000
150000
200000
250000
300000
Impact Velocity (mm/s)
6.35 mm
simulation
REF

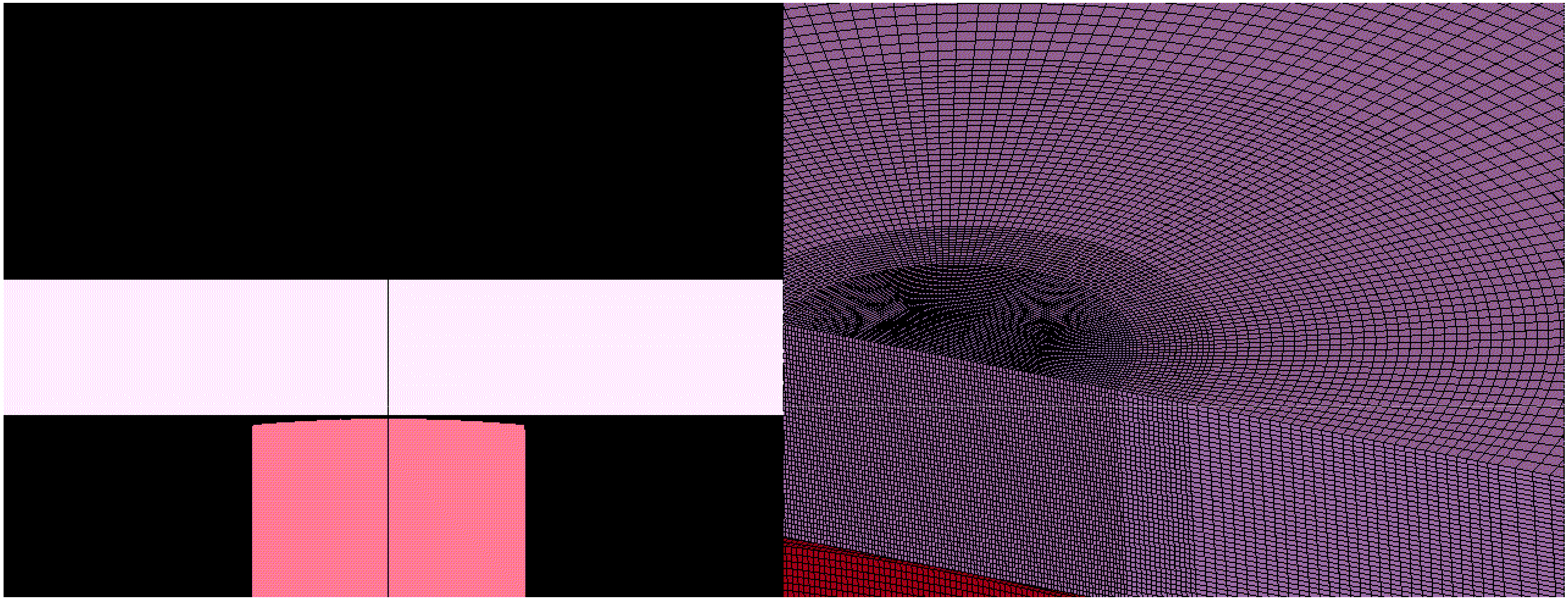

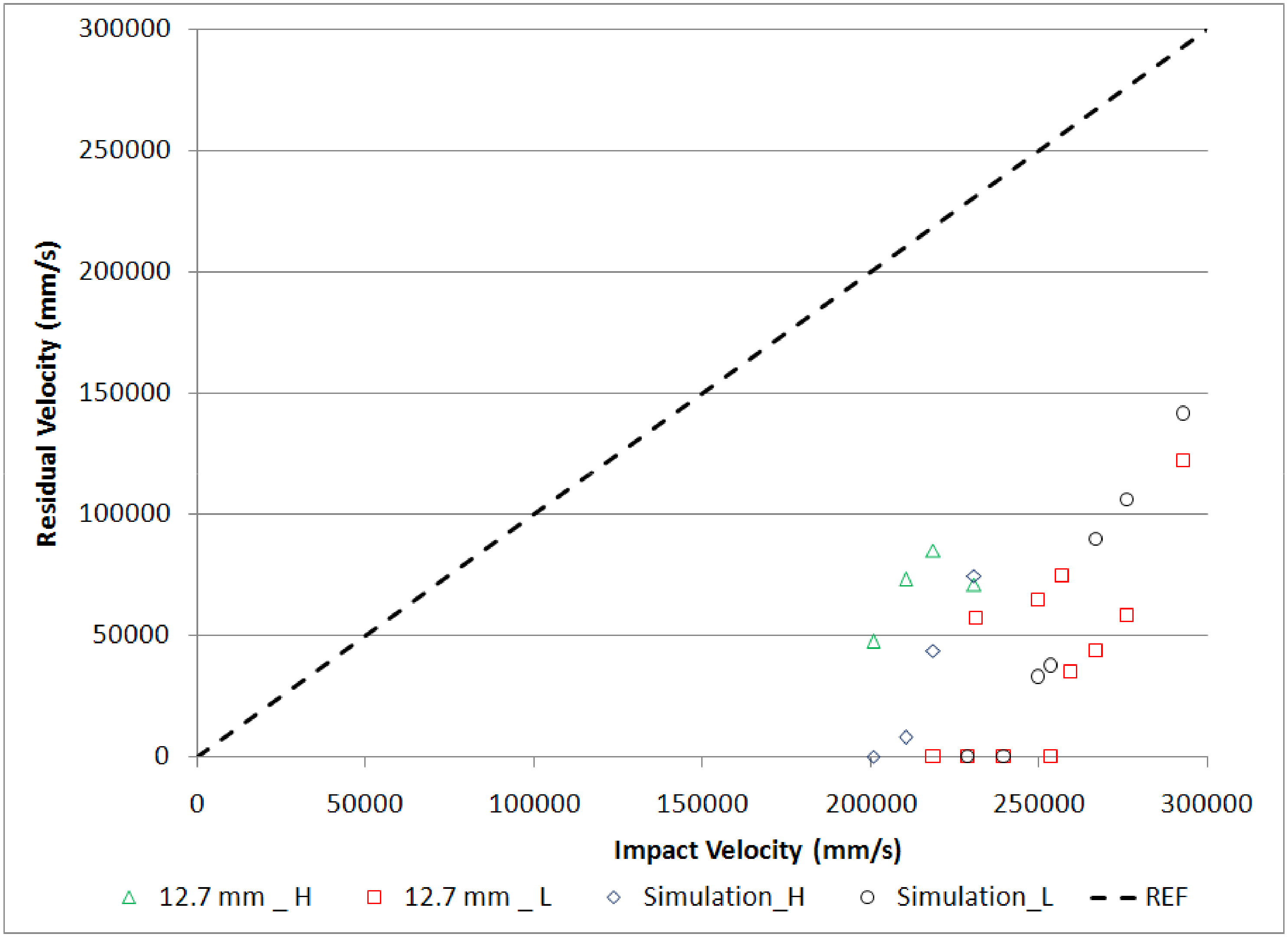

Residual Velocity (mm/s)
300000
250000
200000
150000
100000
50000
0
0
50000
100000
150000
200000
250000
300000
Impact Velocity (mm/s)
12.7 mm _ H
12.7 mm _ L
Simulation_H
Simulation_L
REF

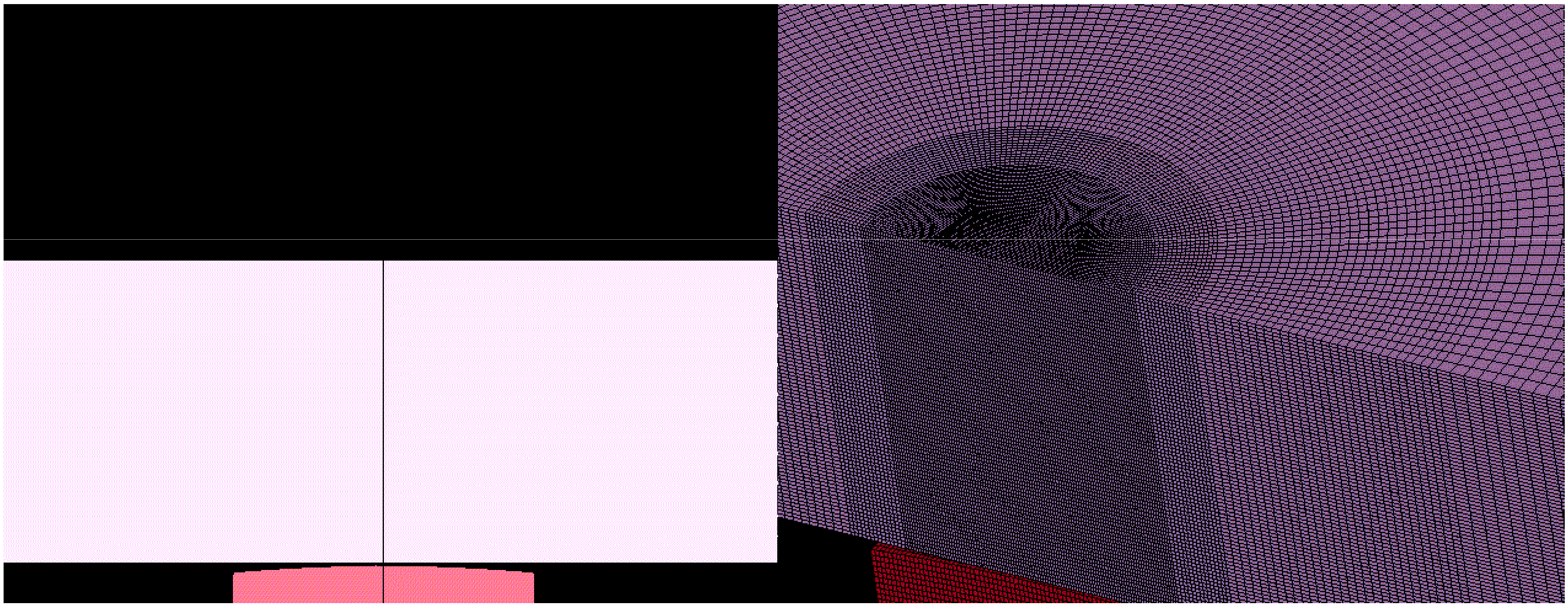

Fuselage 'shielding' tests at China Lake

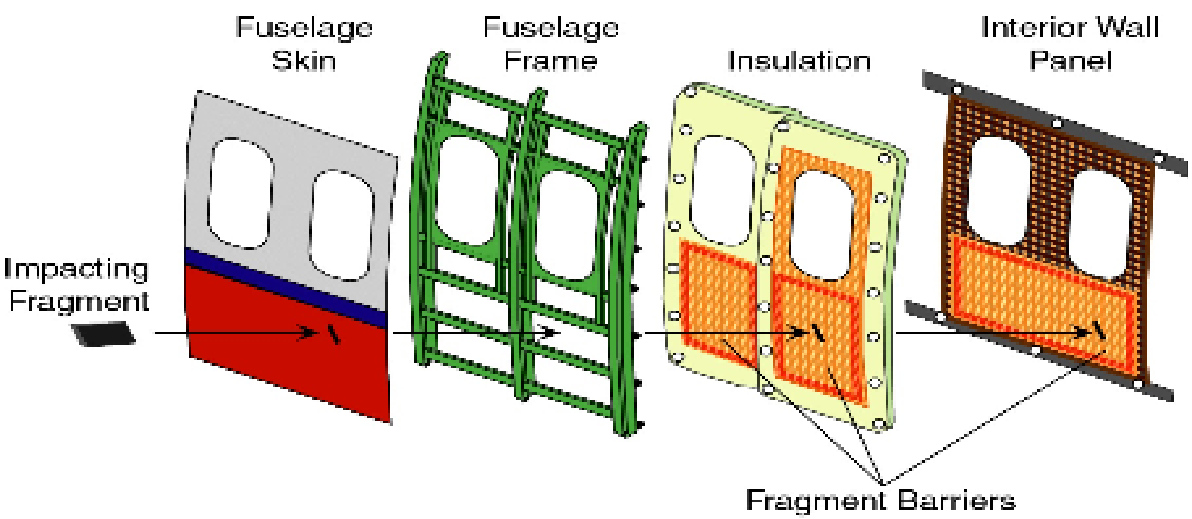

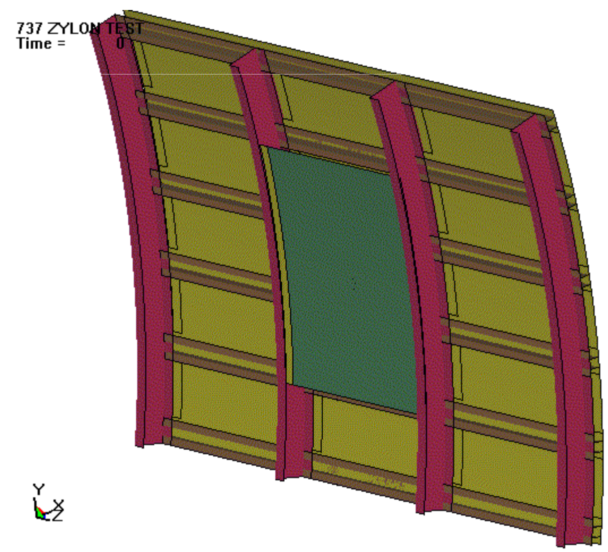

Part 4 :

CONCLUSION

Continuation

- further iterations using the material and punch test results to refine the failure model
- simulation of the ballistic tests performed at GRC to assess the current model
- repeat simulations of the UCB ballistic tests
- simulation of impact tests on fuselage panel performed at China Lake
- titanium and inconel will be investigated next

Conclusions

- **predictive analysis of failure is desirable for materials used in aeronautical structures**
- **to achieve maximum flexibility in the numerical models a tabulated and regularized generalisation of the Johnson-Cook material law was implemented in LS-DYNA**
- **a comprehensive testing program was used to create a material data card for aluminium 2024**
- **it proved possible to predict the complicate crack pattern in dynamic punch tests**
- **large numbers of ballistic limit experiments are available for further validation**